

Human hedonic experience during thermal alliesthesia:

A functional magnetic resonance imaging study

A Thesis

in

The Department

of

Psychology

Presented in Partial Fulfillment of the Requirements

For the Degree of Master of Arts at

Concordia University

Montreal, Quebec, Canada

November 2010

© Brian J. Dunn, 2010

CONCORDIA UNIVERSITY

School of Graduate Studies

This is to certify that the thesis prepared

By: Brian John Dunn

Entitled: Human hedonic experience during thermal alliesthesia:
A functional magnetic resonance imaging study

and submitted in partial fulfillment of the requirements for the degree of

Master of Arts (Psychology)

complies with the regulations of the University and meets the accepted standards with respect to originality and quality.

Signed by the final Examining Committee:

Barbara Woodside Chair

Virginia Penhune Examiner

Natalie Phillips Examiner

Peter Shizgal Supervisor

Approved by

Jean-Roch Laurence
Chair, Psychology Department

December 14, 2010

Graham Carr
Dean of Graduate Studies

Abstract

Human hedonic experience during thermal alliesthesia:

A functional magnetic resonance imaging study

Brian J. Dunn

The primary aim of the present experiment was to distinguish and map the hemodynamic correlates of hedonic experience using functional magnetic resonance imaging (fMRI). To accomplish this, we exploited a functional distinction between thermosensory perception and hedonic valuation. We used a water-perfused suit, both to deviate core temperature and to deliver thermal stimulation to the skin. We acquired two fMRI scans of each participant, under opposite core temperature deviations, in a single experimental session. During each scan we alternated the temperature of the circulating water in the suit from hot to cold every 2.25 minutes, for 18 minutes. Participants rated their thermal comfort and the suit temperature on 11-point Likert scales during alternating nine-second epochs. The critical feature of our design is that the hedonic sequence was the same in the two scans whereas the sequence of peripheral thermal stimuli, and the core temperature deviations were opposite. We present behavioral evidence that the opposite sequences of thermal stimuli induced a common pattern of hedonic experience. Furthermore, concurrent hedonic ratings tracked the blood oxygenation level dependent (BOLD) signal recorded from spatially conjoint cortical areas in pairs of scans from the same individuals. In cross-subject mixed effects analyses, we grouped the functional scans acquired under each core temperature deviation. We then used a conjunction analysis of

the group statistical maps to identify common hemodynamic correlates of the pattern of hedonic experience in both scans. Spatially conjoint (i.e., co-localized) BOLD signal correlates of the hedonic ratings were observed in bilateral subregions of the orbitomedial prefrontal cortex (OMPFC). A second analysis, based on a normative model of hedonic response, yielded spatially conjoint BOLD signal correlates in a more broadly distributed area of the OMPFC, including the subgenual cingulate and bilateral temporal poles.

Acknowledgements

This experiment demands the efforts of a large team of people, all of whom deserve my sincere gratitude. My heartfelt thanks go first to Peter Shizgal, my advisor and the originator of this experiment. Whatever is clear and compelling in this document is due to him; the present account of the experiment captures only a small part of his understanding and much of my confusion. I would like to thank Kent Conover, without whom the scanning and analysis would not have been possible, and who has been a generous colleague and friend. Many thanks to Gilles Plourde and Louise Ulyatt, who cared for me and for our participants, keeping us safe and making the experiment work. Thanks to David Munro, for his clarity and effort from the beginning and for never turning away a request for help. Thanks to Robert Kilgour for his advice and for allowing me to recruit his students. To everyone who assisted us in acquiring these data, including Marie-Pierre Cossette, Levi Riven, Karine Eigenman, Karine Paquin Boisvert, Brendan Parsons, Ian Moreau, and Catherine Cowan, many thanks. Special thanks to Christophe Lower for saving many scans and fixing more than he was ever asked to fix. Thanks to everyone in the Shizgal Lab during my studies, who encouraged and tolerated me: Giovanni Hernandez, Yannick-André Breton, Rebecca Solomon, Ivan Trujillo, Marie-Pierre Cossette, and Marc-André Bacon. I have been a hedgehog among foxes. I must also thank everyone at the Brain Imaging Center of the MNI/H, particularly André Cormier, David Costa, Ron Lopez, Louise Marcotte, Mike Ferreira, and Stacey Peixoto. I

must thank everyone who completed our study, despite the difficulty. And I must thank Gene Heyman for drawing me into psychological research and helping me stay. Finally, my thanks go to my partner, Elizabeth Zeeuw, who took the great risk of coming to Montréal without knowing what would happen and who has cared for me throughout.

Table of Contents

| | |
|--|----|
| List of Tables and Figures..... | ix |
| List of Appendices..... | xi |
| Introduction..... | 1 |
| Method..... | 14 |
| Participants..... | 14 |
| Apparatus..... | 16 |
| Temperature and physiological monitoring..... | 20 |
| Stimuli..... | 21 |
| Procedure..... | 22 |
| Data Analysis..... | 39 |
| Results..... | 50 |
| Behavioral Results..... | 52 |
| Functional Neuroimaging Results: Hedonic ratings..... | 55 |
| Group analyses of hedonic ratings EVs..... | 60 |
| Conjunction analysis of hedonic ratings maps..... | 66 |
| Group analyses of normative alliesthesia EVs..... | 68 |
| Conjunction analysis of normative alliesthesia maps..... | 74 |
| Non-conjoined area in the hedonic conjunction map..... | 77 |
| Discussion..... | 79 |
| Thermal alliesthesia..... | 79 |
| Distinguishing features of the present study..... | 81 |

| | |
|---|-----|
| Behavioral evidence of altered hedonic response..... | 83 |
| Distinction of hedonic responses from sensory processes..... | 85 |
| Location of conjoint hemodynamic response..... | 86 |
| Single-cell recording studies in human subjects..... | 90 |
| Single-cell recording studies in non-human primates..... | 93 |
| A functional model of orbitomedial prefrontal cortex (OMPFC)..... | 100 |
| FMRI studies of hedonic valuation..... | 105 |
| FMRI studies of primary rewards and punishers..... | 112 |
| Limitations..... | 120 |
| Future Directions..... | 129 |
| References..... | 133 |

List of Figures and Tables

| | |
|------------------------|----|
| Figure 1..... | 16 |
| Figure 2..... | 17 |
| Figure 3..... | 19 |
| Figure 4..... | 27 |
| Figure 5..... | 29 |
| Figure 6..... | 30 |
| Figure 7..... | 32 |
| Figure 8..... | 35 |
| Figure 9..... | 36 |
| Figure 10..... | 38 |
| Figure 11..... | 48 |
| Figure 12..... | 48 |
| Figure 15..... | 50 |
| Figure 16..... | 51 |
| Figure 17..... | 53 |
| Figure 18..... | 55 |
| Figure 19..... | 56 |
| Figures 20-22..... | 58 |
| Table 1..... | 59 |
| Figures 23 and 24..... | 61 |
| Table 2..... | 62 |
| Figures 25 and 26..... | 64 |

| | |
|---------------------|-------|
| Figure 27..... | 66 |
| Table 3..... | 66 |
| Figure 28-30..... | 68-69 |
| Table 4..... | 70 |
| Figures 31-34..... | 72-3 |
| Figure 35..... | 75 |
| Figure 36..... | 98 |
| Figure 37..... | 99 |
| Figure 38..... | 106 |
| Figure 39..... | 106 |
| Figures 40- 41..... | 107 |
| Figure 42..... | 116 |
| Figure 42..... | 118 |

List of Appendices

| | |
|--|-----|
| Appendix A: MR Safety Screening Form | 143 |
| Appendix B: Informed Consent Form..... | 145 |
| Appendix C: Exemplary Hyper- and Hypothermia Induction Sheets..... | 151 |
| Appendix D: Ratings Instructions..... | 155 |
| Appendix E: Individual FEAT Script..... | 157 |
| Appendix F: Group FEAT Script..... | 164 |

Introduction

The aim of the present study was to distinguish the hemodynamic correlates of hedonic experience from those of sensory information processing and map them using functional magnetic resonance imaging (fMRI). We pursue this aim as a starting point for a neurobiological analysis of questions regarding what areas of the human brain encode hedonic experience. The challenge of distinguishing the neural correlates of hedonic experience from stimulus perception has limited the inferences that can be made from functional neuroimaging studies of emotion and reward processing (see O’Doherty, 2004; Wiens, 2005). Our objective was to induce hedonic experiences of positive and negative sign, using an experimental design that facilitates the differentiation of hedonic valuation from sensation.

Hedonic experience, defined as subjective pleasantness or unpleasantness, signals the current biological utility of stimuli. For naturally occurring primary rewards or punishers, the hedonic value of a stimulus depends on the internal state. Craig (2003) goes so far as to specify a class of “homeostatic emotions,” of which the hedonic response accompanying thermosensation and thermoregulation is paradigmatic. Homeostatic emotions are the subjective component of regulatory responses, indices of the survival needs of the organism. We have manipulated a determinant of hedonic experience by deviating core temperature and then delivering a sequence of peripheral thermal stimuli.

Sensations, in contrast to hedonic responses, provide information about the external world. The validity of sensory data is predicated upon their relative independence from fluctuations in physiological states. Consequently and necessarily, the sign of sensory percepts is not modulated by shifts relative to homeostasis. In the present experiment, the fact that sensory and hedonic responses to peripheral thermal stimuli are differentially affected by changes in core temperature is the basis of their distinction.

A thermal stimulus can be hedonically positive or negative, depending on core temperature, while its sensory attributes remain unaltered. Thus, the hedonic value of a thermal stimulus can be modulated in the experimental context: warming or cooling of the skin can feel good or bad depending on the direction in which core temperature deviates from a regulated value. This characteristic dependence of hedonic responses on the direction and magnitude of a deviation from the regulated range of core temperature is a phenomenon known as thermal *alliesthesia* (Cabanac, 1971). Defined generally, *alliesthesia* refers to the observation that “a given external stimulus can be perceived either as pleasant or unpleasant depending upon signals coming from inside the body” (Cabanac, 1971, p. 1105).

History and background: Thermal alliesthesia

The primary conceptual and methodological antecedents of the present study are Cabanac’s investigations of hedonic responses, in which he manipulated the relations between sensations and internal states. In his classic study of the physiological role of pleasure (1971), and a later refinement (Cabanac, Massonet & Belaiche, 1972), he and his collaborators established that pleasure and displeasure are not properties of stimuli

per se and that hedonic responses depend on signals from multiple sources in the body. The affective aspect of sensation, as Cabanac termed it (1971), depends on internal signals while being independent of the “descriptive” aspects of sensation.

This he first demonstrated by submerging a subject in a temperature-controlled bath to alter core temperature, while one hand was separately heated or cooled in another container (Cabanac, 1971). The subject rated his hedonic responses to the thermal stimulation of his hand while the investigators monitored his core temperature. Core temperature determined the pleasantness of the thermal stimulation to which the hand was exposed: when core temperature was elevated, cool peripheral stimuli were pleasant while warm or hot stimuli were unpleasant. When lowered, cool peripheral stimuli were unpleasant but warm stimuli were pleasant. Regardless of internal temperature, the subject could sense the temperature of the peripheral stimuli with accuracy. The observation of reversible hedonic responses to the same stimulus under opposite core temperature deviations provided the basis for equating the pleasant with the homeostatically useful (Cabanac, 1971). The conclusion, for non-noxious thermal stimuli, is that pleasure signals the promise of a stimulus to correct a deviation from thermoregulatory set point and displeasure attends a stimulus that threatens to exacerbate such a deviation.

In a more controlled and elaborate follow-up experiment Cabanac, Massonet & Belaiche (1972) attempted to determine the influence of mean skin temperature on thermal preference and generate a quantitative model of the relation between internal temperature, skin temperature and thermal preference. They tested healthy men at different bath temperatures. Subjects controlled a peripheral stimulus themselves by

operating a valve to mix hot and cold water in a specially designed glove. Before entering the bath, subjects either had their internal temperature raised or lowered. Once hyperthermic, subjects were submerged to the neck in a cool, cold or lukewarm bath (23°, 28°, 33° C, respectively); once hypothermic, they were submerged in a bath that was lukewarm, warm or hot (33°, 38°, 40° C, respectively).

The sole instruction was that subjects maintain the peripheral stimulus (i.e., the temperature of the water running through the glove) at a “pleasant” temperature. The constant temperature of the bathwater kept skin temperature constant, while shifting internal temperature. Following the respective gradients (e.g., the difference between an elevated internal temperature and a 23° C bath), core temperatures drifted in the direction of the bath temperature. The preferred glove temperature, as controlled by the subject, moved gradually in the opposite direction. In effect, the pleasant stimulus was shown to be one that regulated a thermoregulatory set point.

The implications of this evidence include an account of mutable biological utility, experienced as hedonic value and determined by regulatory responses that do not vary significantly between individuals. When both the peripheral stimuli and bath were held constant, as in the first experiment (Cabanac, 1971), ratings of the pleasantness and unpleasantness of the peripheral stimuli reversed as a function of internal temperature. When subjects were asked to select what felt pleasant, the resulting choice behavior demonstrated great sensitivity, changing over time as a function of internal temperature (Cabanac, Massonet & Belaiche, 1972). Thus, “(a) given stimulus can be perceived as pleasant or unpleasant according to the inner state of the subject” (Cabanac, 1979, p. 9). To describe the altered hedonic response to a stimulus on the basis of internal signals

Cabanac coined the term *alliesthesia* (defined: Cabanac, 1971, p.1105; Cabanac, Massonet & Belaiche, 1972, p. 699; Cabanac, 1979, p.9), derived from the ancient Greek for “other feeling” or perhaps “altered feeling.”

Subsequent thermal *alliesthesia* experiments were few in number and are directly relevant to the present study. We can consider them in less detail because they represent simple refinements of the two studies by Cabanac and colleagues discussed above. Marks & Gonzalez (1974) observed that hedonic responses evidence spatial summation: for non-noxious radiant heat stimuli, proportional increases in temperature or area yielded equal changes in hedonic ratings. Thus, transient thermal signals from the skin do contribute to the “affective dimension of thermal sensation” (Marks & Gonzalez, 1974, p.474), in a manner that the authors attributed to anticipatory homeostatic responses. The evidence of spatial summation supports our application of thermal stimuli to a broadly distributed area of the skin on the trunk, arms and legs, as opposed to the thermal stimulation of the hand most often used in human neuroimaging studies (Rolls, Grabenhorst & Parris, 2009; McAllen et al., 2006).

Mower (1976) tested the converse of Cabanac’s *alliesthesia* theory, that is, whether changes in internal temperature affected thermosensation. Like those of Cabanac and colleagues (1972), his subjects were submerged in a bath after induction of hyperthermia, hypothermia or at normal core temperature. However, Mower submerged his subjects in a neutral temperature bath (35-36° C) and small test baths, which ranged in temperature from 21° C to 45° C (in 3° increments), served as peripheral stimuli. All peripheral stimuli were then presented in contrast to neutral thermal stimuli: for each trial, subjects removed their hand from a neutral temperature “adapting” bath, immersed

it in a test bath for three seconds, and then returned it to the adaptive bath. Subjects gave hedonic and sensory ratings when their hand was again immersed in the adapting bath.

Mower's (1976) subjects' internal temperatures did not affect their judgments of peripheral temperature. In the context of our discussion, the fact that thermosensation was not affected by changes in core temperature is evidence that modulation by core temperature deviation is specific to hedonic responses. As in Cabanac and colleagues' prior study (1972), deviated core temperatures drifted in the direction of the surrounding bath water. In contrast to the unaltered peripheral temperature judgments Mower observed, the hedonic ratings under core temperature deviations were a dramatic example of *alliesthesia*. Despite having set out to show that *alliesthesia* did not occur, Mower's behavioral results accord with the hedonic ratings obtained under deviated core temperatures by Cabanac and colleagues published that same year (Cabanac et al., 1976), among others.

Attia & Engel (1981), in another study that contributed to the understanding of thermal *alliesthesia*, observed identical hedonic ratings of thermal stimulation to three peripheral locations under passive heating and cooling. In addition to rating pleasantness or unpleasantness and temperature, subjects selected the most pleasant temperature for each stimulus location. Their hedonic selections, like the other behavioral evidence, show perfect *alliesthesia* and no location effect. As predicted by the theory, the preferred temperatures were inversely related to internal and ambient temperatures, almost to the point of inverse proportionality (cf. Cabanac et al., 1972, 1976, Mower, 1976).

So well established was the phenomena of thermal *alliesthesia* that investigators employed it as a means of operationalizing the thermoregulatory set point (e.g., Cabanac

et al., 1969, 1971, 1976), defining hyperthermia and hypothermia (Attia & Engel, 1982; Attia, 1984), and quantifying thermal stress loads (Attia & Engel, 1982). Attia and colleagues (1982) demonstrated the equivalence of any combination of behavior and thermal conditions that produced equal thermal *alliesthesia*. Their finding that the effects of core temperature deviations override those of mean skin temperature is particularly relevant to the present experiment.

Studies predicated on and elaborating the theory of *alliesthesia* altered the definition of thermoregulatory set point. Prior to Cabanac's work, the existing definition stipulated that the thermoregulatory set point was the temperature at which no thermoregulatory responses occurred, a "dead band" of thermoneutrality (in Cabanac & Massonnet, 1977, p.587). The first blow to this definition came when Cabanac and colleagues (1976) demonstrated experimentally that as the resting core temperature shifts over the 24-hour nycthemeral cycle, so do hedonic responses. One necessary, adaptive function of *alliesthesia* was consequently demonstrated: hedonic responses to thermal stimuli must be adjustable because the regulated range of core temperatures changes.

Cabanac & Massonnet (1977) further showed that there is no "dead band" of non-reactive thermoneutrality. They measured the autonomic thermoregulatory responses (i.e., metabolic heat production, sweating, convective heat loss, shivering and vasomotor response) of subjects submerged in series of temperature-controlled baths and compared the thresholds for heat loss and heat production. They found that the thresholds overlap; there was no range of core temperature for which thermoregulation was inactive. On the basis of these observations, they defined the thermoregulatory set point as a dynamic range, one that could not be characterized by the inactivity of autonomic responses.

In a later review Attia (1984) inverted the logic, on the basis of this body of research, defining the thermoregulatory set point hedonically, in relation to *alliesthesia*: “(T)he set point (is) the value of core temperature at which...cool and warm stimuli (are) neither pleasant nor unpleasant” (p. 337). By this definition, hedonic responses to thermal stimuli are indeed the subjective component of regulatory responses, the indices of the changing survival needs of the organism.

The purpose of this brief review of the experimental precedents for thermal *alliesthesia* is to support and illustrate the distinction of hedonic responses from thermosensation. Most consequential is the point that changes in internal states can modulate the hedonic sign but not the sign of sensory percepts (i.e., a deviation in core temperature will not make a subject perceive cold as hot or *vice versa*). Indeed, we might go further to assert that pleasantness and unpleasantness are not “perceived,” in the simple, veridical sense. Rather, hedonic value is generated, “constructed” from comparisons between convergent signals. Afferent temperature signals come from multiple locations in the body (e.g., brainstem, chest, organs, see Boulant & Dean, 1986; Romanovsky, 2007) and must be compared with a regulated temperature range. That state determines the hedonic value of signals from temperature sensors in the skin. The survival utility of both changeable hedonic responses and fidelity in sensory perception should be clear in the case of the relations between core temperature and the temperature of peripheral thermal stimuli.

Thermosensation and thermoregulation

By behavioral and autonomic means, mammals regulate core temperature very tightly. The range of survivable core temperature is narrow, particularly in the direction of its upper limit. The actual or even potential effects of thermal stimuli on core temperature are constantly monitored and adaptively reacted to by dedicated circuits in the central nervous system (Craig, 2000, 2003; Romanovsky, 2007). Afferent and efferent thermoeffector loops, engaged by thermosensory signals along the spino-reticulo-hypothalamic pathway, contribute to the regulation of core temperature value (Romanovsky, 2007).

Critically for our discussion, monitoring (by thermosensory neurons and thermoreceptive neurons in the CNS) and reacting (by autonomic thermoeffector/thermoregulator functions) are separate processes that engage separate systems (Romanovsky, 2007). The monitoring functions of thermosensation are relatively invariable in their function. In healthy mammals, signaling is not modulated by other physiological functions, within a survivable range of temperatures. In contrast, thermoeffector subsystems are adaptive according to relations between multiple afferent values. This functional distinction between thermosensory processes and thermoregulatory (or, more accurately *thermoeffective*) processes maps onto the distinction between sensation and hedonic response¹. The functional distinction between

¹ This is not to assert that thermoeffective responses are limited to hedonic responses. Obviously many other autonomic responses are included (e.g., sweating, shivering, vasodilation or vasoconstriction, respiratory changes, *et cetera*).

thermosensation and thermoregulation makes our experiment possible. It is the physiological basis of *alliesthesia*.

Axiomatic to the theory of *alliesthesia* is the observation that hedonic responses are regulatory in nature. As such, the hedonic experiences that define thermal *alliesthesia* are coincident with autonomic regulation and motivate behavioral efforts at thermoregulation. Regulatory signals can be experienced as feelings of (thermal) comfort and discomfort. Hedonic appraisals, as we will show, are based on comparative regulatory utility: A change in internal temperature shifts the biological utility of a perceived thermal stimulus. Conversely stated, a thermal stimulus is hedonically valued as a function of its bearing on core temperature, specifically on its engagement of autonomic thermoeffector systems.

The modulation of hedonic responses to thermal stimuli occurs both because of the changing environment and because the thermoregulatory balance point is not a point at all, but rather a homeostatic range (Romanovsky, 2007). This was mentioned above in relation to Cabanac and colleagues' (1976) study of changes in hedonic response across the nycthemeral cycle of thermoregulation. This point bears repeating because it is of critical importance: core temperature is dynamic or mutable, within the limited functional range. As a consequence of this, relations between changing core temperature and the changing environment necessitate dynamic thermoeffective responses and hedonic indexing. As demonstrated in Cabanac's efforts and our experiment, hedonic responses are mutable, even reversible, as required to signal the autonomic defense, or motivate the behavioral defense, of a limited homeostatic range.

In the present study, we have applied Cabanac's observations and theory of thermal *alliesthesia* to the fMRI setting as a means of changing the hedonic sign of peripheral thermal stimuli without changing their sensory characteristics. The cardinal features of the theory are first, that the hedonic value of a thermal stimulus is reversible according to its relation to core temperature. As a consequence, the identical stimulus can be hedonically positive or negative. Second, the sign and direction of change in thermosensation are not modulated by alterations in core temperature. This difference between thermosensation and hedonic valuation is the basis for distinguishing their neural correlates.

Rationale for the current study: prior neuroimaging studies

Human neuroimaging experiments have contributed to the identification of the neural substrates of hedonic value representation and emotion experience (for reviews see O' Doherty, 2004; Rolls & Kringelbach, 2004, Kringelbach, 2005; Berridge & Kringelbach, 2007; Rolls & Grabenhorst, 2008; Dolan, 2002; for meta-analyses of emotion induction and experience in neuroimaging see Steele & Lawrie, 2004; Phan et al., 2002; Murphy et al., 2003; Wager et al., 2003). Correlational evidence from fMRI studies indicates that subregions of the anterior ventromedial and orbital prefrontal cortex (vmPFC/OMPFC) encode the hedonic value of stimuli. Blood oxygenation level dependent (BOLD) signal changes in the mid-anterior subdivisions of the vmPFC have been uniquely associated with hedonic experience, notably in studies designed to distinguish it from other concurrent processes (Small et al., 2003; Anderson et al., 2003; Dolcos et al., 2004; Kringelbach et al., 2003; see reviews in Rolls & Kringelbach, 2004;

Berridge & Kringlebach, 2007; Kringlebach, 2005).

One line of evidence from neuroimaging echoes William James's (1884, 1890, 1894/1994) identification of emotion with the feeling of bodily changes (Damasio, 1999; Craig, 2002, 2003, 2004; Wiens, 2005; Critchley, Wiens et al., 2004; Critchley, 2004; see also Dolan, 2002). Perceiving the physiological condition of the body and the physiological responses to stimuli is central to the subjective experience of emotion, according to this view. The localization of these functional representations in the vmPFC is consistent with correlational evidence of a role in self-monitoring (Northoff & Bermpohl, 2004; Northoff & Panksepp, 2008; meta-analysis in Northoff et al., 2006) and the processing of affective valence as distinguished from arousal or intensity (Kinglebach, 2005; Heinzl et al., 2005; Northoff et al., 2006; Grimm et al., 2006; Anderson et al., 2003; Small et al., 2003; Dolcos et al., 2004; *inter alia*).

Findings from fMRI and positron emission tomography studies indicate that the subgenual region of the anterior cingulate cortex (i.e., ventral to the “*genu*” of the anterior cingulate) contributes to the encoding of the subjective experience of emotion and mood (e.g., Mayberg et al., 1999; Liotti et al., 2000; see Drevets, 1998 and 2000 for reviews). This has been demonstrated in imaging studies of induced and recalled emotion (e.g., Lévesque et al., 2003; Beauregard et al., 2001; Gemar et al., 2007; Damasio et al., 2000), and hedonic experience (e.g., Rolls, Grabenhorst & Parris, 2009), among other paradigms. It is significant, in this respect, that the subgenual cingulate has been identified as a primary functional correlate of mood disorders and a marker of treatment response (Drevets et al., 1997; Drevets, 1998, 2000; Drevets and Raichle, 1992; Drevets, Savitz, & Trimble, 2008; Mayberg et al., 1999).

On the basis of this evidence, our expectation was that we would observe BOLD signal changes correlated with the pattern of hedonic experience in the subgenual cingulate and ventromedial prefrontal cortex. In the present study, we have designed experimental conditions to induce a common pattern of hedonic experiences during two functional magnetic resonance imaging scans of the same subject. We have manipulated biological utility by controlling determinants of hedonic value, in the modality of thermosensation and thermoregulation, to induce experiences of positive and negative hedonic sign. By altering the internal state (i.e., core temperature) and varying external conditions (i.e., peripheral thermal stimuli) according to an optimized pattern, we have attempted to disambiguate neural correlates of hedonic experience from those of sensory processing. This distinguishes the present study from its predecessors.

To summarize our method briefly, we induced mild hyperthermia (+1°C) and hypothermia (-1°C) using a water-perfused suit. We scanned each participant twice, during each respective core temperature deviation. Our two fMRI scans entailed a block design, during which we alternated the temperature of the circulating water in the suit from hot to cold every 2.25 minutes, for 18 minutes. During alternating nine-second epochs, participants rated their thermal comfort and the suit temperature on 11-point Likert scales. The critical feature of our design is that the hedonic sequence was the same in the two scans, while the sequence of peripheral thermal stimuli and the core temperature deviations were opposite. We used a conjunction analysis to identify common hemodynamic correlates of the pattern of hedonic experience.

Our experimental approach is broadly informative because hedonic experience, as an index of biological utility, is a motivator of behavior. Whether expressed in terms of

pleasure principle or principles of instrumental reinforcement, behavior is orderly in its relation to rewarding or punishing conditions. Yet the conditions themselves do not have an inherent hedonic quality; that is a feature of subjective experience that can be modulated by internal states. Mapping the hemodynamic correlates of this feature of subjective experience can inform the understanding of neural systems that represent reward value, the hedonic dimension of emotion, the state of the body, and the self.

Method

Participants

Sixteen healthy, unmedicated adults (nine women and seven men), aged 19 to 26, have participated in the study. All reported being right-handed. Nine of the sixteen participants were naïve to the magnetic resonance (MR) environment; ten had never undergone brain scans. All sixteen were sufficiently fit to tolerate moderate exercise under heat stress; their physical conditioning ranged from irregular team sport participation and non-competitive distance running to daily cross training. However, none was an elite athlete preparing for competition. Participants were recruited via word of mouth from the community of students and researchers at Concordia University, were screened for contraindications to magnetic resonance scanning (Appendix A) and gave informed consent (Appendix B) according to the regulations of the Research Ethics Board of the Montréal Neurological Institute and Hospital (MNI) as well as the Concordia University Human Research Ethics Committee.

Screening procedures: In an informal screening interview with one of the investigators (BD) we confirmed participation in regular aerobic exercise and excluded participants with the most obvious contraindications to magnetic resonance imaging. Psychological screening comprised the Structured Clinical Interview for DSM-IV-TR (SCID, First et al., 2002)(BD interviewer), Beck Depression Inventory (BDI) (Beck et al., 1961), Tri-dimensional Personality Questionnaire (TPQ) (Cloninger et al., 1991), and Barratt Impulsivity Scale (BIS) (Barratt, 1975; Barratt, 1985). As might be expected of participants in contact sports, some had history of mild head injury, for which they did not seek medical attention. Others reported known histories of concussion. Therefore, in consultation with a neurologist (Dr. Alain Dagher), we established an exclusion criterion. Past concussion or non-traumatic head injury without symptoms was not exclusionary, if the injury occurred longer than five years before screening.

Having passed this screening, participants underwent a medically supervised cardiac stress test. Dr. Marcel Fournier, M.D., a board-certified cardiologist practicing at the Royal Victoria Hospital and Queen Elizabeth Health Center, evaluated the 12-lead ECG results and cleared fourteen candidates for participation. Dr. Gilles Plourde, M.D., an anesthesiologist on staff at the MNI and co-investigator in this study, briefly interviewed all participants prior to the experiment to collect information relevant to emergency treatment, such as medication allergies, and he confirmed the absence of any medication or condition that might affect a participant's cardio-vascular response to the experimental manipulation. Female participants were screened for pregnancy with a urine assay and scanned during their self-reported luteal phase, unless using oral

contraceptives. On the morning of the scans, all participants were screened for substances of abuse using a ten-panel urine assay.

The experimental procedures have the approval of the Research Ethics Board of the Montréal Neurological Institute and Hospital (#NEU-04-51) as well as the Concordia University Human Research Ethics Committee (#UH2004-107-2). Participants were debriefed following completion of the scanning day by the team of investigators and compensated for the cardiac stress test and scanning day (\$300.00 total).

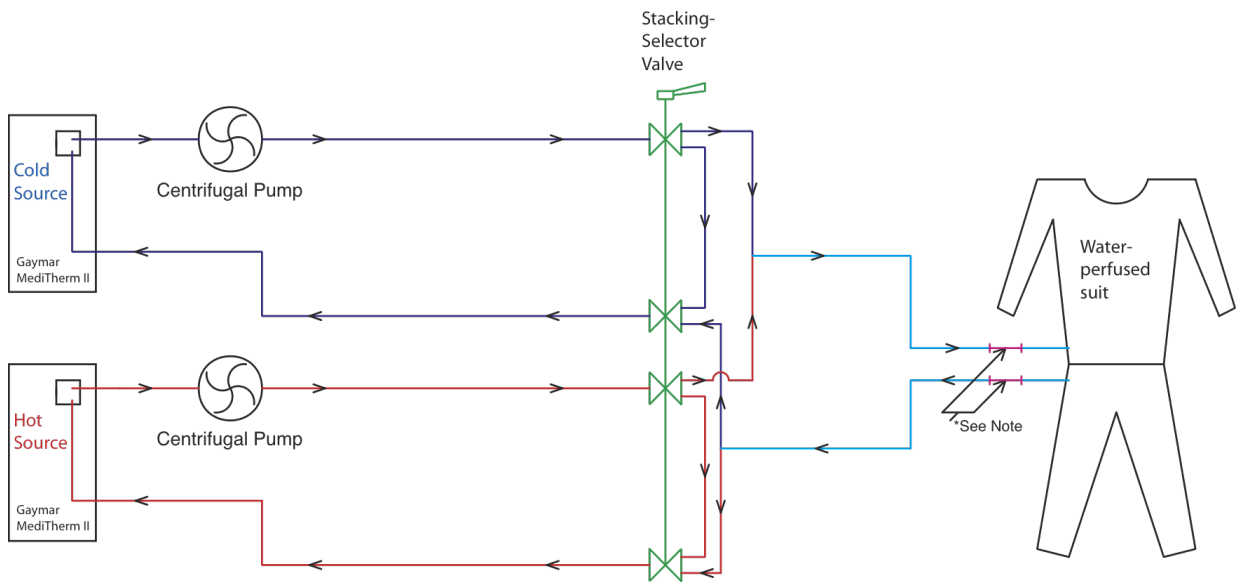
Apparatus

Thermal Control: Throughout the experiment day, participants wore a Med-Eng Systems® COOL-TUBE suit (Fig.M1, below), which we used to deviate core temperature and deliver thermal stimuli. The suit resembles a set of long undergarments. It has a 200-275 foot network (depending on suit size) of 0.097” Tygon tubing sewn into the inner surface. Heated and cooled water entered the tube suit through 1/8” flow valved coupling connectors. These connect to a manifold on the left side of the suit top



Figure 1. Tube suits in detail.

(indicated by red square above); from that entry point water flowed through the tubing attaching the suit top and bottom and circulated throughout the network of tubes. The single point of entry is a significant detail because the perception of temperature change during each suit perfusion begins at the point of origin in the manifold, and “spreads” over the participant’s skin from that point. This perfusion time lasts approximately 90 seconds. Our participants wore their own undergarments and polypropylene long underwear (top and bottom) underneath the suit to obviate the risk of burns.



*Note: Sections of thin-walled brass tubing. Fluoroptic probes are attached here to monitor the temperature of the water entering and exiting the suit.

Figure 2. Thermal control schematic.

To heat and cool the water, we employed four Gaymar® Medi-Therm II Hyper/Hypothermia systems. The demands of this experiment exceed those of the post-operative use for which these systems were designed. Therefore, we made significant modifications aimed at intensifying the stimuli and increasing the speed of transitions.

Two units were designated to provide hot stimuli and Gaymar engineers increased the set points to 52°C. This modification made it possible to deliver ~47°C water to the tube suit entry point. The remaining two units served as the cold-water supply. Among the modifications made to limit restrictions on flow, the stock output hoses (3/16" ID) were modified to terminate in larger bore (1/4" ID) valved Colder Products Company® plastic coupling connectors.

We boosted the flow rate to compensate for a mismatch in impedance: the pumps in our Gaymar® Medi-Therm systems were not sufficient for the combined impediments of the surface area of tubing and distance between the sources of hot and cold water and tube suit. Using a pair of centrifugal booster pumps we achieved the necessary increase in flow, driving the heated or cooled water through twenty-five foot insulated two-channel hoses (1/4" ID). The addition of booster pumps increased flow rates for the complete circuit from 8 gallons per hour (GPH) (i.e., full system, without booster pumps) to greater than 15 GPH (i.e., full system, with booster pumps).

By necessity, all of this equipment remained outside the Faraday shield; 25-foot hoses connected it to an MR compatible stacking selector valve, which regulated the flow of water to the tube suit. The valve (Fig. 2 above and detail in Figure 3 below) was configured to provide three states of flow: hot water, cold water and no flow. The respective hot and cold circuits had separated send and receive channels. Shunt connections allowed the hot or cold supply circuit to flow uninterruptedly when that respective circuit was not in use. This configuration placed unadulterated hot or cold water immediately at hand: With the valve positioned directly next to the scanner bed, delays between thermal stimuli were kept to a minimum.

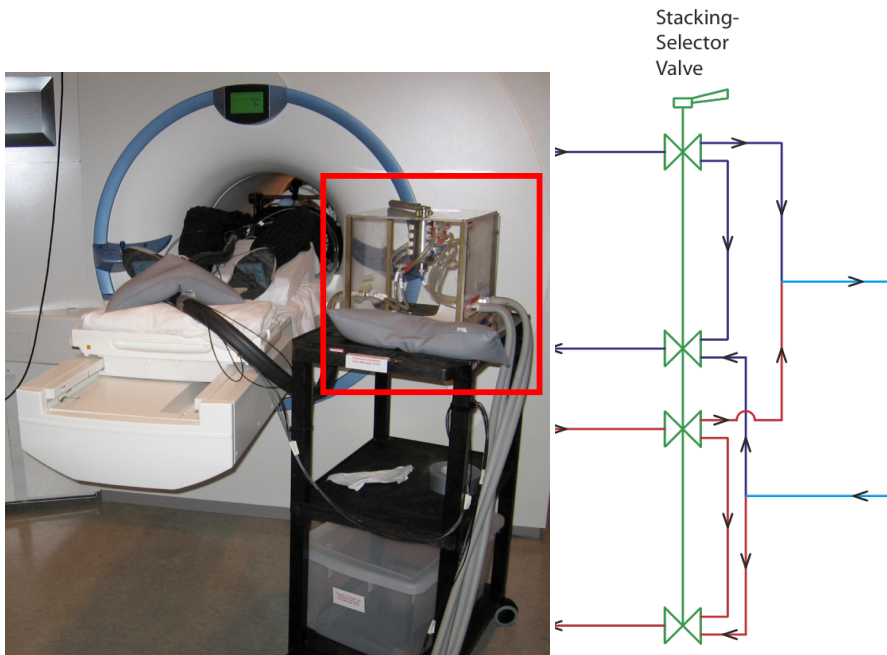


Figure 3. Stacking selector valve in use.

The use of the valve reduced transition time between thermal stimuli to the combined latency of the time from valve output, the flow through an eight-foot hose connecting it to the tube suit, and the perfusion time of the tube suit itself.

The final path for water flowing into and out of the suit was this eight-foot hose, or “umbilicus.” It comprised send and receive channels made of reinforced Tygon tubing, each of which “stepped down” from 12-inches of ¼” ID tubing to the remaining 84 inches of 1/8” ID tubing, as needed to match the tube suit input and output connections. The ends of the umbilicus were fitted with brass connectors, to which we attached fiber optic probes to monitor the temperature of the water flowing into and out from the tube suit, as described in the following.

Temperature and physiological monitoring: We acquired temperature records using an MR compatible Luxtron® m3100 four-channel Biomedical Fluoroptic® Thermometry kit. (This equipment was the used for the first nine participants and later superseded by the new model, the Luxtron/Lumasense® m3300, for the last five scans). Positioned outside the Faraday shield and connected to probes by 25-foot fiber-optic extensions, the thermometry unit's four channels were allocated to monitoring participants' (i.) oral temperatures, (ii.) skin temperatures, and the temperature of water flowing (iii.) into the tube suit ("suit in") and (iv.) out of the tube suit ("suit out").

The details of physiological monitoring were as follows. The oral temperature probe we passed through a modified snorkel mouthpiece; our participants adjusted the depth of the probe and we secured it with tape, to be held in the sublingual pocket throughout the experiment. The skin probe was secured with surgical tape to the skin over the left intercostal muscle. We acquired temperature readings from the four probes once per second and logged them with our data acquisition software running on a laptop computer. The laptop was located in the control room, allowing the investigators to view the temperature readings as they were acquired. Medical staff in the control room (Dr. Plourde and Louise Ulliyatt, RN) monitored participants' oral and skin temperature, and were able to monitor pulse rates, as measured by a pulse oxymetry sensor secured on the index finger of the participant's non-dominant hand.

Stimuli

Thermal stimulus control and presentation: We used a Toshiba Tecra laptop (Operating system: Microsoft Windows XP; processors: Intel® Pentium® 1.86GHz) running Labview® software (versions: 7.4- 8.6) to control stimulus presentation and monitoring functions, and to amass non-fMRI data. The functions of the Labview® software included the following: presentation of cues to the valve operator, presentation of alternating Likert-type visual analog rating scales to the participant, recording and displaying subjective rating responses, and displaying the four fluoroptic temperature readings to the investigators. The Labview® software ran continuously, serving these functions and collecting data prior to and between scans; a synchronization pulse from the scanner triggered the trial sequence routine.

Thermal stimulus presentation: During fMRI scanning, participants experienced alternating sequences of thermal stimulation, applied over a broad area of the skin on the trunk, arms and legs. As dictated by the trial sequence, hot or cold water coursed through the tube suit in alternating blocked trials of 135 seconds (see trial sequence in Figures 4. and 5., pages 27 and 29, respectively) and valve operator check sheets. The valve operator executed the trial sequence, monitoring an LED display as the countdown to each valve state change proceeded. In order to verify the sequence of thermal stimulus conditions, the valve operator and an investigator in the control room checked off each transition on trial sequence documents and confirmed the transition by signaling each other. We also assured the correct stimulus presentation by other means: From the control room, we viewed the cues presented to the valve operator on the LED display, the

position of the selector valve itself, and the temperature of water flowing into and out of the tube suit².

Procedure

Pre-scanning procedures: Orientation, Consent, and Self-Report Questionnaires.

Because of the demanding nature of participation, which necessarily included some thermal discomfort, potential participants received detailed informed consent documents for their review before any screening appointments were scheduled. They were thus able to consider the challenges and responsibilities involved in their commitment to proceed, in their own time, unaffected by the presence of an investigator. Potential participants were not solicited after receiving informed consent documents, but contacted the investigators when they had reviewed the details of participation and decided to proceed with screening. The first step was a visit to the Shizgal laboratory at Concordia University's Loyola Campus for a screening interview and orientation. Once participants had signed the informed consents (Appendix B), and passed a screening with the SCID (First et al., 2002), they completed magnetic resonance screening forms and mood questionnaires. The second step was a cardiac stress test, as described above.

Fitting. Contingent upon having passed the cardiac stress test, a second brief visit to the lab was scheduled for the week of the scanning date; participants were then fitted for long underwear, tube suits, snorkel mouthpiece and stabilizing neck brace. They were oriented to the thermal control equipment and safety procedures and received satisfactory responses to remaining questions regarding the procedures.

² *Nota bene:* In thirty-two scans, one valve state error occurred, albeit before the collection of functional data.

Scanning day: Arrival and orientation. On the scanning day, our participants reviewed the informed consent document a second time and then completed the Profile of Mood States (POMS) (McNair et al., 1992; Coupland et al., 2001; Leyton et al., 2003). These data are not included here. They received subjective rating instructions and practiced providing hedonic and sensory ratings using a laptop that displayed rating scales, later to be displayed throughout the functional scans. If the results of the urine screening were negative, as they were in all cases, the scanning day proceeded.

Head stabilization and scanning preparation. We adopted a preliminary 30-minute fitting session in the scanner; this helped to minimize delays in the set up for scans, assuring that the core temperature deviations were maintained and reducing the passive heating of hyperthermic participants. We used this session to configure the head stabilization, adjust and focus the subjective rating scale display, test the response device and synchronization pulse. By design, this experiment includes a scan under hypothermia and thermal stimulus transitions that may induce head motion, therefore, in addition to the standard head stabilization, our participants wore a padded plastic neck brace of the type used to stabilize patients with whiplash injuries. This brace was loosely fastened to provide a point of reference contact with the jaw, while not contributing to the likelihood of claustrophobic reaction or altering the position of the head. Other supplementary head stabilization included pads pressing lightly on the center of the forehead and zygomatic arches, firmly braced by an armature mounted around the head coil. (The most recent six participants were scanned with a 32-channel head coil, which provides excellent head stabilization with the use of compressed foam pads at 360° contact points. In these later six scans, the armature was not used, but the 30 min fitting was still executed.)

For thirteen of the sixteen participants, this fitting session was their first exposure to the MR environment (i.e., the interior of the scanner, the fit and feeling of the head coil and supplementary stabilization). As such, they had the opportunity to acclimate themselves and ask for adjustments needed for their comfort before the insertion of the mouthpiece made spoken communication impossible. We designed the scanning day to include this limited initial exposure with the aim of reducing participants' anxiety and its potentially confounding effects on hedonic responses. Participants also had ample time to practice using the response device to give subjective ratings during this period.

Experimental sequence: Baseline temperature measurement. Once the preliminary setup and testing were complete, participants and investigators moved from the scanner suite to an ancillary room for the determination of baseline temperature. Relative to this baseline, we set the targets for core temperature deviations. In consideration of diurnal core temperature fluctuation, it is important to note that we conducted all experiments on the same schedule: all baseline temperatures were determined at approximately the same time of morning.

Participants slowly pedaled a bicycle ergometer with no load, while oral temperature was sampled at 3-minute intervals using a digital oral thermometer. (Fiber optic probes were not yet connected to the interface at this stage.) From baseline temperature acquisition throughout the remainder of the experiment, the snorkel mouthpiece remained in the oral cavity; the tip of the digital thermometer and the fiber optic probe passed through ports in the mouthpiece to rest comfortably in the sublingual pocket. The digital thermometer, initially used in place of, and to determine any offset in, fiber optic thermometry, remained in the mouthpiece until the subject entered the scanner

each time (the fiber optic probe is MR compatible and remained in place throughout the scanning day). Sampling of the baseline temperature continued until we recorded stable values for two consecutive sampling periods. Eight tenths to one degree centigrade (+/- 0.8-1.0° C) in each respective direction was the standard core temperature deviation (see Appendix C for an example of individual baseline and target temperatures)³.

Experimental sequence: Hyperthermia induction. In preparation for hyperthermia induction, investigators and medical staff attached a second fiber-optic probe to the skin over the left intercostal muscle for skin temperature monitoring during scans. Participants were assisted into PolarTech 200 fleece jacket and pants, covered by a Tyvek jumpsuit, two layers of gloves (first layer surgical, outer layer thick vulcanized rubber extending to mid-forearm) a fleece neckband, and polypropylene hat. Once the participant was dressed and pedaling, oral temperature sampling at three-minute intervals recommenced.

We induced hyperthermia by circulating hot water (44-48 °C) through the tube suit as the participant pedaled at a self-chosen pace and resistance. When the target oral temperature of +0.8-1.0° C had been reached for two consecutive samples (~6 min.), the team prepared to transfer the participant and thermal control gear to the scanner suite. The duration of the hyperthermia induction process varied individually, but generally required ~25 minutes (See Appendix C for exemplary induction sheet).

Experimental sequence: Transfer to scanner. With the participant now hyperthermic, and with the care and sense of urgency appropriate to that condition, we disconnected the flow of hot water and medical staff assisted them to a prepared seat in the foyer outside the scanner suite. The team proceeded to prepare the participant (i.e.,

³ Note: this range allowed us to moderate the deviation when it appeared that the participant could not tolerate a full degree.

removing digital thermometer, inserting earplugs, checking for symptoms or undue discomfort) and assisted them to the scanner bed. There, the head was again stabilized, response device tested, pulse monitor attached, and display re-aligned as needed.

Magnetic Resonance Imaging. All data were acquired using the 3-Tesla Siemens Magnetom Trio scanner at the McConnell Brain Imaging Center of the MNI. The 19-minute and 17 second functional scanning sequences (see scanner sequence, Figure 4) consisted of either 512 or 542 full brain volume measurements of gradient-echo, echo-planar, T2*-weighted images with blood oxygen level dependent (BOLD) contrast (time to echo (TE) = 30 msec, time to repeat (TR) = 2.25 sec, flip angle = 90°, field of view (FOV) = 256mm). We acquired a full volume of 36 contiguous slices, in interleaved mode (direction: anterior to posterior), every 2.25s. Isotropic functional volume elements (“voxels”) were 4x4x4 mm.

| Phase | Time (sec) | Time (min) | Cumulative Time (min) | # TRs | Cumulative TR | Trial # | Suit temperature (hyperthermia) | Suit temperature (hypothermia) | Label for on-line BOLD |
|---|------------|---|-----------------------|-------|---------------|---------|--|--------------------------------|------------------------|
| AA Scout | 46 | 0.77 | 0.77 | | | | hot | cold | |
| localizer | 15 | 0.25 | 1.02 | | | | hot | cold | |
| TRUFISP | 30 | 0.50 | 1.52 | | | | hot | cold | |
| functional scan | 104 | 1.73 | 3.24 | 46 | 46 | dummy | hot | cold | bad |
| functional scan | 135 | 2.25 | 5.49 | 60 | 106 | 1 | hot | cold | bad |
| functional scan | 135 | 2.25 | 7.74 | 60 | 166 | 2 | cold | hot | good |
| functional scan | 135 | 2.25 | 9.99 | 60 | 226 | 3 | hot | cold | bad |
| functional scan | 135 | 2.25 | 12.24 | 60 | 286 | 4 | cold | hot | good |
| functional scan | 135 | 2.25 | 14.49 | 60 | 346 | 5 | hot | cold | bad |
| functional scan | 135 | 2.25 | 16.74 | 60 | 406 | 6 | cold | hot | good |
| functional scan | 135 | 2.25 | 18.99 | 60 | 466 | 7 | hot | cold | bad |
| functional scan | 135 | 2.25 | 21.24 | 60 | 526 | 8 | cold | hot | good |
| functional scan | 36 | 0.60 | 21.84 | 16 | 542 | dummy | cold | hot | good |
| gre field-mapping scan | 130 | 2.17 | 24.01 | | | | neutral | neutral | |
| anatomical hi-res | 540 | 9.00 | 33.01 | | | | neutral | neutral | |
| last modified: 01/10/09 | | filename: trial_sequence_2p25min_BIC_v14_BD.xls | | | | | | | |
| Neutral = no flow through the tube suit; hot = 52 °C MediTherm set-point; cold = 8 °C MediTherm set-point | | | | | | | This design supports the use phase lags of up to 30 TRs (38, if no lead volumes are dropped) during data analysis. | | |
| TR = | | 2.25 | sec | | | | | | |

Figure 4. Functional magnetic resonance imaging scan trial sequence.

Scanning sequence and experiment design. This experiment requires that we acquire the functional data before the anatomical scan, in order to deliver the thermal stimuli while the participant's core temperature is still deviated from its baseline. Therefore, only three brief scans (lasting ~90 sec.) preceded the acquisition of functional data. To establish neuroanatomical landmarks for use in aligning subsequent scans, we performed an auto align (AA). Following the AA scout were two localizer scans needed to position the field of acquisition. The first was a 15 sec. low-resolution localizer of the coronal, sagittal and axial planes; the second (TruFISP) was a high resolution T2 weighted scan of the sagittal plane only. Because of its improved signal to noise ratio, the TruFISP provides excellent resolution and tissue differentiation, allowing a clear delineation of the corpus collosum. In consultation with the MR technician, we used the TruFISP image to select the 3D volume, with a ventral boundary along the anterior-posterior commissure. The field of view (FOV) was tilted ~30° upward, depending

slightly on the individual's anatomy, and re-evaluated by "stepping through" the sagittal slices to assess coverage. (The investigators gave final approval of the FOV selection.) This technique has been established as an effective means of reducing susceptibility artifacts, caused by the proximity of the orbitofrontal cortex to sinus cavities and mouth, (Gottfried et al., 2002; Deichmann et al., 2003), though it may exacerbate artifacts in areas of lesser interest for our study. It is now widely used (Pessiglione et al., 2008; Lamm et al., 2007; Dillon et al., 2008; Lewis et al., 2007; *inter alia*).

Trial sequence. The trial sequence commenced with the first synchronization pulse from the scanner. As described above, the water circulating through the tube suit was varied in alternating 2.25-minute blocks (135 sec, 60 TRs)(see trial sequence, Fig. M5, below). Understood in terms of hedonic sign or valence, the sequence of trials presented during functional scanning was *identical* in hyperthermia and hypothermia scans. Our participants underwent a sequence starting with a "dummy trial" (46 TRs, 104 sec.) and then a second trial (60 TRs, 135 sec.), both in the hedonically "bad" condition. Thermal stimuli alternated in subsequent trial blocks (See Figure 5., below).

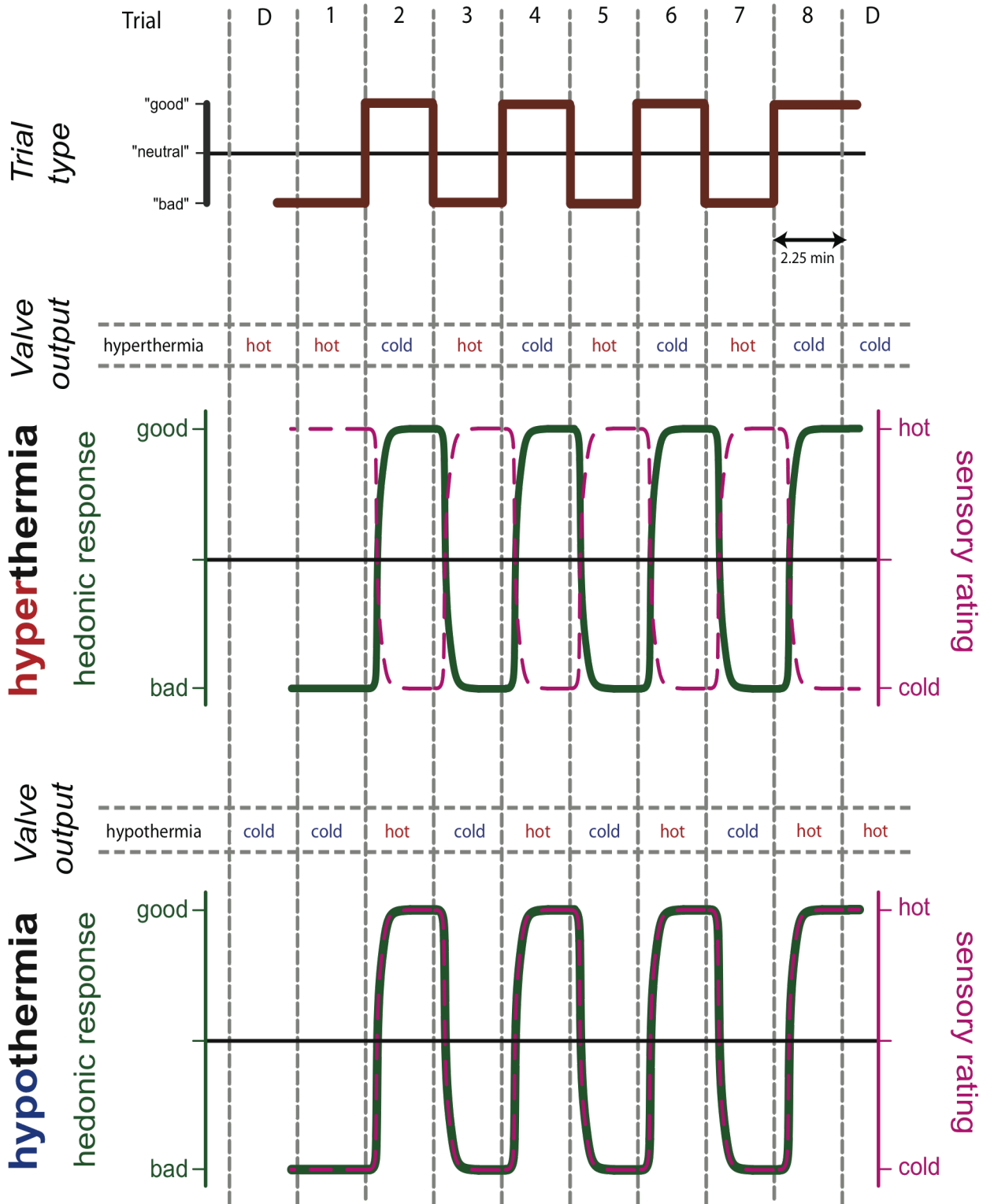


Figure 5. Experiment design schematics.

Hyperthermia and hypothermia sequences consisted of a block of eight experimental trials, preceded and followed by a single dummy trial. The first dummy trial allows for scanner stabilization and subtraction of eight leading volume measurements; the final dummy trial extends the period of data acquisition sufficiently for the investigation of phase lags within the range of hemodynamic response (following 67.5 sec of ratings).

Understood as hedonic stimuli (i.e., in terms of hedonic sign or “valence”), the sequence of ten trials, including dummy trials in parentheses, ran: (BAD), BAD, GOOD, BAD, GOOD, BAD, GOOD, BAD, GOOD, (GOOD) (for hyperthermia sequence, see Figure 6., below).

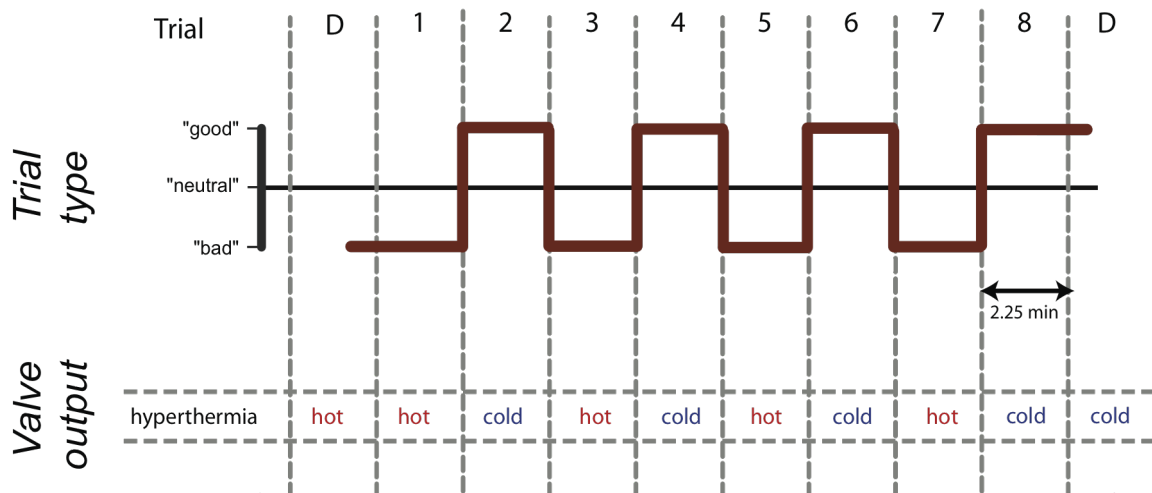


Figure 6. Detail of experiment design schematic: common hedonic response pattern with valve output for hyperthermia scan.

An hedonically bad, or unpleasant trial entailed the delivery of thermal stimulation congruent with the direction of core temperature deviation (i.e., hot water while hyperthermic). Such an experience threatens to worsen the shift away from homeostasis.

A hedonically good trial entailed thermal stimulation incongruent with the deviation (i.e., cool water while hyperthermic). Such an experience promises a return to homeostasis.

Additional scans: Gradient Echo field mapping and anatomical. Acquired following each functional scan were a ~2 min. gradient echo (GRE) field mapping scan, used to correct static (B0) field inhomogeneities, and a 13 min. high-resolution T1-weighted 3D anatomical scan (voxel size: 1×1×1 mm) for anatomical localization of the functional data.

Subjective ratings, hedonic and sensory. Participants were directed to rate their sensory and hedonic experience throughout the functional scans; their hedonic ratings constituted our primary regressors. To assure uniformity of presentation and thereby control some of the potential variability due to misunderstanding of the ratings directions, an investigator read the directions aloud to each participant as they read along with a copy of the text (see Appendix D). This procedure was repeated three times during the scanning day: first during the initial orientation, and once prior to each scan. Participants were asked if they had any questions about the instructions and whether the distinction between rating temperature and rating what we described as “thermal comfort” was clear to them. All concurred and reported having understood the directions when asked during the debriefing session.

Beginning during the Auto align (AA) scout, localizer, and TRUFISP scans (see Fig. M4 above for trial sequence), participants gave alternating hedonic and thermal ratings every 9 seconds. Participants therefore had no less than five minutes (300 sec) of practice prior to the data acquisition during the functional scan. It is relevant to note that in all fourteen cases, additional minutes were added to the period prior to the acquisition

of functional data, either for the positioning and tilting of the field of view, difficulties with software, or problems with the initial synchronization pulse. In effect, this extended the period of rating practice.

Subjective ratings: Visual analog scales. In a mirror mounted to the head coil and secured over the bridge of the nose, participants viewed (the reflection of) two alternating 10-increment visual analog scales (resolution: 1024 X 768). The horizontally oriented rectangular projection was enlarged to fill the maximum width visible from inside the scanner bore (approximately 152 cm X 30 cm). The two scales appeared in alternation for periods of 9 seconds, respectively.

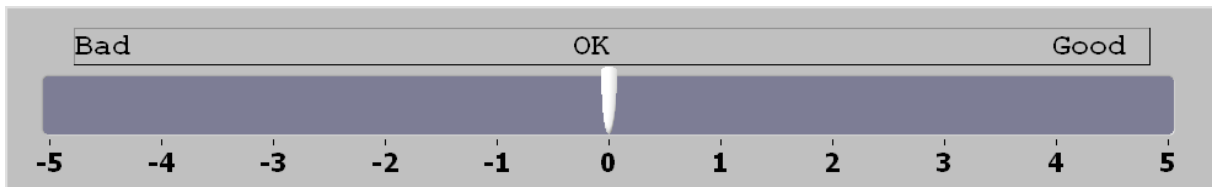


Figure 7. Hedonic ratings scale.

The hedonic rating scale, pictured above in Figure 7., ranged from -5, (labeled above the polar negative digit as “BAD”) to 5 (labeled above the polar positive digit as “GOOD”). The zero point, in the middle of the scale, was labeled “OK”. The sensory scale we differentiated by its labels, range, color of text and color of the cursor. This second scale comprised integers from 0 to 10; zero (0) was labeled “COLD” above the digit, 5 “NEUTRAL” and 10 “HOT”. The respective scales always started at the midpoint, when each new 9-second rating period began.

Participants moved the cursor right or left along the ratings scales by pressing one of two buttons on a fiber-optic response device connected to the experiment laptop. The response device was placed in their dominant hand (all reported being right handed). Participants chose which fingers to use to press the respective buttons, but the response box was always oriented so that the right button moved the cursor to the participants' right and the left to the left. A single button press moved the cursor one increment; it was not possible to move the cursor over multiple increments or in an accelerated fashion by holding down a button.

Subject comfort during anatomical scans. During the (~14 min) anatomical scans that followed the functional scans, the valve operator monitored the ongoing hedonic ratings, using the ratings to determine a comfortable water temperature. For example, having ended the hyperthermia functional scan with the valve in a state of cold water flow and then neutral (in which no water flowed to the suit), participants were instructed by the MR technician to continue their subjective ratings. Whenever their hedonic ratings dipped below neutral, the valve operator changed the state to maintain hedonically positive ratings. Thus, hedonic ratings were used to maintain a comfortable range and steer the participant toward normothermia. During most of the anatomical scans after hyperthermia, the hedonic ratings dictated that the participant receive cold water or no flow through the tube suit.

Experimental sequence: Hypothermia induction. After the completion of the anatomical scan under hyperthermia, the team assisted the participant from the scanner bed and brought them to a prepared seat outside the Faraday shield. Investigators removed the Tyvek suit, fleece garments, hat and gloves. Fiber-optic temperature

recording and measurements from the digital oral thermometer overlapped for no less than six minutes, to establish the offset between the measurements obtained with the two devices. Once insulating garments had been removed and oral temperature offset determined, investigators escorted the participant into an air-conditioned machine room adjoining the scanner (n.b., ambient air temperature $\sim 15^{\circ}\text{C}$). Eleven of the fourteen participants were drenched with sweat following hyperthermia, and the cool air on the exposed wet garments enhanced the hypothermia induction. Once again participants pedaled the bicycle ergometer, this time with no load and at a slow, self-selected pace. The slow pedaling with no load was intended to promote circulation of cooled blood from the periphery without causing significant muscular heat production.

We induced hypothermia (-0.8 to -1°C below baseline) by circulating cold water (8 - 12°C) through the tube suit, as an air-conditioning vent blew directly on the participant's head from above and a fan moved cool air over their face. To accelerate the process, participants could opt to have cold water sprayed on their head and face, a cold, wet towel placed around the neck, and/or hold a pair of ice packs in their hands or armpits. All opted for some combination thereof. In addition to constant monitoring and encouragement by the research team, Dr. Plourde monitored participants at intervals by assessing their degree of shivering and changes in the hue of fingernail beds. When two consecutive (3 min) sampling periods at the target temperature had been achieved, the participant was prepared for transfer back to the scanner.

In the foyer just outside the Faraday shield, the team again prepared the participant (i.e., removing digital thermometer, inserting earplugs, checking for symptoms or undue discomfort). We then assisted MR technicians in adjusting the head

stabilization apparatus, re-attaching the pulse oxymetry probe, and placing the response device in the hand of the participant. In cases of visible shivering, the flow of cold water was suspended during these preparations. The scans described above for the hyperthermia condition were then repeated exactly, with the single exception of an inverted sequence of thermal stimuli (see *Figure 8., below*).

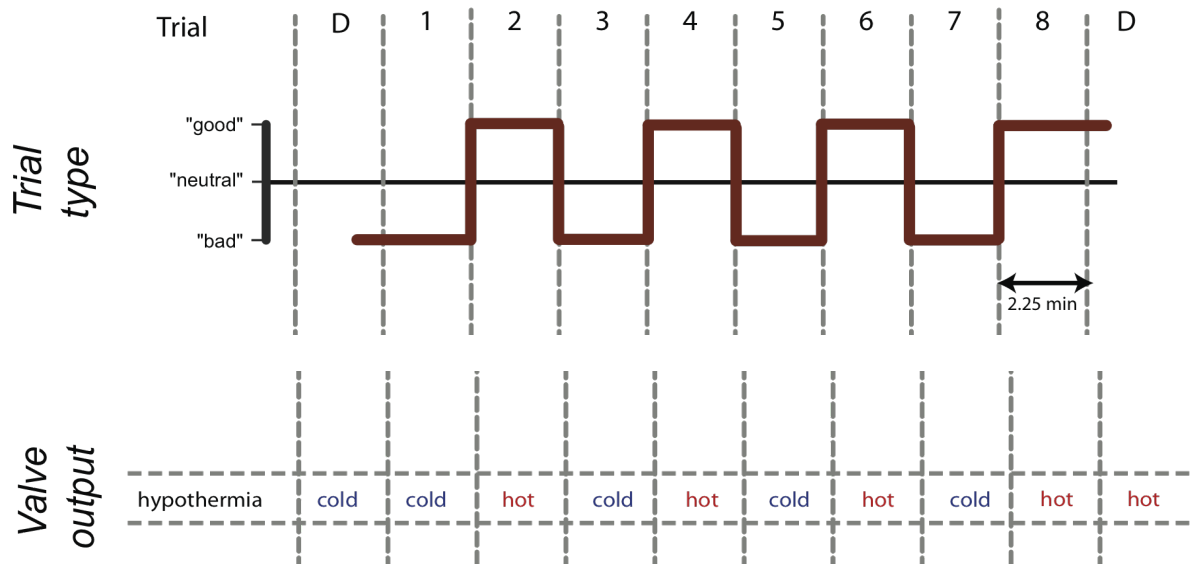


Figure 8. Detail of experiment design schematic: common hedonic response pattern with valve output for hypothermia scan.

Subjective ratings regressors: Our primary hypothesis concerns hedonic signals, those hemodynamic responses that we can associate statistically with the ongoing experience and behavior of the participants. Therefore we started our analysis with an explanatory variable (EV) that modeled ongoing hedonic appraisal. To construct these regressors for each individual scan, we sampled the final hedonic rating of each respective 9-second epoch. Figure 9., below (top panel), is an example; values within blue circles are our selections. The relative stability of the ratings, once the target value is

reached, is evident. Having selected the end of epoch ratings, we then interpolated linearly between the sampled values, using MATLAB, to create a ratings vector for each scan (see Figure 9., bottom panel). Finally, we rescaled the hedonic ratings vectors from 0 to 1, to accord with the scaling of parameter estimates (i.e., β values) in the univariate steps of the individual subject, or “first level” analyses (Smith, 2001; Worsley, 2001, 2003; Smith et al., 2004).

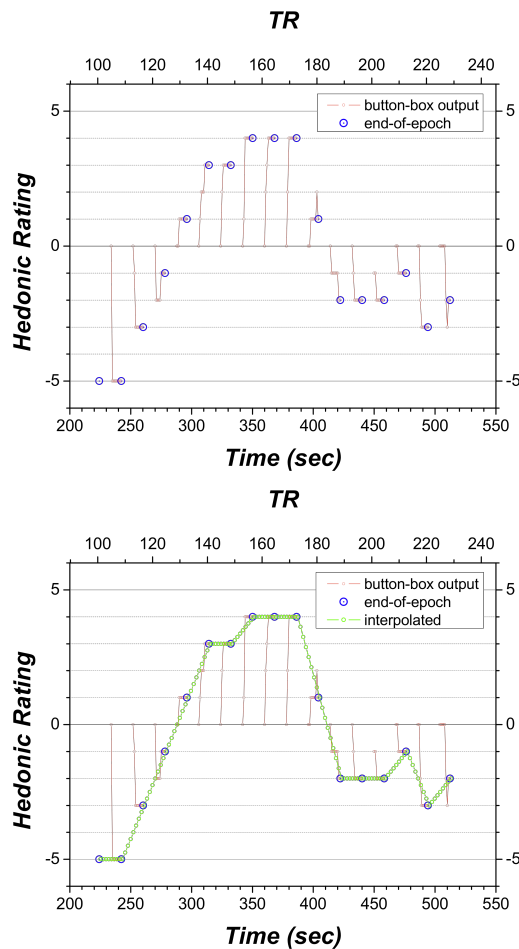


Figure 9. Hedonic ratings sampling and interpolation. Top panel: Selected hedonic ratings values in blue circles. Bottom panel: Interpolation between selected ratings values.

“Normative alliesthesia” regressors: Secondly, we investigated the possibility that the hemodynamic responses we observed could be modeled followed the pattern predicted by the theory of *alliesthesia*, as distinct from participants’ subjective ratings. The normative account of alliesthesia stipulates that sensations predictive of, and promoting a return to homeostasis engage neural circuitry mediating reward; sensations that predict and promote (further) deviation from homeostasis engage neural circuitry mediating aversion. Accordingly, in order to model this phenomenon, we started with the sensations themselves, as rated by our participants: we sampled the sensory ratings exactly as described above. We selected the final sensory rating of each respective 9-second epoch, interpolated linearly between the sampled values to create a ratings vector for each scan and rescaled the vectors from 0 to 1.

The crucial difference between these “normative alliesthesia” predictors and simple sensory predictors is that, in the case of the hyperthermia scans, the ratings vectors are inverted. The necessity of inverting the sensory ratings obtained during hyperthermia scans to model alliesthesia is evident from Figure 5. above and Figure 10., below. Sensory and hedonic responses are distinguished by their inversion during hyperthermia: in hyperthermia scans, a positive hedonic sign is determined (or induced) by negative stimulus temperature.

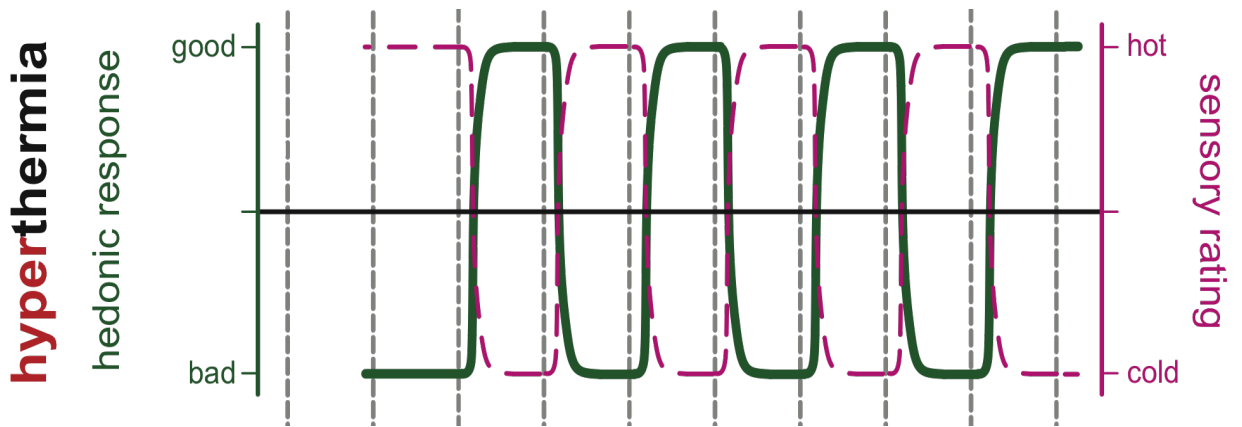


Figure 10. Experiment design schematic: inverted value of sensory and hedonic during hyperthermia scans.

It is critical to note that the “normative alliesthesia” regressors for hypothermia scans were, in fact, the sensory ratings. However, our data analysis approach, to be described in the following section, consisted of identifying significant, conjoined BOLD responses common to *pairs* of group statistical maps. We produced these group maps by analyzing scans from hyperthermia and hypothermia conditions, respectively. Their conjunctions, we argue, are indicative of common signaling, despite opposite sensory characteristics. We did not analyze the hypothermia scans using the normative alliesthesia regressors in isolation and interpret them as evidence of lawful hedonic signaling. Rather, when appropriately grouped and paired, we used these regressors to model putative hedonic response, as predicted by alliesthesia.

FMRI Data Analysis

FMRI data analysis steps: Transfer and Conversion. Upon completion of the scanning day, DICOM files, containing the reconstructed brain images, were transferred to DVD. These files we converted NiFTI format, using mricron (<http://www.sph.sc.edu/comd/rorden/mricro.html>).

FMRI data analysis steps: Pre-processing, extraction, motion correction and registration. We executed all our analysis steps, using FSL, the fMRI Software Library developed at the Center for Functional Magnetic Resonance Imaging of the Brain (FMRIB) (Woolrich et al., 2009; Smith et al., 2004; www.fmrib.ox.ac.uk/fsl). Brain tissue in the functional and anatomical data sets was isolated and extracted from the surrounding tissue and bone with the Brain Extraction Tool (BET2)(Smith, 2002). We transformed each respective pair of anatomical scans (i.e., those acquired after hyperthermia and hypothermia functional scans) from neuroscience to radiological coordinates, and then registered them to the MNI 152 1mm standard space using 12 degrees of freedom (six rigid transformations: 3 rotations, 3 translations; and 6 affine: 3 scales and 3 shears). Gradient echo (GRE) field map scans we rescaled into radians per second, and, as a measure of B0 field non-linearity, later employed in compensating for this defect. This step reduces distortions in the functional images and improves the quality of their registration. Static or B0 (“zero”) magnetic field distortions and motion effects in the functional scans were simultaneously corrected.

We used the McFLIRT tool (Jenkinson et al., 2002), to unwarp, motion correct and linearly register each 3D slice volume or “frame” of the functional scans. In this

procedure a template frame, in native space, is used as a reference. Subsequent frames (i.e., 2-514 or 2-542) were registered to the template using six degrees of freedom (i.e., 3 rotations, 3 translations) and motion corrected.

FMRI data analysis steps: Filtering. The 4D functional data sets we temporally filtered using a high pass filter, to remove low frequency signal far below that of expected hemodynamic responses to the experimental stimuli. Low frequency signal can occur due to mean scanner output change over time, known as “scanner drift” and, notably though less often cited, slow fluctuations in resting arterial carbon dioxide (Wise et al., 2004). For these reasons, the temporal filtering window--the frequency range for retention in the data set and below which signal was eliminated--was set to 1.5 times the target period of our stimulus cycle, as recommended (Smith, 2001; Worsley, 2001). Because one full cycle of stimulus presentation (i.e., a full cycle of one trial of each stimulus type, hot and cold) occurs over 270 sec. (2 X 135 sec trials), we set the filtering window at 405 sec (180 TRs).

In order to increase signal to noise ratios, we applied spatial averaging (sometimes referred to as “smoothing” or “blurring”) using a 5mm Gaussian kernel at full wave, half maximum (FWHM). This replaces respective voxel signal time courses with weighted averages, which include neighbors in a spherical range just beyond the 4mm cubic volume elements in the functional data. This smoothing choice was based on the expectation that potential areas of interest would exceed 5 cubic millimeters; in effect, it reduces the number of statistical comparisons made, and thus the likelihood of family-

wise error. By averaging across contiguous voxels, one yields fewer independent volume elements.

As recommended, we ran the Multivariate Exploratory Linear Optimized Decomposition into Independent Components, or MELODIC, tool (Beckmann and Smith, 2004), and then used the reports to filter out artifacts in the functional data prior to linear modeling. MELODIC is a form of model-free multivariate analysis, in which all voxel time courses, and their interactions, are analyzed together (McKeown et al., 1998; Jenkinson & Beckmann, 2001; Beckmann & Smith, 2002). MELODIC yields spatially differentiated signals, distinct from Gaussian noise, with the maximal likelihood of having distinct sources. On the basis of this automated probabilistic independent component analysis (ICA), each 4D functional data set was decomposed into statistically independent, localized time courses with component maps (Jenkinson & Beckmann, 2001; Beckmann & Smith, 2002). In the MELODIC reports, thresholded component maps were represented axially in 36 slices, rendered on a background anatomical image, with attendant Fourier power spectra transformation graphs.

Our procedure involved manually identifying and filtering out those independent, non-random components most obviously due to gross, well-understood and clearly recognizable noise sources or nuisance factors. The visual signature of “structured noise,” which comprises head motion, dropped slices, spoiled gradients, high frequency noise and inhomogeneities in the B0 field, is well established and documented (see <http://www.fmrib.ox.ac.uk/analysis/research/melodic/>). These visual signatures and attendant time courses are strikingly distinct from hemodynamic responses. FSL provides a MELODIC manual (<http://www.fmrib.ox.ac.uk/analysis/research/melodic/>) with

examples of structured noise, which we used to identify the types artifacts we chose to filter out. Among the examples they offer, we selected only those most clearly factitious types.

Because of their broad spatial distribution and artificially elevated values, such artifacts can make up a significant portion of the overall signal we seek to model. This is evident in the uniform peak signal values visible in the “slice drop” and head motion artifacts. In such cases the signals are independent, massive and inarguably factitious. Their statistical significance in an independent components analysis (ICA) captures their prominence, making them easy to identify and more critical to eliminate (see, for example, Tohka et al., 2008). These filtering steps greatly reduce systematic, non-Gaussian noise in the functional data sets.

We have mapped variance change estimates, per voxel, for each individual functional data set. Notably, as evidence of the independence of noise sources, in the brain regions most susceptible to artifactual, structured noise, such as the outermost rim the neocortex, our filtering reduced variance; while in the areas responsive to our manipulation (e.g., ventromedial prefrontal cortex, orbitofrontal cortex, limbic areas, temporal cortices), this filtering actually increased variance.

Data analysis: Linear modeling of individual data sets. After filtering, the first eight 3D slice volumes or “frames” were discarded, due to gradient instability at the beginning of the functional scan. The remaining signal comprises the “denoised” data set for each functional scan. Using standardized scripts to avoid errors, we conducted first-level univariate analyses of individual whole-brain functional scans using the fMRI

Expert Analysis Tool (FEAT 5.98) for linear modeling. The first stage comprises fMRIB's Improved Linear Modeling, or FILM, a validated Generalized Least Squares (GLS) method (see for example, Woolrich et al., 2001; Smith et al., 2004) for minimizing biased estimations caused by temporal autocorrelation. Using FILM, autocorrelation is estimated locally for each voxel, and normalized, including differential estimations for tissue type. Accounting for autocorrelation is particularly necessary because it is greater in grey matter, where precise sensitivity to activation is most needed. FILM "prewhitening" increases sensitivity by reducing the autocorrelated components of the variance. We used FILM, along with high-pass filtering, spatial averaging, and MELODIC filtering as part of a four-part approach.

The time varying BOLD signals comprising each filtered 3D data set we then regressed against the corresponding truncated and normalized hedonic ratings vector or normative alliesthesia vector. The individual motion parameters and volume mean time course (VMT) from each functional scan we used as confounding variables (i.e., explanatory variables of no interest). Ratings vectors, motion parameters and VMTs were convolved with FSL's canonical gamma hemodynamic response function, and high-pass filtered (sigma=405 sec.) using the same parameters as applied to the data.

Following the GLM as instantiated in FSL (Worsley, 2001), t-values were calculated by dividing parameter estimates (per voxel betas) by the standard error term (standard error of per voxel beta). Mapped t-values were converted to Z-values and rendered at a threshold of $Z \geq 2.3$. In the interests of supplying sufficient information for exact replication (Poldrack et al., 2008) a complete, exemplary set of individual FEAT

commands with sample general linear model matrices are included as an appendix (see Appendix E).

Data analysis: Mixed effects modeling of group data. As part of the FEAT higher-level analysis process, we registered the individual functional scans to the MNI 152 1mm standard space using 12 degrees of freedom (six rigid transformations: 3 rotations, 3 translations; and 6 affine: 3 scales and 3 shears). This registration process involves two stages, using three matrices: First, a registration matrix is generated for transforming each participant's functional data to their anatomical scan. This registration matrix includes 6 degrees of freedom (DOF) (six rigid transformations: 3 rotations, 3 translations). The expectation is that the participant's functional scans will be similar to their anatomical scans, which were acquired immediately following, but this "simpler" 6 DOF registration matrix must then be concatenated with the 12 DOF registration of the respective anatomical scan to the MNI 152 standard space. Finally, the concatenated matrix was applied to the functional data, when the individual statistical maps were submitted to group-level FEAT analyses.

Summary statistics (i.e., betas, covariances and error terms) and supplementary information in the individual-level FEAT directories (i.e., Z-maps, constituent files, registration matrices) were then submitted to cross-subject mixed effects analyses using fMRIB's Local Analysis of Mixed Effects or FLAME, within FEAT (Beckmann, Smith & Jenkinson, 2001; Beckmann 2003, Woolrich, 2004). This tool provides improved group level Z-value estimates by including covariances and heterogeneity from individual-level analyses in the group calculations, along with automatic outlier detection

(Woolrich, 2008). Scans acquired under hyperthermia (n=16) and those acquired under hypothermia (n=16) were grouped together, respectively.

Using mixed effects modeling in FLAME (Woolrich et al., 2003), we first fit a “fast approximation” higher-level model, estimating a group parameter. Voxels at or near the threshold are then submitted to a sophisticated Markov Chain Monte Carlo sampling to which a t-distribution is fit. Finally, these t-maps are converted to Z-maps. To account for multiple comparisons, we used FSL’s cluster-wise correction; Z maps were thresholded using clusters determined by $Z > 2.3$ and a corrected cluster significance threshold of $P < 0.05$ (Worsley, 2001).

In the interest of supplying sufficient information for exact replication (Poldrack et al., 2008) a complete, exemplary set of higher-level group FEAT commands is included as an appendix (see Appendix F).

Conjunction analysis. The present study is concerned with the common hemodynamic responses, across core temperature deviations and stimulus conditions, in the two groups of scans. In this experiment the same hedonic pattern occurs in both scans, while peripheral thermal stimuli are opposite. Our hypothesis dictated that conjoint BOLD signal in group Z-maps from both hyper- and hypothermia instantiate the representation of patterned hedonic responses.

We created a conjunction analysis tool, coded in MATLAB, and applied it to each respective pair of Z-maps. Using this tool, we applied a simple logical “AND” operation to each voxel in a group map. Any voxels that had spatially conjoint values in the group Z-maps were included in a resulting conjunction map; the value of voxels in the resulting conjunction map represents the mean of the conjoint voxel values from the two statistical

maps submitted. Once conjunction maps were completed we scrutinized them as overlays on the MNI 152 1mm brain. Conjunctions and their coordinates were confirmed by simultaneous viewing of the two opaque constituent group Z-maps overlaid. We have adopted the same convention in the Results section. Initial general localization and anatomical labeling was taken from four selected atlases (Harvard-Oxford cortical structure atlas, Harvard-Oxford subcortical structure atlas, MNI structural atlas, and Talairach daemon labels) within FSL's atlas tools. More detailed atlases were then consulted to localize peaks and clusters in confirmed conjunctions (Chiavaras et al., 2001; Petrides et al., 2001; Duvernoy et al., 2009).

Results

Data integrity

We have excluded two scans from this sample. In the first case, delays in the setup prior to the hyperthermia scan combined with the participant's discomfort made it necessary to perfuse the suit with cold water for 3-4 minutes. This decision (to maintain her comfort during a delay of unforeseeable length) caused the loss of core temperature deviation and by definition thermal *alliesthesia* was therefore impossible during the first scan. The graph in Figure 11., left side, below illustrates the oral temperature record for the excluded scan. This participant's baseline temperature was 36.6°; the target temperature for hyperthermia was therefore 37.6°. At the start of the trial sequence, this participant was normothermic: the magenta trace never rose above 36.6 during the scan. (In fact, it is evident in the graph that her oral temperature was actually climbing back to baseline prior to the first trial.) Compare that to a graph from a more typical hyperthermia scan on the right (n.b., data from a woman of comparable body mass), in which the oral temperature remains above target throughout the scan.

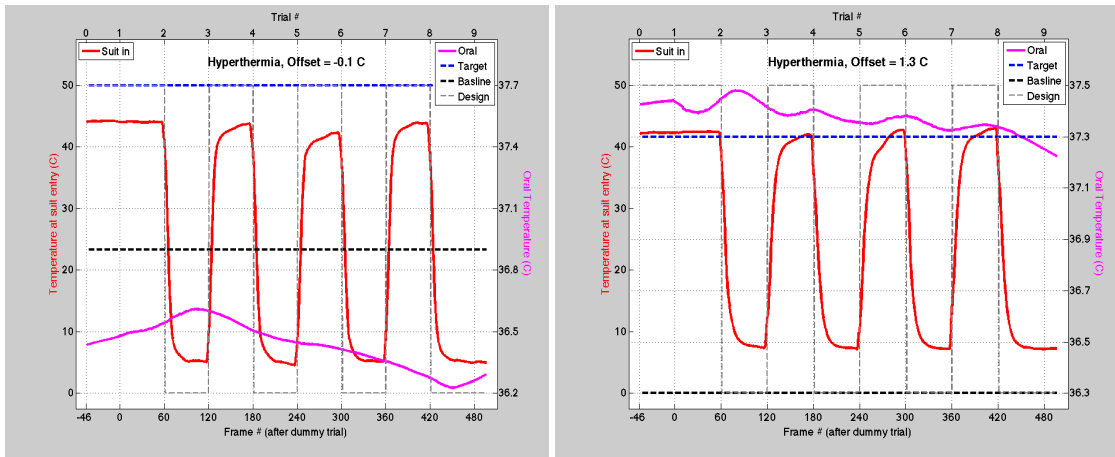


Figure 11. Oral temperature records during hyperthermia scans (left, excluded scan; right, typical scan).

In the second excluded case, head motion during the hypothermia scan exceeded 1mm of absolute displacement, the standard criterion for exclusion based on the capability of motion correction tools in FSL. Furthermore, during this scan there were no less than two instances of pronounced movement. Each instance would have merited exclusion from our sample: In the figure below, it is evident that the initial absolute displacement preceded a spike in absolute displacement (blue trace) just before 350s. This spike alone exceeds 1mm; another just after 450s approaches the exclusion criterion.

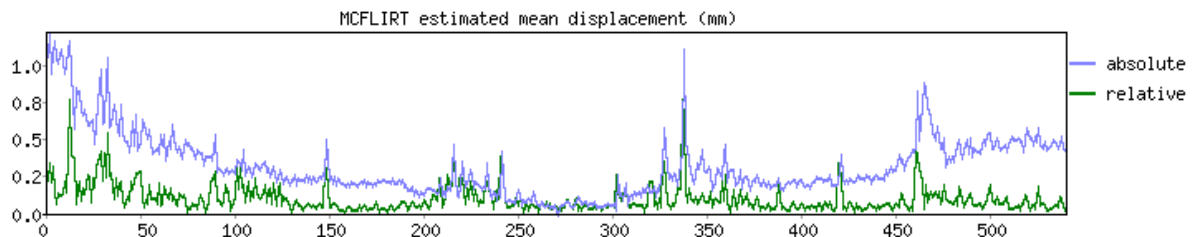


Figure 12. FEAT motion record from excluded scan.

Behavioral Results: Hedonic ratings

Subjective ratings: Concurrent hedonic ratings tracked the sequence of and transitions between trials. The ratings are consistent with the theory of *alliesthesia* in direction, if not always in magnitude and frequency. As hypothesized, participants communicated hedonic appraisals that reflect the relative or adaptive homeostatic value of the stimuli: contrast between deviated core temperature and a peripheral thermal stimulus was rated as pleasant and congruence was rated as unpleasant.

Below are two mosaic images showing the hedonic ratings plotted against the stimulus presentation from all scans. Each cell within the mosaic includes three traces: These are the participant's concurrent hedonic ratings (blue trace), the stimulus (i.e., "suit in" temperature, red trace), and the trial sequence ("design" grey dashed trace in background), respectively. The cells are shown in order of the experiment dates, with gaps for the excluded scans.

Viewed as a group, the hedonic appraisals recorded during hyperthermia scans vary significantly in magnitude and frequency. In contrast, hedonic appraisals follow more closely the stimulus conditions (i.e., the "suit in" trace in red) during hypothermia scans. This issue will be considered in the Limitations section of the Discussion.

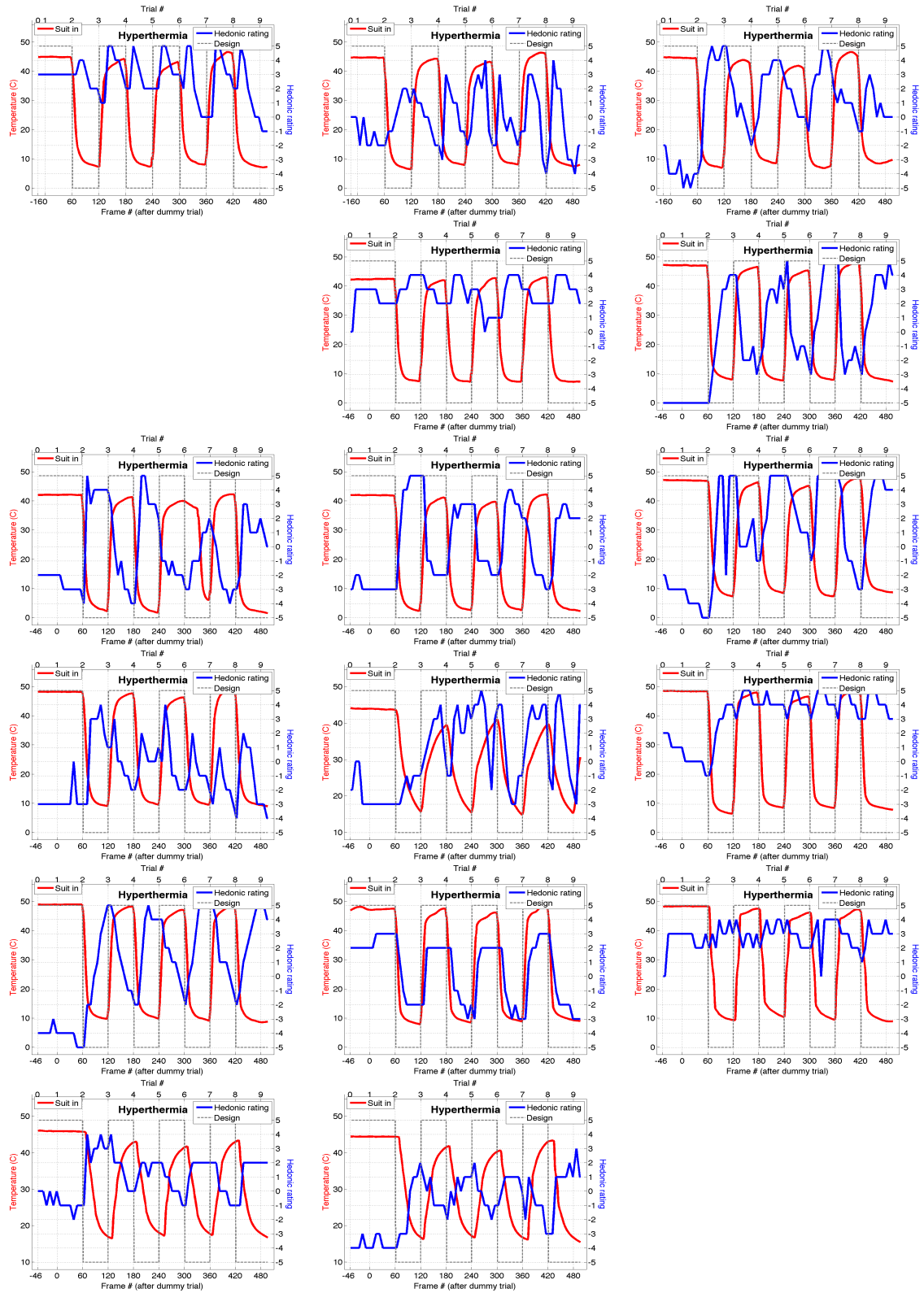


Figure 15. Hedonic ratings mosaic, hyperthermia scans.

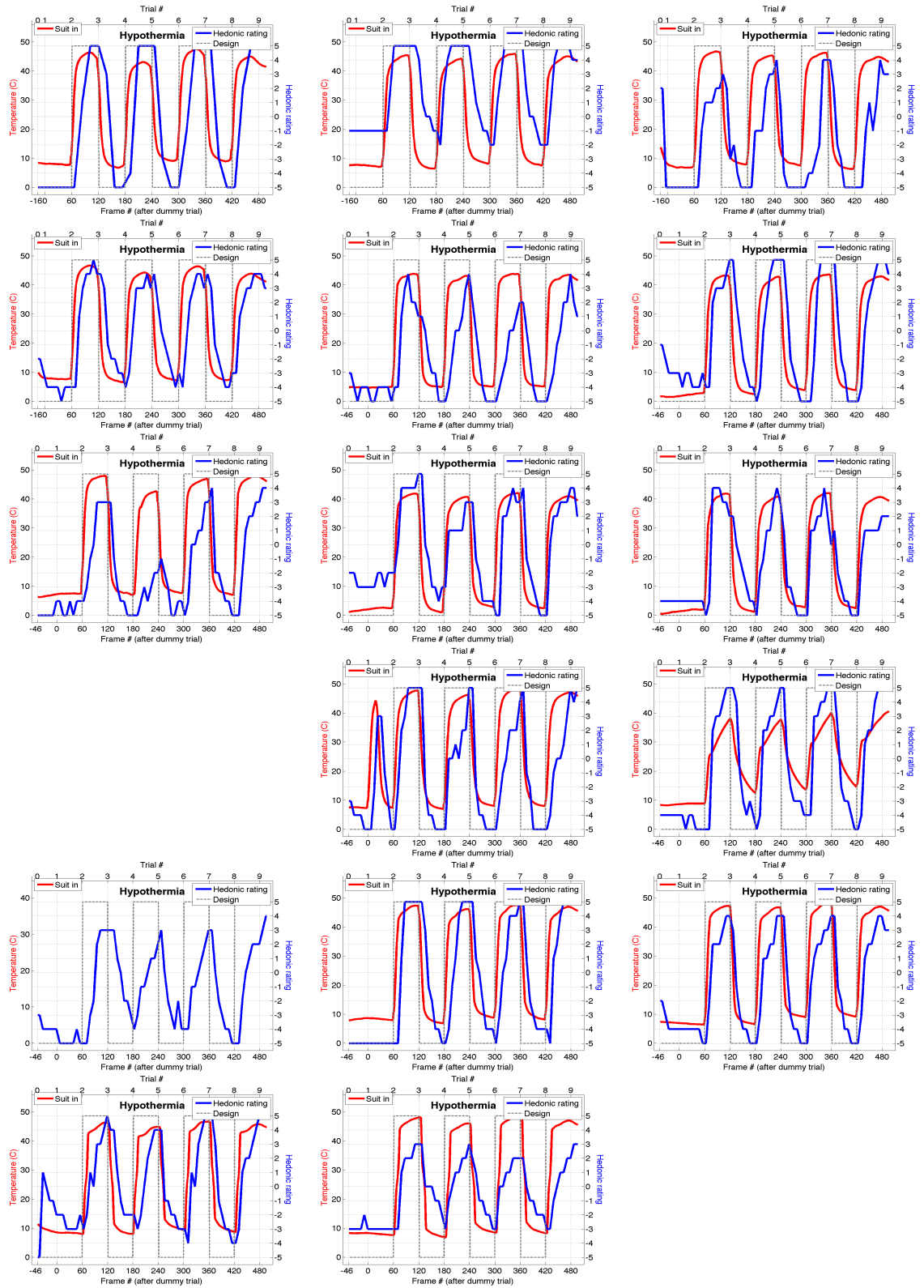


Figure 16. Hedonic ratings mosaic, hypothermia scans

Functional Neuroimaging Results: Hedonic ratings

Individual participant data, hedonic ratings: Concurrent hedonic ratings also tracked the BOLD signal recorded from individual volume elements in individual scans. Furthermore, as predicted, we observed co-localized volume elements in pairs of statistical maps derived from individual participants' respective hyperthermia and hypothermia functional scans. Illustrated by an exemplary case below (Figure 17., 18 and 19.), the raw BOLD signal acquired from co-localized medial prefrontal voxels (red trace) covaries with concurrent hedonic ratings (green trace) and the "full model" (blue trace) of explanatory variables, which includes seven nuisance variables with the concurrent hedonic ratings.

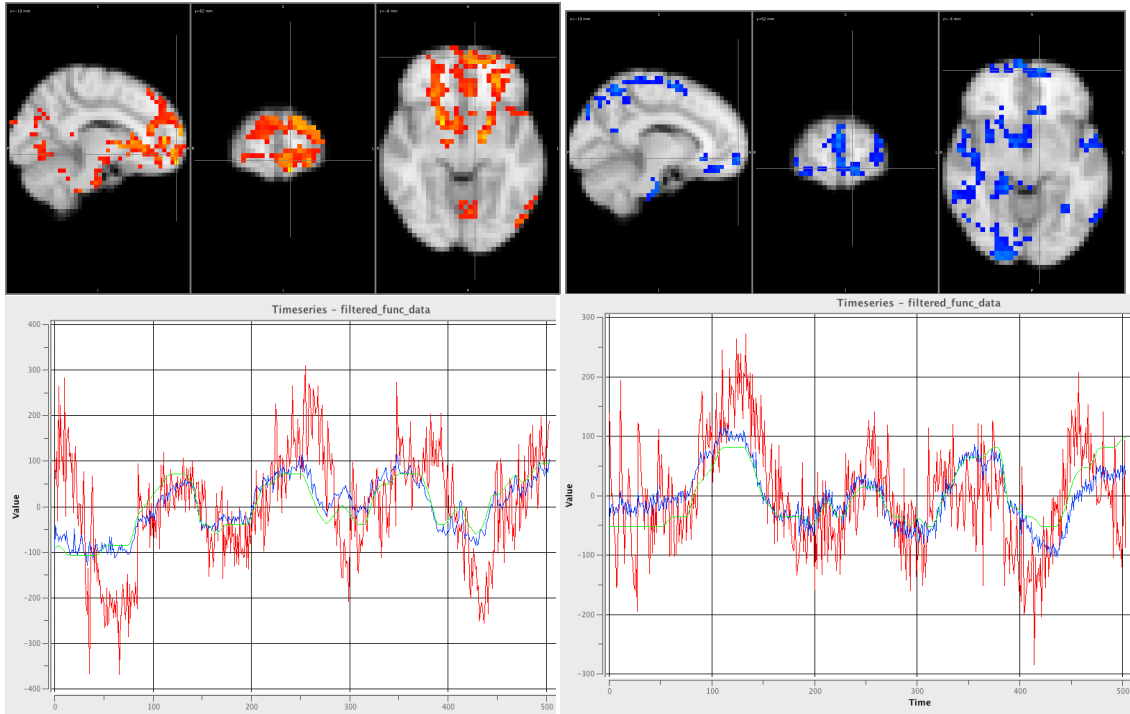


Figure 17. Individual participant z-maps from hyperthermia (top row, left) and hypothermia scans (top row, right) overlaid on MNI152 standard brain (downsampled to 4mm resolution).

Raw BOLD signal timecourses (red traces) are from the voxels shown in crosshairs, plotted against all explanatory variables (“Full Model”, blue traces) and the hedonic ratings vectors (green traces).

Importantly, for each individual volume element we have determined what portion of the variance in the BOLD signal is accounted for by confounding or nuisance explanatory variables (EVs). As described in the Methods section above, these confounding variables include the six motion parameters (i.e., three rotations and three translations) and the whole-brain volume mean time courses. By making this determination, we have isolated, to the best of our ability, the BOLD signal that can be directly compared with our explanatory variables (EVs) of interest. All the statistical maps surveyed in what follows are based on the linear fit between the variance that remains in the BOLD time courses after the partitioning out of nuisance variables and our EVs of interest.

The graphs below (Figures 18. and 19., middle panels) illustrates the final result of this process for an individual participant's conjoined orbitomedial PFC volume element (OMPFC, area 11m, see Kringlebach, 2005, p.693, also reproduced in Discussion), as in Figure 17. above. For the sake of clarity of presentation, the two figures below bring together the individual z-maps (at their native 4mm isotropic resolution), the isolated (i.e., non-confounded) BOLD signal time course plotted against our EV of interest, and the conjoined coordinate shown in the participant's own registered anatomical scan.

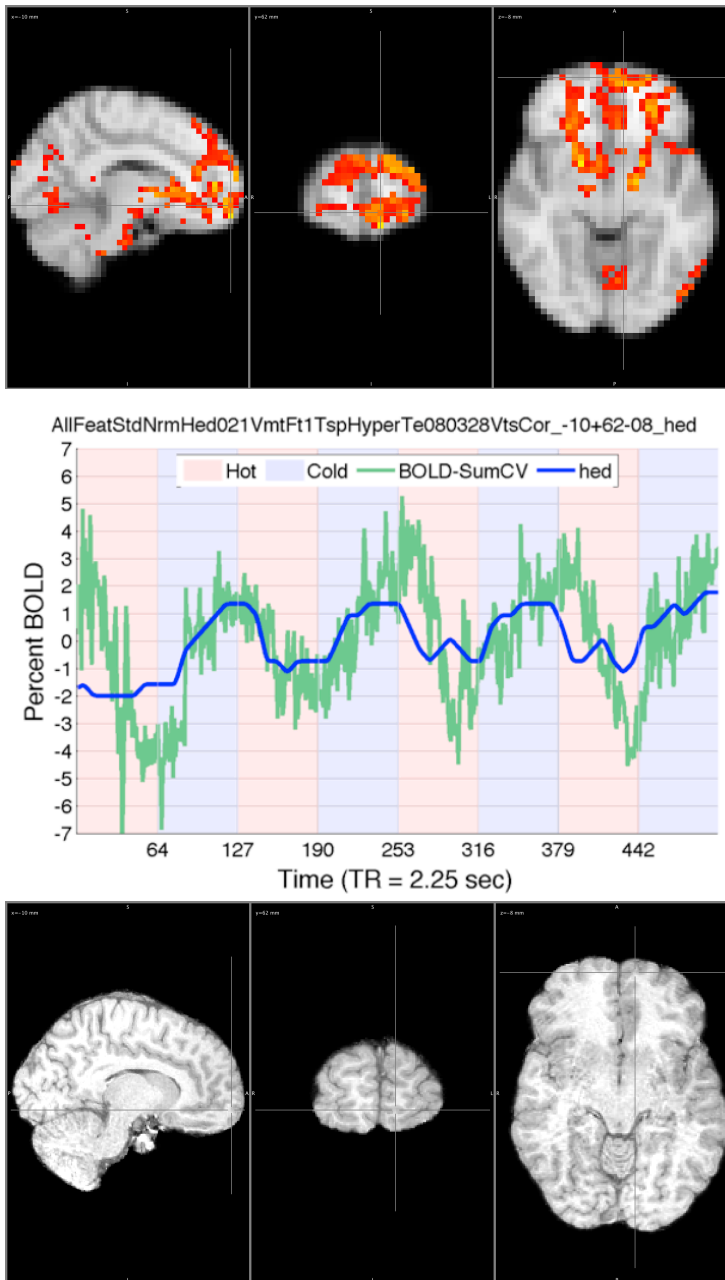


Figure 18. Top: Hyperthermia scan: individual z-map at original 4mm resolution; Middle: BOLD signal time course minus the sum of confounding variables (green trace) plotted against hedonic ratings vector (blue trace); and Bottom: Conjoined coordinate in individual registered anatomical scan at 1mm resolution.

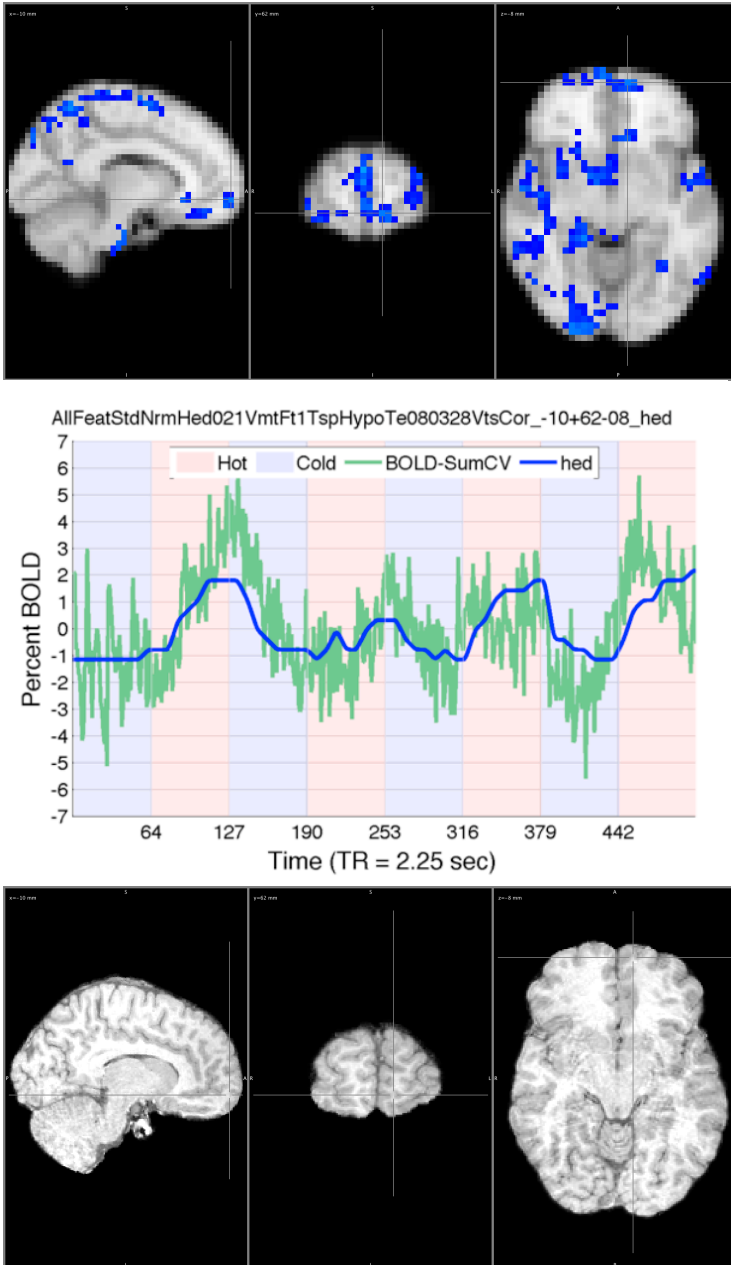


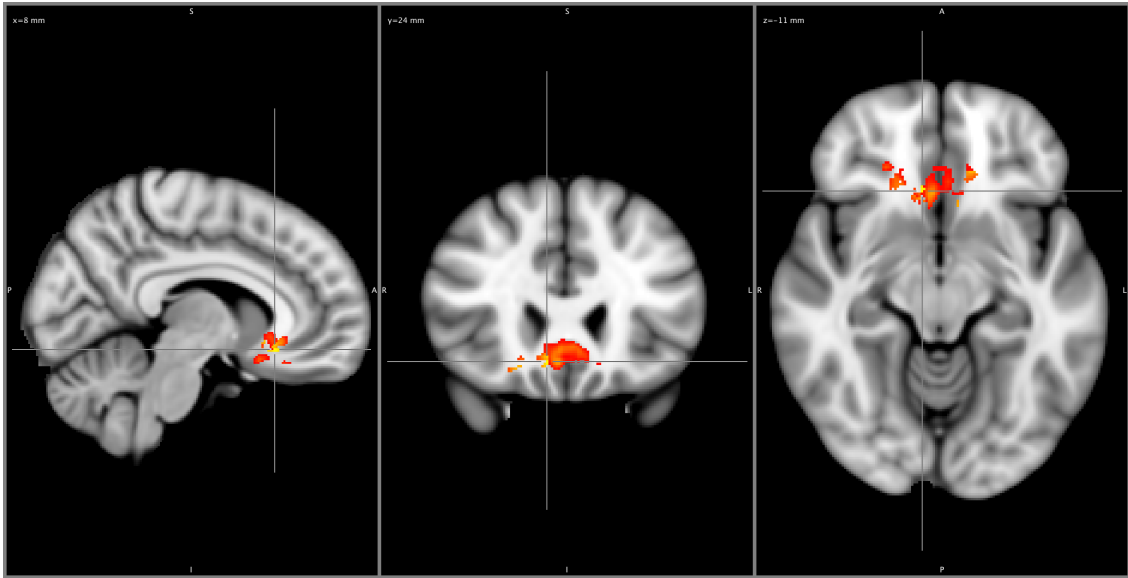
Figure 19. Top: Hypothermia scan: individual z-map at original 4mm resolution; Middle: BOLD time course minus the sum of confounding variables (green trace) plotted against hedonic ratings vector (blue trace); Bottom: conjoined coordinate in individual registered anatomical scan at 1mm resolution.

Group analysis, hedonic ratings explanatory variables (EVs), hyperthermia condition: Below are selected images of local maxima from group Z -maps (i.e., “gaussianized t statistic” maps) comprising 16 hyperthermia scans. Our explanatory variable (EV), in this case, was the concurrent hedonic rating sampled, interpolated and truncated as described above. Peak cluster Z values and coordinates are listed above each figure. The gap in the crosshairs represents 5mm, equal to our smoothing kernel (FWHM). False color scales range from the conventional threshold value of $Z > 2.3$ to the maximum Z value in the respective map. This practice will be maintained in all the statistical maps to follow. Likewise, all statistical maps will be superimposed on the MNI 152 standard brain and corresponding millimeter coordinates used. We will survey the conjoined maxima, in descending order of Z value.

Figures 20., 21., 22. Conjoined local maxima, hedonic ratings group analysis, hyperthermia scans

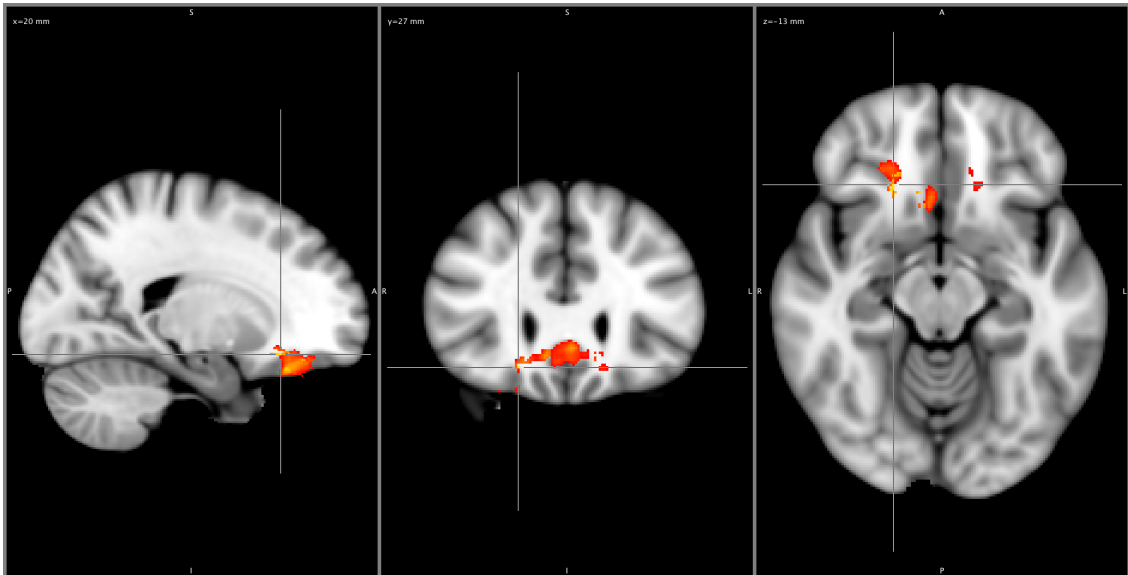
| Z | x | y | z |
|------|---|----|-----|
| 4.24 | 8 | 24 | -11 |

2.3  4.24



| Z | x | y | z |
|------|----|----|-----|
| 4.08 | 20 | 27 | -13 |

2.3  4.08



| | | | |
|------|----|----|-----|
| Z | x | y | z |
| 4.03 | 31 | 33 | -19 |

2.3  4.0

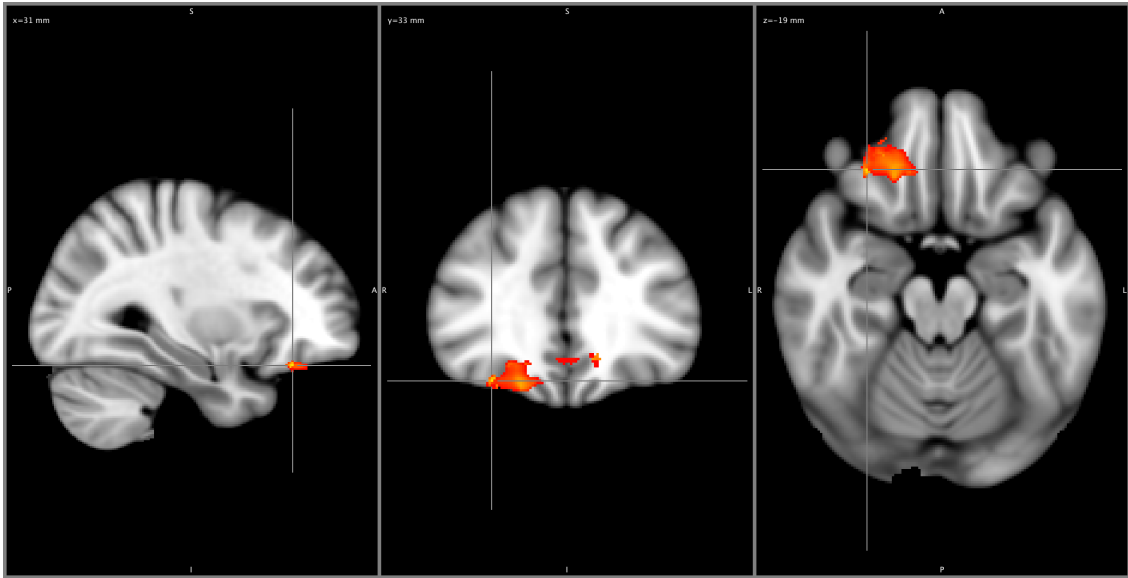


Table 1

Local maxima, hedonic ratings group analysis, hyperthermia scans (MNI coordinates); “CJN” column indicates conjoined or not (0 indicates not conjoined)

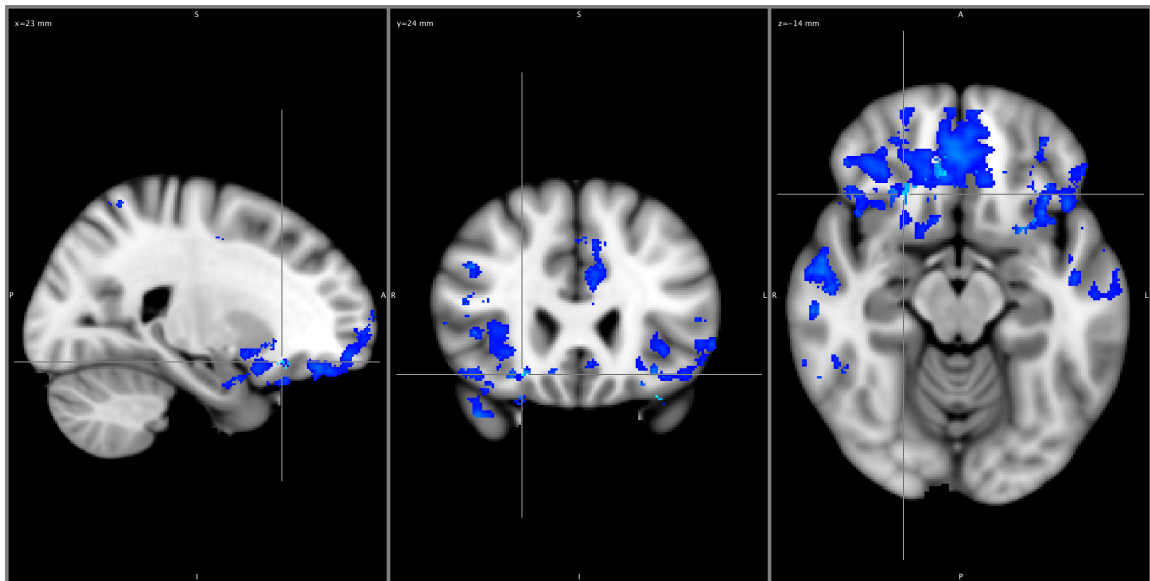
| Z-value | x | y | z | Region | CJN |
|---------|----|----|-----|---------------------|-----|
| 4.24 | 8 | 24 | -11 | Subgenual Cingulate | 0 |
| 4.08 | 20 | 27 | -13 | OFC dorsal | 1 |
| 4.03 | 31 | 33 | -19 | OFC Right lateral | 1 |
| 3.96 | 20 | 30 | -20 | OFC Right lateral | 0 |
| 3.96 | 8 | 21 | -12 | Subgenual Cingulate | 0 |

Group analysis, hedonic ratings regressors, hypothermia condition: Below are selected images of local maxima from group Z -maps comprising 16 hypothermia scans. Our explanatory variable was the concurrent hedonic ratings sampled and interpolated as described above. Peak cluster Z values and coordinates are listed above each figure. The gap in the crosshairs represents 5mm, equal to our smoothing kernel (FWHM). False color scales range from the threshold value of $Z > 2.3$ to the maximum Z value in the respective map. We will survey conjoined maxima in descending order of Z value.

Figures 23. and 24. Conjoined local maxima, hedonic ratings group analysis, hypothermia scans

| Z | x | y | z |
|------|----|----|-----|
| 4.96 | 23 | 24 | -14 |

2.3  4.96



| Z | x | y | z |
|------|----|----|-----|
| 4.87 | 18 | 30 | -16 |

2.3  4.87

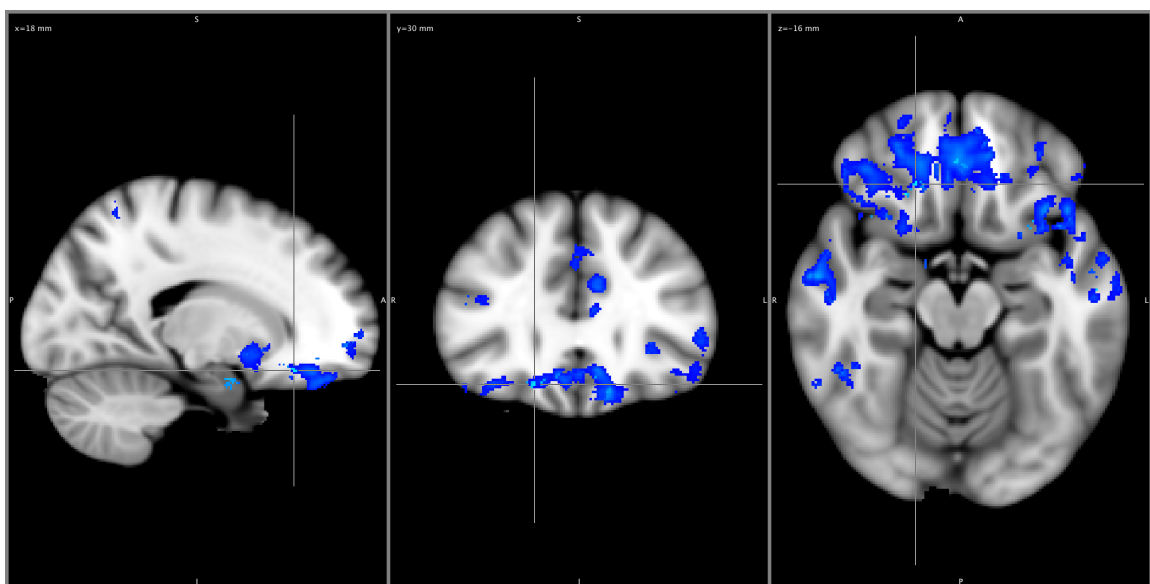


Table 2

Local maxima in cluster order, hedonic ratings regressors, hypothermia condition (MNI coordinates); “CJN” column indicates conjoined or not (0 indicates not conjoined)

| Z | x | y | z | Region | CJN |
|------|-----|-----|-----|-------------------------------------|-----|
| 5.04 | -32 | 24 | -23 | OFC L | 0 |
| 4.96 | 23 | 24 | -14 | OFC R | 1 |
| 4.87 | 18 | 30 | -16 | OFC R | 1 |
| 4.87 | 22 | 26 | -16 | OFC R | 0 |
| 4.67 | 20 | 32 | -18 | OFC R | 0 |
| 5.14 | 1 | -50 | 66 | intrahemispheric: Precuneus | 0 |
| 5.07 | -2 | -74 | 50 | intrahemispheric: Precuneus | 0 |
| 4.89 | 1 | -50 | 60 | intrahemispheric: Precuneus | 0 |
| 4.85 | 5 | -51 | 70 | precun/PC gyrus | 0 |
| 4.74 | 1 | -48 | 61 | intrahemispheric: Precuneus | 0 |
| 4.73 | -8 | -49 | 70 | Postcentral Gyrus L | 0 |
| 4.62 | -51 | -28 | 51 | Postcentral Gyrus L/ Brodmann 40 | 0 |
| 4.59 | -47 | -29 | 48 | Postcentral Gyrus L/ Brodmann 40 | 0 |
| 3.98 | -45 | -26 | 52 | Postcentral Gyrus L/ Brodmann 40 | 0 |
| 3.82 | -55 | -18 | 41 | Postcentral Gyrus L | 0 |
| 3.82 | -31 | -41 | 45 | L parietal sulcus | 0 |
| 3.78 | -33 | -40 | 46 | L parietal sulcus | 0 |
| 4.95 | -13 | -22 | 36 | Posterior Cingulate | 0 |
| 4.74 | -13 | -25 | 38 | Posterior Cingulate | 0 |
| 4.74 | -13 | -24 | 36 | Posterior Cingulate | 0 |
| 4.04 | 5 | 8 | 27 | Vent-Anterior Cingulate/Brodmann 24 | 0 |
| 4.04 | 4 | -33 | 32 | Posterior Cingulate | 0 |
| 3.93 | -9 | -18 | 37 | Posterior Cingulate | 0 |

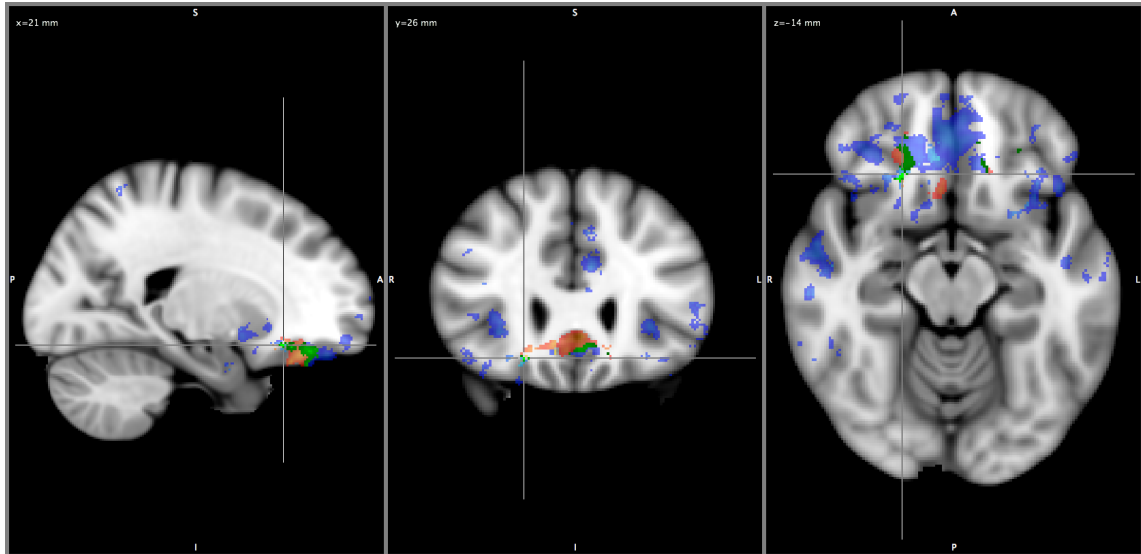
Conjoined areas in group statistical maps for hedonic ratings regressors: We have observed that BOLD signal in a number of brain areas covaries with hedonic ratings. In order to identify common regional hemodynamic response in groups of scans acquired under different conditions, we applied a logical conjunction to the two group maps surveyed above. Any volume elements above threshold value in both maps appear in the resulting conjunction map (with their mean voxel value). In the figures below, conjoined volume elements appear in green on a scale of $Z > 2.3$ to the highest value in the map; for clarity of presentation, the constituent group maps (i.e., from hyperthermia and hypothermia conditions) appear opaque behind the resulting conjunctions.

BOLD signal covaries with concurrent hedonic ratings in a cortical network comprising the ventromedial prefrontal cortex (vmPFC), bilateral orbitofrontal cortices (OFC), bilateral temporal poles, bilateral superior and inferior temporal gyri and subgenual cingulate gyri. Critically, the localized correlation of hemodynamic responses with hedonic ratings is common to scans acquired under opposite core temperature deviations and with opposite sequences of thermal stimulation. This was precisely the objective. Our observations support the hypothesis that common processes occur during conscious hedonic appraisals of thermal *alliesthesia*.

Figures 25. and 26. Maximum values in the conjunction map, hedonic ratings EV.

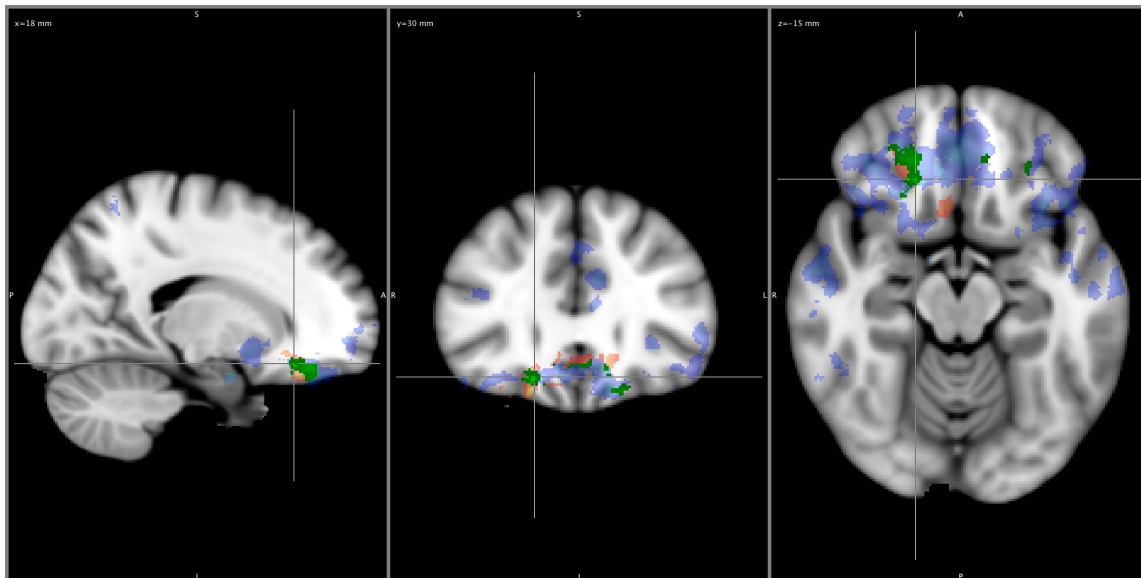
| Mean Z | x | y | z |
|--------|----|----|-----|
| 4.11 | 21 | 26 | -14 |

2.3  4.11



| Mean Z | x | y | z |
|--------|----|----|-----|
| 3.74 | 18 | 30 | -15 |

2.3  3.74



Group analysis, normative alliesthesia EVs, hyperthermia condition: Below are selected images of local maxima from group Z -maps comprising 16 hyperthermia scans. Our explanatory variable (EV), in this case, was the model of normative *alliesthesia* response derived from each participant's sensory ratings, sampled and interpolated as described above. The reader will recall that the normative *alliesthesia* regressors are the sensory ratings from hypothermia scans (i.e., in which the putative hedonic condition was in phase with peripheral thermosensation) and the inverted sensory ratings from hyperthermia scans (i.e., in which the putative hedonic condition was out of phase peripheral thermosensation).

Peak cluster Z values and coordinates are listed above each figure. As in the foregoing sections, the gap in the crosshairs represents 5mm, equal to our smoothing kernel (FWHM). False color scales range from the conventional threshold value of $Z > 2.3$ to the maximum Z value in the respective map. In each sub-section, we survey conjoined maxima in descending order of Z value.

Figure 27. Conjoined local maximum, normative alliesthesia group analysis, hyperthermia scans.

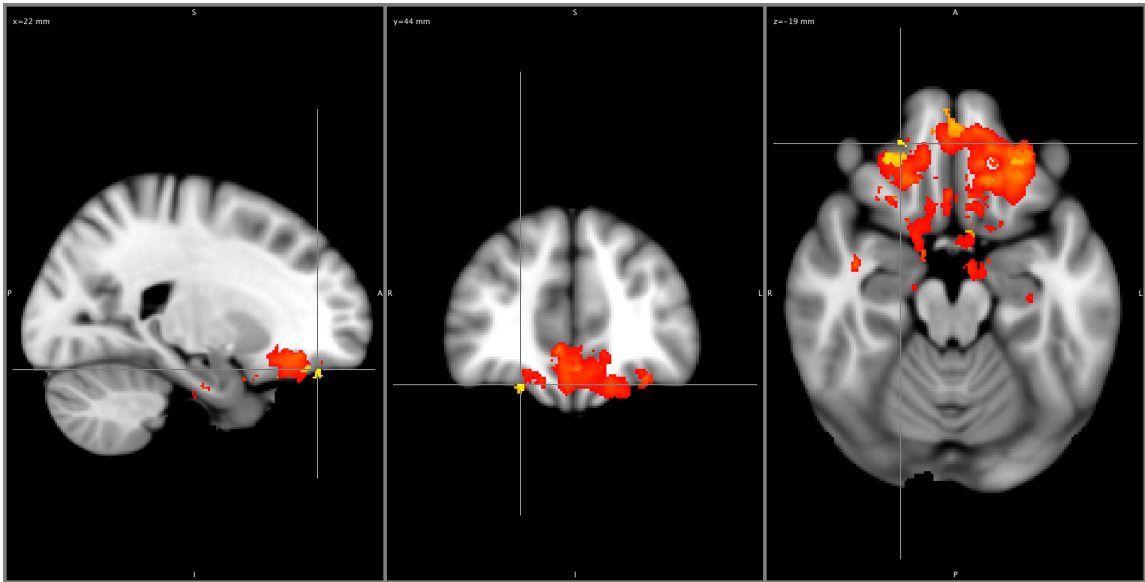


Table 3

Local maxima in cluster order, normative alliesthesia group analysis, hyperthermia scans (MNI coordinates); “CJN” column indicates conjoined or not (0 indicates not conjoined)

| Z | x | y | z | | CJN |
|------|----|----|-----|--|-----|
| 5.48 | 22 | 44 | -19 | Frontal pole/OFC | 1 |
| 5.26 | 28 | 35 | -21 | Frontal pole/OFC/Brodmann 11 | 0 |
| 5.24 | 41 | 4 | -42 | Temporal pole/inferior Temp gyrus/Brodmann21 | 0 |
| 5.24 | 39 | 10 | -40 | Temporal pole/inferior Temp gyrus/Brodmann21 | 1 |
| 5.21 | 44 | 6 | -44 | Temp Pole | 0 |
| 5.19 | 43 | 8 | -40 | Temp pole | 0 |
| 5.16 | 44 | 8 | -42 | Temp Pole | 0 |

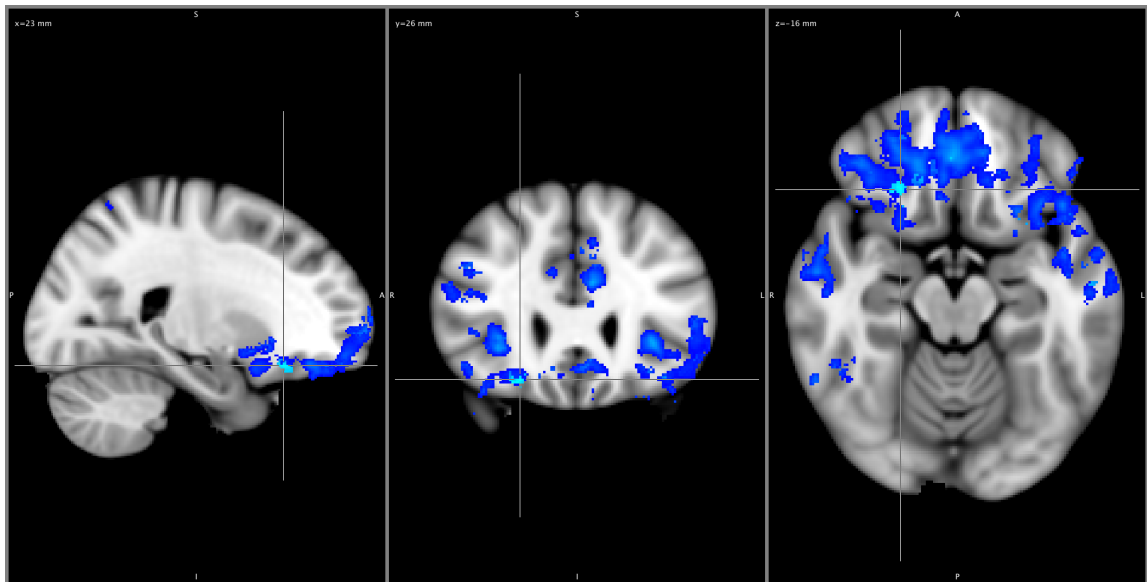
Group analysis, normative alliesthesia EVs, hypothermia condition: Below are selected images of local maxima from group Z -maps comprising 16 hypothermia scans. Our explanatory variable was the model of normative *alliesthesia* response derived from each participant's sensory ratings, sampled and interpolated as described above. Because the normative *alliesthesia* regressors are the sensory ratings recorded during hypothermia scans, the Z -map is widely distributed and the majority of the local maxima are not conjoined. Indeed, this is an elementary demonstration that distinct networks represent peripheral thermosensation. Only a subset of these hemodynamic responses, which occurred in the OFC, is hedonically relevant.

As in the foregoing, peak cluster Z values and coordinates are listed above each figure. The gap in the crosshairs represents 5mm, equal to our smoothing kernel (FWHM). False color scales range from the threshold value of $Z > 2.3$ to the maximum Z value in the respective map. We survey the few conjoined maxima in descending order of Z value.

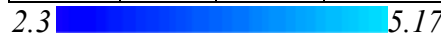
Figures 28., 29., and 30. Conjoined local maxima, normative alliesthesia group analysis, hypothermia scans.

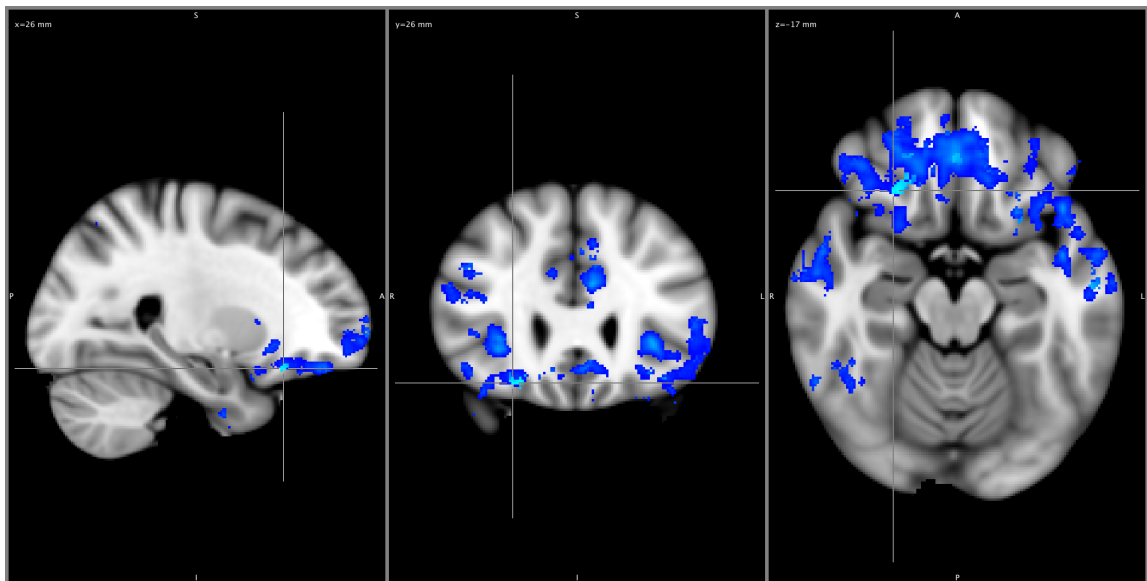
| Z | X | y | z |
|------|----|----|-----|
| 5.20 | 23 | 26 | -16 |

2.3  5.2



| Z | x | y | z |
|------|----|----|-----|
| 5.17 | 26 | 26 | -17 |

2.3  5.17



| Z | x | y | z |
|------|----|----|-----|
| 4.91 | 24 | 28 | -19 |

2.3  4.91

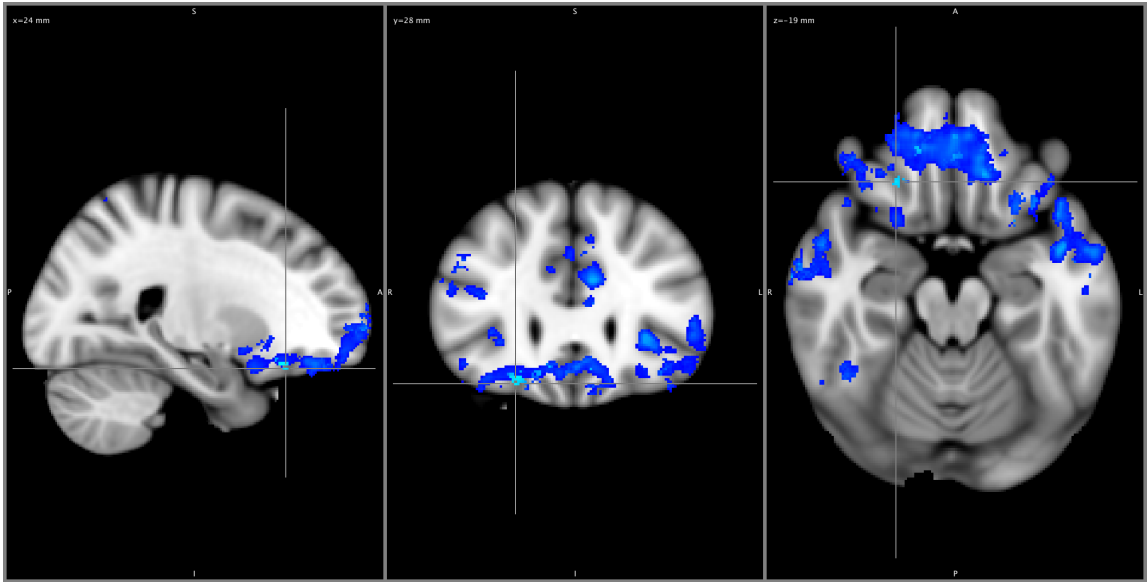


Table 4

Local maxima in cluster order, normative alliesthesia EVs, hypothermia condition (MNI coordinates); “CJN” column indicates conjoined or not (0 indicates not conjoined)

| Z | x | y | z | | CJN |
|----------|----------|----------|----------|-------------|------------|
| 5.2 | 23 | 26 | -16 | OFC | 1 |
| 5.17 | 26 | 26 | -17 | OFC | 1 |
| 4.92 | -33 | 22 | -4 | OFC | 0 |
| 4.91 | 24 | 28 | -19 | OFC | 1 |
| 4.8 | 32 | 14 | 4 | insula | 0 |
| 4.8 | 19 | 30 | -17 | OFC | 1 |
| 4.79 | 46 | -21 | 45 | PS GYR | 0 |
| 4.66 | 48 | -22 | 44 | same | 0 |
| 4.61 | 42 | -32 | 49 | PS GYR | 0 |
| 4.58 | 51 | -21 | 39 | PS GYR | 0 |
| 4.41 | 50 | -19 | 47 | same | 0 |
| 4.26 | 62 | -25 | -9 | post_temp | 0 |
| 5.19 | 0 | -49 | 61 | precuneus | 0 |
| 5.13 | -2 | -74 | 50 | mask: prec. | 0 |
| 4.88 | 5 | -52 | 70 | mask: prec. | 0 |
| 4.81 | -8 | -49 | 70 | precuneus | 0 |
| 4.8 | -13 | -21 | 36 | Cingulate | 0 |
| 4.77 | -13 | -25 | 38 | same | 0 |
| 4.79 | -51 | -28 | 51 | precun L | 0 |
| 4.63 | -47 | -30 | 48 | same | 0 |
| 4.61 | -47 | -38 | 51 | same | 0 |
| 4.61 | -45 | -28 | 49 | same | 0 |
| 4.31 | -46 | -25 | 51 | same | 0 |
| 3.82 | -33 | -40 | 46 | PS GYR | 0 |
| 4.14 | -59 | -38 | 7 | mid-temp | 0 |
| 3.98 | -68 | -38 | 2 | same | 0 |
| 3.9 | -51 | -46 | 7 | mid-temp | 0 |
| 3.7 | -50 | -21 | -3 | same | 0 |
| 3.6 | -50 | -20 | -6 | same | 0 |
| 3.57 | -52 | -27 | 1 | same | 0 |

Conjoined areas in group statistical maps for normative alliesthesia regressors:

BOLD signal in a broadly distributed group of brain areas covaries with our individually derived normative models of *alliesthesia*. As with the hedonic ratings conjunction, in order to identify common regional hemodynamic response in groups of scans acquired under different conditions, we applied a logical conjunction to the two group maps surveyed immediately above. Any volume elements above threshold value in both maps appear in the resulting conjunction map (with their mean voxel value). In the figures that follow, conjoined volume elements appear in green on a scale of $Z > 2.3$ to the highest value in the map; for clarity of presentation, the constituent group maps from hyperthermia and hypothermia scans appear opaque behind the resulting conjunctions.

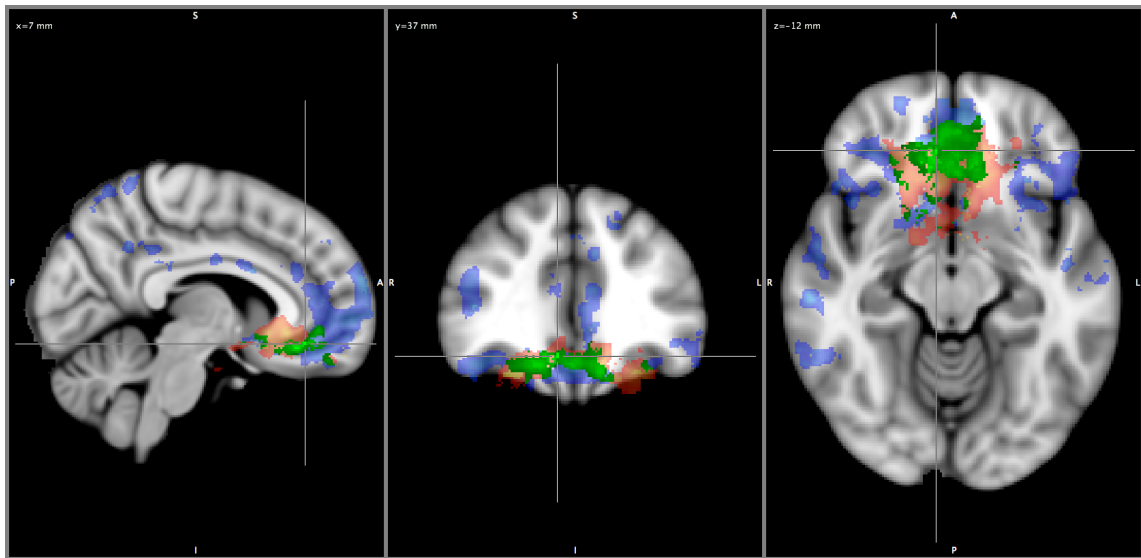
BOLD signal covaries with normative alliesthesia regressors in a dense cortical area covering the ventromedial prefrontal cortex (vmPFC), bilateral orbitofrontal cortices (OFC), bilateral temporal poles, bilateral superior and inferior temporal gyri and subgenual cingulate gyri. The conjoined area extends caudally to paralimbic areas including the head of the caudate nucleus and putamen.

Critically, the localized correlation of hemodynamic responses with normative alliesthesia models is common to scans acquired under opposite core temperature deviations and with opposite sequences of thermal stimulation. By design, this was precisely the objective. Our observations support the hypothesis that common processes can be extracted from whole brain functional scans using explanatory variables constructed from individual sensory ratings to model putative hedonic conditions, i.e., normative thermal alliesthesia.

Figures 31., 32., 33., 34. Maximum values in the normative alliesthesia conjunction map

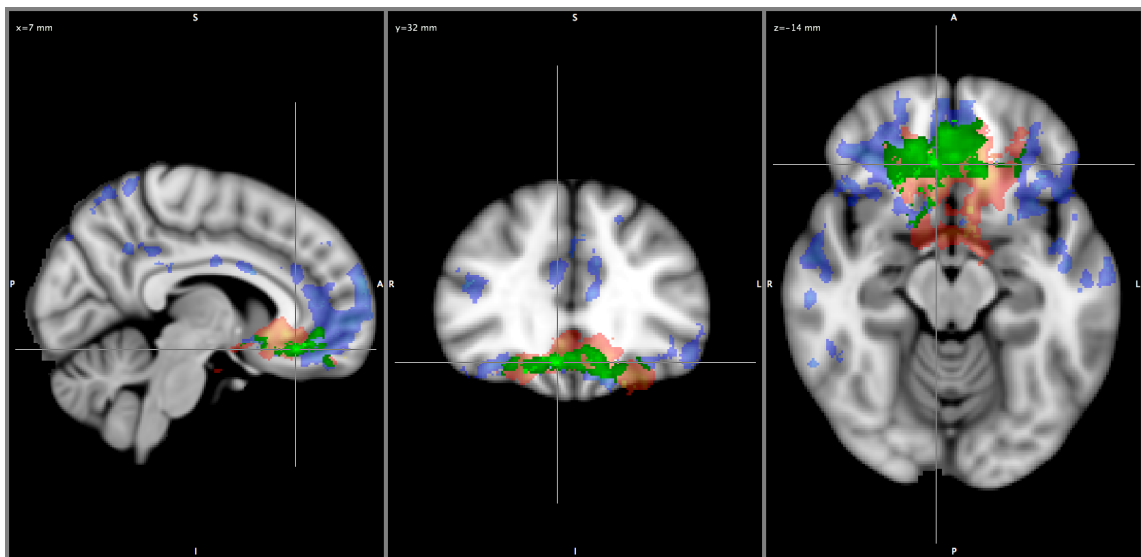
| Z | x | y | z |
|------|---|----|-----|
| 4.24 | 7 | 37 | -12 |

2.3  4.24



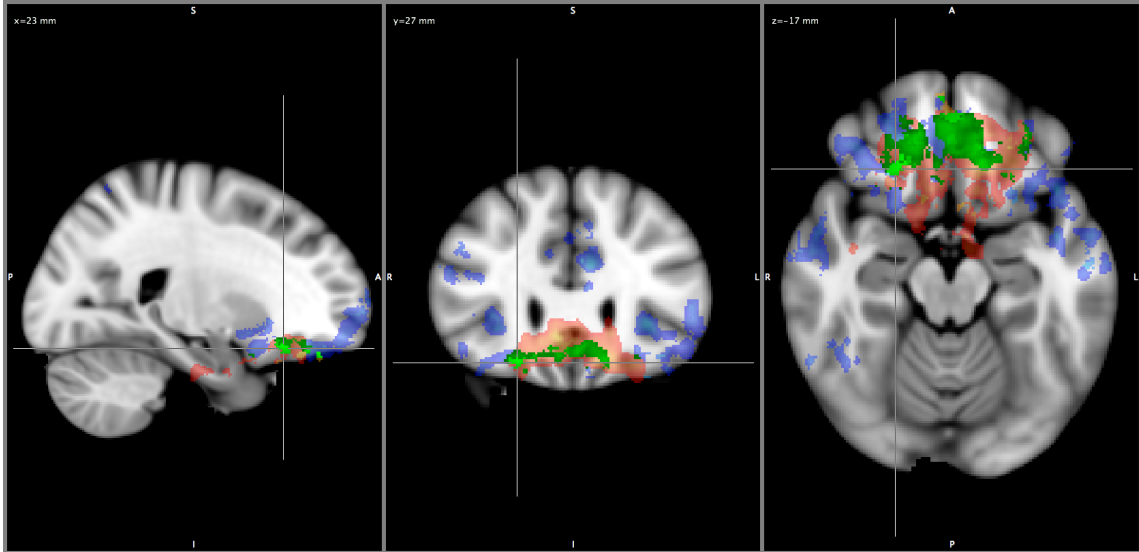
| Z | x | y | z |
|------|---|----|-----|
| 4.23 | 7 | 32 | -14 |

2.3  4.24



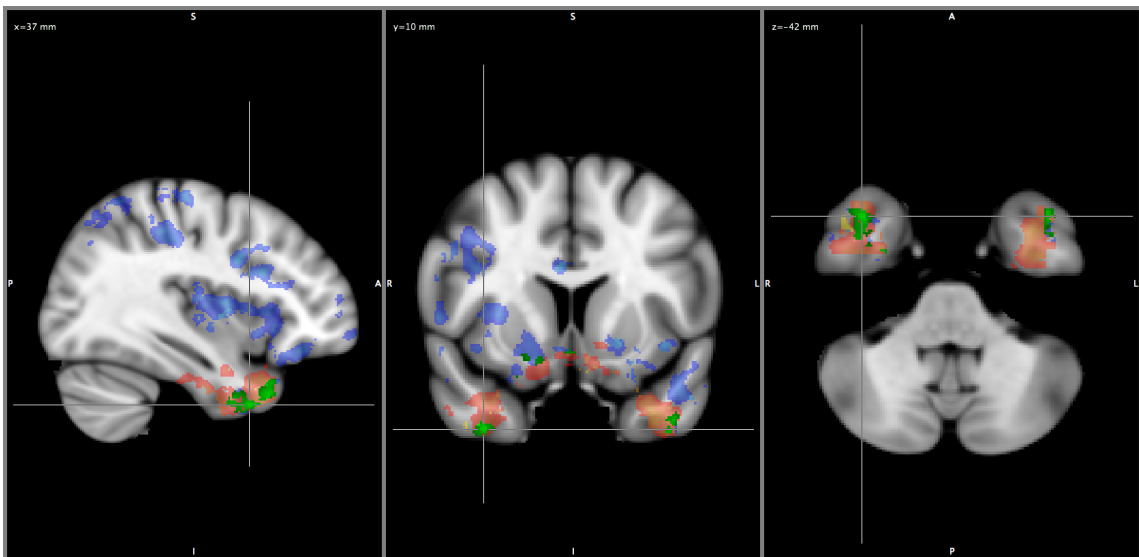
| Z | x | y | z |
|------|----|----|-----|
| 3.97 | 23 | 27 | -17 |

2.3  4.24



| Z | x | y | z |
|------|----|-----|-----|
| 3.58 | 37 | -10 | -42 |

2.3  4.24



Unique area in the hedonic conjunction map: In order to identify common regional hemodynamic response in groups of scans acquired under different conditions, we applied a logical conjunction. In the resulting conjunction maps, it is clear that the spatial extent and z-values of the conjoined normative alliesthesia map exceed those of the conjoined hedonic ratings map. In order to clarify whether the hedonic conjunction analysis has simply yielded a subset of the normative conjunction analysis we compared the two conjunction maps, masking the shared areas. The following figure shows an area of the hedonic conjunction map that is not shared with the normative conjunction,

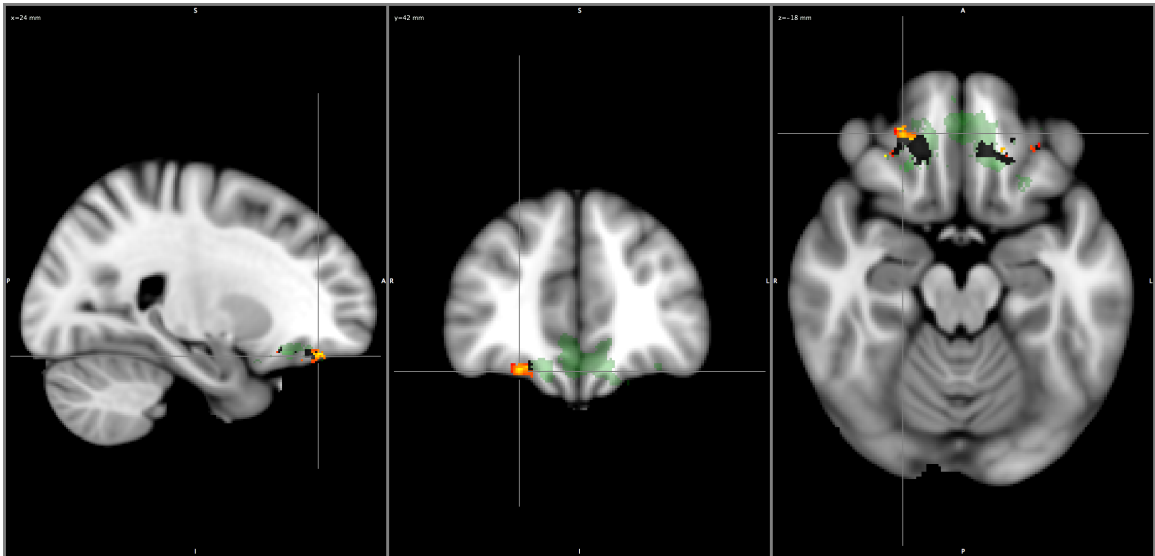
In a neuroanatomically important subregion of the orbitofrontal cortex, namely the right medial orbital sulcus⁴ (and possibly middle frontal gyrus), the hedonic analysis has yielded a distinct area of spatial conjunction. The conjoined volume elements appear in red to yellow on a scale of $Z > 2.3$ to the highest value in the map (i.e., $Z=4.11$). For clarity of presentation, the normative alliesthesia conjunction map appears opaque in green, and the area shared by the normative and hedonic conjunction maps appears in black. Critically, the localized correlation of hemodynamic responses with the hedonic ratings is common to scans acquired under opposite core temperature deviations and with opposite sequences of thermal stimulation. Our observations support the hypothesis that common hedonic processes have a unique neural representation in the right OFC.

⁴ For comparison see Chiavaras et al., 2001, Figure 8B., page 485.

Figure 35. Unique area in hedonic conjunction map: right medial orbital sulcus.

| Z | x | y | z |
|------|----|----|-----|
| 3.58 | 24 | 42 | -18 |

2.3  4.11



Discussion

Thermal alliesthesia as a means to distinguish hedonic from sensory processes

The primary aim of the present study was to distinguish and map the hemodynamic correlates of hedonic valuation using functional magnetic resonance imaging (fMRI). We pursued this aim by twice deviating core temperature and applying opposite alternating sequences of thermal stimuli to the skin over the course of two fMRI scans. Deviations of core temperature in opposite directions, combined with opposite sequences of thermal stimuli, were used to induce a common sequence of hedonic experiences in two fMRI scans. Importantly, core temperature deviations modulated the hedonic value of peripheral thermal stimuli without affecting the perception of temperature. Consequently, we were able to distinguish spatially conjoint correlates of an *a priori*, normative model of hedonic response, and correlates of hedonic ratings, from those of thermosensation. Our results show that cortical areas in the OMPFC, inclusive of the subgenual cingulate gyrus and superior-anterior temporal and paralimbic subregions, encode the hedonic value of thermal stimuli during alliesthesia.

The hedonic quality of experience is defined in dimensional models of human emotion (e.g., Russell, 1980; Russell, 2003; Posner, Russell and Peterson, 2005; Posner et al., 2009) as the phenomenal or subjective pleasantness or unpleasantness. In order to communicate or record hedonic experience, we can quantify it as a value on a continuum from pleasure to displeasure⁵. Precisely how we might characterize the hedonic quality of

⁵ The empirical origins of dimensional models of affect are relevant to our experiment because these models were derived from analyses of reported emotions (e.g., Russell, 1980). As such, their dimensions are representative of conscious experiences and the

experience in terms of states and processes of the central nervous system is a foundational question for affective neuroscience and for this study. We begin that characterization deductively, from the premise that cardinal features of hedonic experience make it distinguishable from sensory perception.

First and foremost, changes in the conditions of the internal milieu sufficient to determine the hedonic value of primary rewards and punishments do not alter the sign of sensory perception. Modulation by the magnitude of shifts in core temperature applied in this experiment is a property of hedonic responses, but not of sensory perception. We manipulated the determinants of the hedonic value of peripheral thermal stimuli by deviating core temperature. Consequently, the “external stimulus (was) perceived either as pleasant or unpleasant depending upon signals coming from inside the body” (Cabanac, 1971, p. 17).

Using this method, we were able to modulate hedonic value in both directions (i.e., changed the hedonic sign of stimuli from positive to negative and *vice versa*) without degrading other information processing. Thermally opposite stimuli induced common hedonic responses when core temperature was deviated in opposite directions. A striking example of this can be seen in one exemplary case above. Figures 17., 18. and 19. (pages 56 and following) show an individual participant’s conjoined anterior OFC voxels, corresponding BOLD signal time courses, and their close relation to hedonic ratings. What others have observed of selective satiety is also true of thermal *alliesthesia*. It is “a particularly useful phenomenon for studying affective representation in the brain, as it provides a means of altering the affective value of a stimulus without modifying its

language used to communicate them, but not necessarily of the neural circuitry or processes.

physical attributes” (Kringelbach et al., 2003, p.1064).

It was possible to manipulate thermal *alliesthesia* in the magnetic resonance environment and to acquire concurrent behavioral and physiological data during fMRI scans, as we have shown. Moreover, our behavioral evidence indicates that opposite sequences of peripheral thermal stimuli delivered during opposite core temperature deviations induce a common pattern of hedonic valuation. Thus, we have altered the hedonic value of the stimuli without modifying their physical attributes. We developed the methodology of inducing a common sequence of hedonic experiences in pairs of functional scans to surmount the challenge of disambiguating the neural representation of hedonic value from sensory information processing. Similarly, the design of complementary fMRI experiments has facilitated the isolation of hedonic processing from other affective and cognitive processes (e.g., Anderson et al., 2003, Small et al., 2003; Grimm et al., 2006; Anders et al., 2004; Lewis, Critchley, Rotshtein and Dolan, 2007; Nielen et al., 2009; Heinzl et al., 2005).

Distinguishing features of the present study

Our approach is unique. The application of a conjunction analysis predicated on thermal *alliesthesia* is a novel contribution to the experimental literature on reward processing and emotion experience. Employing concurrent hedonic ratings as explanatory variables (EVs) is a means of mapping and quantifying an objective physiological correlate of subjective emotional experience. This approach complements studies in which hedonic ratings were sampled after stimulus presentation (e.g., Rolls, Grabenhorst & Parris, 2009; Grimm et al., 2006; Phan et al., 2004).

The use of broadly distributed peripheral thermal stimuli for the induction of intense affective states of both positive and negative hedonic sign is another notable attribute of our study. We have seen evidence that spatial summation affects the hedonic valuation of thermal stimuli. Specifically, proportional increases in temperature or area yield equal changes in hedonic ratings (Marks & Gonzalez, 1974). Thus, our method of stimulus delivery complements prior studies in which non-noxious, focal thermal stimuli were applied to the hand (Rolls & Grabenhorst, 2009, McAllen et al., 2006).

The use of prolonged trials (2.25 minutes per condition) complements prior functional neuroimaging studies in that we acquired data during sustained emotional responses (for the temporal dynamics of sustained emotions, see Verduyn et al., 2009; Ekman & Davidson, 1995; Davidson, 1998; Eaton & Funder, 2001; Hemenover, 2003; for a current view on short timescales of affective responses measured by fMRI see Waugh, Hamilton & Gotlib, 2010). Furthermore, longer stimulus duration reduces the temporal mismatch between neuronal activity (i.e., local field potentials) and BOLD signal changes (Logothetis et al., 2001; Shmuel, personal communication). The delay in hemodynamic response is rendered less significant on this timescale.

The delivery of primary rewards and punishers⁶, such as thermal stimuli, has several merits. The equation of hedonic value with biological utility is only valid for naturally occurring primary rewards and punishers.⁷ The present study is among a small

⁶ Following Rolls (1999, 2000), we define a reward as anything for which an organism will work and a punishment as anything which an organism will work to avoid (or terminate or delay). Using these definitions, peripheral thermal stimulation in the present experiment is a potent, unlearned (i.e., primary) reward or punishment.

⁷ Indeed, the divergence of hedonic value and biological utility could serve as a definition of aberrance. (For example, in the case of refined drugs of abuse hedonic value is highly

group that have involved the delivery of naturally occurring primary rewards and punishers during fMRI and which were designed to isolate hedonic processing (see Anderson et al., 2003, Small et al., 2003; Kringelbach et al., 2003). This class of primary reward stimuli exerts potent effects without necessitating cognitive elaborations or higher order associations, an attribute that Anderson and Sobel term “acute emotional primacy” (2003, p. 581). As such, thermal stimuli, like tactile, olfactory and taste stimuli, are prototypical emotion inducers (see also Rolls, Grabenhorst & Parris, 2009). The regulatory function of hedonic responses to these stimuli accounts for their primacy. Moreover, the fact that the hedonic value of naturally occurring primary rewards and punishers is determined as part of well understood regulatory systems is a feature advantageous to the experimenter. For secondary or abstract rewards and punishers (e.g., images of social scenes, money, faces) hedonic value is dependant upon learning histories and higher order associations that may be unavailable for measurement or manipulation.

Behavioral evidence of altered hedonic response

In Figures 15 and 16 above (pages 53 and 54, respectively) we present behavioral evidence, in the form of hedonic ratings, that our participants did indeed experience intense affective states of both positive and negative hedonic sign. Critically, core temperature deviations modulated hedonic responses to peripheral thermal stimuli in all participants. Moreover, the observed modulation of hedonic responses extends to complete reversals of sign, consistent with the homeostatically determined biological value of heating or cooling the skin. Notwithstanding the more variable hedonic ratings

divergent from biological utility. Beyond sustaining the shifted homeostasis involved in dependence, drugs of abuse oppose biological utility).

provided during the positive hedonic trials under hyperthermia (in which some participants found the cold stimulus unpleasant after an initial period), the behavioral and physiological evidence presented here provides confirmation that we largely succeeded in our manipulations and demonstrates that hedonic valuation processes are distinguishable from peripheral thermosensation.

Participants in our study gave remarkably accurate and consistent temperature ratings, which confirm the subjective experience of opposite sequences of thermal stimulation. The record of temperature probes attached to the input and output of the tube suit provides objective confirmation of the trial conditions and stimulus characteristics (See red traces in Figure 13, p. 51; Figures 15 and 16, pages 53 and 54, respectively). Measures of core temperature confirm that data acquisition occurred while participants endured opposite core temperature deviations (e.g., see Figure 13, p. 51, right panel). The combined behavioral and physiological records show that the magnitude of opposite core temperature deviations was sufficient to modulate hedonic responses without affecting thermosensation.

Most critical to our objective of distinguishing sensory from hedonic processing is the observation of behaviorally correlated BOLD signal modulations occurring in the same areas of cortex during both functional scans. According to our experimental design, conjunction analysis isolates common processes occurring under physiologically opposite conditions. The critical aspects of thermosensory and thermoregulatory processes, namely the sequence of stimuli and the core temperature deviations, were not common but opposite in the two scans. The hedonic ratings are evidence that the sequences of hedonic experiences, in contrast, were indeed common to both scans. We delivered

opposite sequences of thermal stimuli under opposite deviations of core temperature expressly to identify the common information processing involved in the hedonic valuation of a salient primary reward and punisher⁸. By doing so we exploited a functional distinction between thermosensory perception and hedonic valuation.

Distinction of hedonic responses from sensory processes

The validity of sensory data is predicated upon their relative independence from fluctuations in physiological states. As an example of this, the sign of thermosensory percepts should not be by altered by moderate physiological shifts relative to homeostatic range⁹, as we have seen. With respect to sign and direction of change, sensory data processing captures the objective world with fidelity. For our purposes, the feature of note is that, despite the psychophysical transforms of sensory systems, the sign of the objective input (i.e., hot or cold) is not altered by internal state.

Hedonic valuation serves a different purpose and therefore functions differently. The current biological value of stimuli depends on physiological states, which change over time. Hedonic valuation processes, and the subcomponent of hedonic experiences, index¹⁰ the changing relations between states and stimuli that determine biological utility.

⁸ Following Rolls (1999, 2000), we define a reward as anything for which an organism will work and a punishment as anything which an organism will work to avoid (or terminate or delay). Using these definitions, peripheral thermal stimulation in the present experiment is a potent, unlearned (i.e., primary) reward or punishment.

⁹ This is leaving aside cases of pharmacological effects that affect perceptual processes, and extreme cases of shifts away from homeostasis so extreme that they have a systemic effect, for the purpose of this discussion.

¹⁰ Throughout this discussion, we will follow prior authors in the field and use the verb "to index" in the following specific sense, meaning: "to provide a value on a scale of measurement derived from a series of observed facts, which can reveal relative changes as a function of time" or "to employ a numerical scale to compare variables with one

That being the case, hedonic processes are distinct from sensory processes in two respects: the conditions under which they are mutable differ and sensory processes are not subject to the inversions in sign that we observe with hedonic value. The present study is predicated on the fact that hedonic responses are indices of the immediate biological circumstances that determine hedonic value. Hedonic valuation processes and responses are, by functional necessity, uniquely context-determined. We were able, consequently, to modulate hedonic responses in the experimental context without affecting sensory perception.

The experience of hedonic value is paradigmatic of subjectivity, the phenomenal dimension of experience termed *qualia*¹¹ in contemporary philosophical discourse (for *qualia*, see Churchland, 1984, 1985; Loar, 1990; Block, 1990, p.58ff. ; also Kringelbach, 2005, p. 697-8). Signals encoding biological utility are subjective phenomena: Hedonic data are subject to and conditional upon the state of the organism. Our aim was to characterize objectively the neural correlates of one type of *qualia*¹².

Location of conjoint hemodynamic response

As in prior fMRI studies involving the ongoing appraisal of induced emotion or the valuation of primary rewards and punishers, we have observed that participants' hedonic ratings covaried with robust BOLD signals in an ensemble of ventromedial prefrontal, rostro-ventral anterior cingulate (i.e., subgenual cingulate) and anterior

another” (see O’Doherty, 2003; Dolan, 2004, Rolls & Kringelbach, 2004)

¹¹ “the introspectively accessible, phenomenal aspects of our mental lives” <http://plato.stanford.edu/entries/qualia/>; the “intrinsic character of one’s experiences” (Churchland, 1984, citing Nagel)

¹² Or rather one “*quale*”, singular, for the Latin grammarians who may read this

temporal cortical regions (see Small et al., 2003; Anderson et al., 2003; Kringelbach et al., 2003; Phan et al., 2004; Taylor et al., 2003; Kalisch et al., 2006). A normative model of thermal *alliesthesia*, constructed from individual sensory ratings to model the physiologic determinants of hedonic experience, correlated with the BOLD signal over a more broadly distributed cortical area¹³ and with higher *z* values. To a lesser extent, conjoint BOLD signal in anterior temporal and paralimbic areas (i.e., head of caudate/putamen) was also correlated with these behavioral measures. These results are notable because, unlike data from the majority of neuroimaging studies of hedonic processing, perceptual processes are differentiated (see this objection in Wiens, 2005, p. 3; O’Doherty, 2004). The location of the conjunctions is consistent with prior observations of primary hedonic valuation processes in humans and non-human primates, to be reviewed in the following subsections.

Our observations are consistent with multiple lines of evidence from neuroimaging. Briefly stated, many investigators have produced correlational evidence that the ventromedial prefrontal cortex (vmPFC), and the antero-medial orbitofrontal cortex in particular, is a location for the representation of hedonic value (see O’ Doherty, 2004; Kringelbach & Rolls, 2004, for reviews). Others have produced correlational and morphological evidence that the subgenual region of the anterior cingulate cortex and the orbitofrontal cortex are instrumental to the processing of intense affect and the subjective experience thereof (Drevets et al., 1997; for neuroimaging review, see Drevets, 1998, 2000; additional reviews extending beyond imaging evidence in Drevets & Raichle, 1992; Drevets, 1999). In light of this, it should not surprise that Drevets has marshaled

¹³ Although this may be due to the reduced individual variability in this model, a matter to be addressed in the following section.

evidence for the subgenual cingulate as a substrate for disorders of mood and affect, especially Major Depressive Disorder (MDD) and Bipolar Disorder (BD) (see Drevets et al., 2008; Drevets, Price & Furey, 2008; Drevets et al., 1997; Price and Drevets, 2010).

Other investigators have produced correlational evidence that the right anterior insula and right orbitofrontal cortex are interconnected sites for monitoring and experiencing the internal state of the body, which they term interoception (Craig, 2002, 2003, 2004; Wiens, 2005; Critchley, Wiens et al., 2004; Critchley, 2004; Pollatos, et al., 2007a, b., and c.). Craig has long been the champion of what he calls a homeostatic afferent pathway, which he has mapped using multiple techniques in primates and humans, to monitor changes in the physiological condition of the body (2002, 2003, pp. 500-502) and represent the subjective evaluation of these states. He is very specific in his stipulation that the resultant hedonic sign of a state of the body is represented in the right OFC (Craig, 2002). It is of considerable importance for the present study that much of Craig's evidence comes from thermosensation (e.g., Craig et al., 2000; Craig, Bushnell, et al., 2002).

There is also a small but intriguing literature reporting correlational evidence of temporal pole activity in response to induced emotion of both hedonic signs (Aalto et al., 2001; Lane et al., 1997), episodic recall of emotion (e.g., Dolan et al., 2000, *inter alia*), empathically shared emotion (Vollm et al., 2003, 2006), and inference or appraisal of the emotional states of others (reviewed in Frith and Frith, 2003). Conjunction analysis of hedonic experience induced using multiple sensory modes has shown common temporal pole correlates (Royet et al., 2000; Aalto et al., 2001).

Comparing the spatial location of our results in relation to prior studies is a means of corroborating data from this correlational method: significant covariance between BOLD signal and a behavioral measure is worthy of our attention, but subsequent inferences are conditional upon appearance in neuroanatomically valid locations. The conjoint peak correlates reported here are notable because of their *z*-values and because this evidence meets conservative standards of statistical and logical inference. Specifically, we conjoined only statistically significant correlates of hedonic ratings or a normative *alliesthesia* model, respectively, corrected for multiple comparisons, modeled using the minimum of spatial averaging and rigorous denoising methods. Only significant group effects in the same areas appear in the final conjunction maps. Finally, among the spatially conjoint, statistically significant areas of correlated activity, we will focus on the peak value observations least susceptible to Type I error (i.e., “false positive” observations).

By identifying conjoint hemodynamic correlates we adduce one form of correlational evidence for the role of these brain areas in hedonic valuation processes: According to our hypothesis, a necessary condition for a neural representation of hedonic value is that the areas with correlated signal must be coextensive. By “coextensive” we mean showing a common temporal and spatial pattern in pairs of scans. The correlated signals we have acquired, when coextensive, meet the logical criterion we have set for distinguishing cortical areas that can be both statistically and anatomically associated with the encoding of hedonic value.

When combined with prior evidence from single neuron recording studies and neuroimaging, our observations contribute to the empirical basis for linking the

subgenual cingulate, ventromedial prefrontal cortex (vmPFC), particularly anterior medial orbitofrontal subdivisions, and bilateral anterior temporal areas with hedonic valuation and the experience of hedonic value or *qualia*. In the following subsections we will adduce the relevant findings from studies of primary hedonic valuation in primates and humans (conducted using single-cell recording) and neuroimaging of induced human emotion. We will now turn to these lines of evidence, in order, then address limitations to the study and draw some broader conclusions.

Single-cell recording studies in human subjects

The spatial localization of the conjoint hemodynamic responses we report here is consistent with prior evidence for the role of the orbitomedial prefrontal cortex and subgenual anterior cingulate cortex in the indexing of hedonic value and the experience of intense emotions at the poles of hedonic range. Evidence from single-cell recording studies of both humans and non-human primates human single-cell recording studies corroborates our findings of spatially conjoined, peak hedonic correlates in the right ventromedial prefrontal cortex (vmPFC, specifically, the innermost/dorsal-most right medial orbital gyrus, see Chiavaras et al., 2001). Though these studies may complicate the interpretation of fMRI data, due in part to the mismatch in spatial and temporal resolution, they provide direct evidence of localized neural response to rewards and punishers in vmPFC.

In the first study of its kind to characterize unambiguously the selective response of vmPFC neurons to emotional stimuli, Kawasaki, Adolphs and colleagues (2001) recorded from depth electrodes in a single subject during the presentation of facial affect

images and the International Affective Picture System (IAPS, Lang & Ohman, 1988). They observed a distinctive pattern of immediate suppression followed by sustained bursts of neuronal activity in ventromedial, but not ventrolateral, prefrontal cortex (PFC) following presentation of aversive IAPS stimuli and fearful faces. The investigators consequently attribute the “encoding of emotional value” (Kawasaki et al., 2001, p. 16) to a subgroup of right ventromedial PFC neurons.

Despite the understandable limitations of presurgical study, such as the inability to probe for vmPFC neurons¹⁴ selectively responsive to pleasant stimuli, responsive to multiple hedonic values, or those encoding reversals of value, as reported in the non-human primate literature (e.g., Thorpe, Rolls & Maddison, 1983; Rolls et al., 1989; Critchley & Rolls, 1996, Morrison & Saltzman, 2009), two elements of these results are highly significant to our discussion. First, vmPFC neurons fired selectively to the presentation of aversive IAPS stimuli, despite differences in stimulus content and despite the fact that the investigators’ selections from the IAPS stimuli were matched for sensory characteristics, described in terms of lower level perceptual features (e.g., brightness, contrast, size, color composition). This rules out the interpretation that responses are mixed with perceptual processes or the appraisal of individual stimulus features.

Second, emotion selective neural responses occurred at short latencies (120-170ms) and continued for prolonged periods (>1400ms). This observation suggests that

¹⁴ In a book chapter on the human OFC, the authors describe the extraordinary difficulty of acquiring these data, stating that: “Once implanted, the electrodes in humans cannot be moved” (Adolphs et al., p.358, in Zald & Rauch, 2006). Their hybrid clinical-research probes do have multiple contacts, but their probe placements were determined by estimated seizure foci, not the objectives of the experiment. The investigators have a small time window to test their subjects between recovery from implantation surgery (and medication) and the incipient seizures.

encoding proceeds on two time scales, exemplifying both a quick and necessarily covert indexing¹⁵ of emotion categorization (i.e., an unconscious process by definition, see Zajonc, 1980, 1984; Ohman et al., 2007; Morris, Ohman & Dolan, 1999; Carlsson et al., 2004; Mineka & Ohman, 2002; Katkin, Wiens & Ohman, 2001; *inter alia*) and sustained activity, which occurs on a timescale that would allow for conscious emotional experience (Kawasaki et al., 2001). While this slower phase of encoding is sufficient for conscious experience, it does not follow that conscious processing necessarily occurs. Nonetheless, the possibility of vmPFC neural activity indexing emotional value both unconsciously, due to the relative immediacy, and then potentially consciously, due to a longer duration of firing, is intriguing in the context of our fMRI results.

Evidence from a subsequent elaboration by the same group (Kawasaki et al., 2005) substantiates the conclusion, based on non-human primate single cell recording studies, that vmPFC neurons selectively fire to pleasant, neutral and aversive stimuli. In this second depth electrode study of epileptic patients awaiting surgery, the investigators were able to record from 267 neurons in four subregions of the bilateral vmPFC, inclusive of the subgenual cingulate cortex. Stimulus presentation again consisted of the IAPS. Of the vmPFC neurons that fired to the IAPS images in these four patients, those tuned to aversive stimuli were again the majority; yet there were subpopulations selective for neutral and pleasant stimulus categories as well.

Patterns of selective firing were not differentially associated with a class of hedonically positive or negative stimuli, with levels of arousal or of valence (i.e., position

¹⁵ as noted above, the verb "to index" is used in the following specific sense, meaning: "to provide a value on a scale of measurement derived from a series of observed facts, which can reveal relative changes as a function of time" or "to employ a numerical scale to compare variables with one another"

on simple continua extending from pleasant to unpleasant). Nor was selective firing lateralized or differentially distributed according to emotion category in vmPFC and subgenual cingulate. In sum, neurons highly selective for hedonic value are densely, but perhaps unequally interspersed in the human vmPFC, OFC and contiguous areas of subgenual cingulate cortex.

Single-cell recording studies in non-human primates

Observations of selective vmPFC/OFC firing to images of emotional value, and hedonic value specifically, accord with prior evidence from non-human primate electrophysiological studies. The extensive work done by Rolls and colleagues has made a significant contribution to what is known about hedonic processes in the OFC (Thorpe, Rolls & Maddison, 1983; Rolls et al., 1986; Rolls et al., 1989; Critchley & Rolls, 1996; Rolls, 1999, 2000, 2004). The relevant kernel of this comprehensive line of research is that subpopulations of OFC neurons fire selectively to encode hedonic value. Other regions, specifically the primary sensory areas for each modality, encode the sensory features of stimuli. With exquisite selectivity, single neurons in the bilateral vmPFC/OFC robustly fire to the taste, smell, “mouth-feel”, sight, touch or sound of gustatory rewards and punishers (e.g., Thorpe, Rolls & Maddison, 1983; Rolls et al., 1989). Furthermore, these same neurons fire in response to stimuli predictive of, or associated with, such primary rewards and punishers. Illustrative of a functional dissociation from sensory processing, selective OFC firing is both poly-modal and cross-modal (e.g., the sight, taste, touch, sound and smell of the same stimulus will fire the neuron); selective firing occurs in response to perceptually dissimilar but associated stimuli (including those in other sensory modalities); and is uniquely modulated by changes in internal state.

To establish the role of satiety in modulating hedonic valuation, Rolls and colleagues have repeatedly demonstrated that selectively tuned OFC neurons only fire in response to food-related stimuli when the animal is deprived (Thorpe, Rolls & Maddison, 1983; Rolls et al., 1989; Critchley & Rolls, 1996; Rolls, 1999). Furthermore, the modulating satiety is not general but highly selective (Rolls et al., 1989). Firing rates will drop to zero or return to the spontaneous baseline rate when the animal is satiated on a particular gustatory stimulus, indicated behaviorally by their refusal of it. The same neurons will fire robustly to other stimuli, including the sight and smell of a different food, a different rewarding “tastant,” or an object or behavior with a learned association specific to them. Stimuli whose value is not degraded by satiety are encoded as such by OFC neurons, despite differences in sensory characteristics, in sensory modality, or reversals in reward association. The specific evidence follows.

Rolls’ group located neurons tuned to the sensory characteristics of gustatory stimuli (e.g., in the nucleus of the solitary tract) and showed that the sensations making up taste processing, *per se*, are not modulated by hunger (Yaxley et al., 1985). In effect, they were distinguishing neurons selectively responsive only to sensory characteristics, later to distinguish those neurons selectively responsive to, and indexing, hedonic value. These latter neurons they identified in subdivisions of the caudal OFC, described as a secondary taste area and a convergence site for the coding of multimodal hedonic signals (e.g., Thorpe, Rolls and Maddison, 1983, Rolls et al., 1989; Critchley and Rolls, 1996).

They demonstrated two defining features of selective stimulus-dependent activity (i.e., “tuning”) that are directly relevant to our observations of OFC responses in humans. First, a subpopulation of OFC neurons selectively fire in response to both rewards and

punishers, regardless of sensory characteristics. And second, selective firing is mutable: it can be modulated by changes in motivational state. Indeed, selective firing in OFC neurons could be modulated to the extent of being fully reversible in sign or being extinguishable. According to the conditions, including learned associations or the “meaning” of the stimulus, as Rolls put it (1983, p. 113), hedonically selective OFC neuronal firing depends on motivational state.

Thorpe, Rolls and Maddison (1983) recorded single OFC units in awake rhesus monkeys and observed selective firing to visual, gustatory and auditory stimuli, but critically, also to their contextually determined hedonic value. For example, just as in the Kawasaki studies of humans (2001, 2005), single OFC neurons fired selectively to the sight of a variety of aversive stimuli that differed in their identity and sensory characteristics (e.g., realistic toy snakes and tarantulas)¹⁶. One illustrative example of an exquisitely selective hedonic index was the reversible and extinguishable responsiveness of right OFC neurons to the sight of a syringe. A subpopulation of neurons would fire when the animal caught sight of the syringe, if and only if the syringe had just been used to deliver an aversive saline bolus. Firing to that visual stimulus was extinguished after a single trial of the reverse hedonic value, in which the syringe held glucose, and reinstated again after a single saline trial.

Other right OFC neurons showed the inverse, firing only to stimuli associated with rewards, demonstrating that subpopulations of OFC neurons code both reward and punishment associations. Strikingly, the investigators also observed that valuations were

¹⁶ Intriguingly, the short latency observed in the single human patient’s vmPFC response to aversive images (Kawasaki et al., 2001) matches almost exactly the latency observed by Thorpe, Rolls and Maddison (1983) in rhesus monkeys’ response to aversive visual stimuli.

matched in bi-modal coding: the same OFC neurons fired selectively to the sight and taste of a given rewarding stimulus when presented in separate randomized trials (e.g., a trial for the sight of a banana and a trial for the taste of banana). To reiterate a core concept, what the authors cite as evidence of cross-modal matching in single OFC neurons (Thorpe, Rolls & Maddison, 1983, p. 111) illustrates the encoding of hedonic value irrespective of the mode of perception, and thus irrespective of incommensurate sensory characteristics (i.e., sight and taste).

Rolls and colleagues subsequently made definitive observations of selective satiety in macaques (Rolls, Sienkiewicz and Yaxley, 1989; Critchley and Rolls, 1996). In one study, recording in the caudolateral OFC, they applied six stimuli directly to the tongue using a syringe. It is of primary interest, in the context of this discussion, that OFC neuronal responses tracked behavior. When the animals were satiated and the satiating solution was again presented, firing in previously responsive OFC neurons was extinguished. However, the presentation of other solutions induced unaltered, vigorous firing. An impressive mosaic illustrates the near perfect correlation between the descending behavioral ratings and the decreasing firing rate of single OFC neurons, as satiety progressed during each trial (Rolls, Sienkiewicz and Yaxley, 1989, p.56).

In a second study, Critchley and Rolls (1996) demonstrated that satiety selectively modulates neuronal responses to visual and olfactory presentation of food stimuli as well. Activity in OFC neurons responsive to the sight or odor of foods and in those neurons responsive to multiple sensory modes decreased with satiety. Again, consistent with the interpretation that these OFC subpopulations encode hedonic value, decreases in acceptance of food stimuli tracked decreased OFC firing. Notably, in both experiments

all observed decreases in selective firing reversed when the animal was given ample time between trials.

This evidence directly bears on our discussion because the modulation of hedonic valuation by satiety is one form of evidence that the hedonic value of primary rewards and punishers is equivalent to their biological utility, which is determined by the vicissitudes of homeostatic regulation. Just as in thermal *alliesthesia*, in manipulations of satiety OFC activity encodes changing hedonic value, signaling the biological utility of the stimulus in relation to changing internal or motivational states (i.e., need or deprivation versus regulation or satiety).

One recent study of both primary rewards and punishers in particular strongly supports the notions of encoding value irrespective of the sensory characteristics. Recording from right OFC in two rhesus monkeys, Morrison and Salzman (2009) demonstrated that individual OFC neurons respond to both primary rewarding and aversive stimuli, despite their different modalities of presentation and location of delivery. Both liquid rewards and air puffs to the face reliably fired this subpopulation of neurons. Moreover, the responsiveness of these neurons could be associated with abstract conditioned stimuli (i.e., yet a third sensory mode of presentation, with varied characteristics) and the selective firing to associated stimuli was completely reversible.

The investigators used a reversal of hedonic value, specifically of reinforcement contingency, to distinguish activity encoding the sensory features of abstract stimuli from that encoding hedonic value. Consistent with our observations, the firing of a subpopulation of neurons in the right OFC tracked the context-determined hedonic value,

but not the varied sensory attributes. This contextual modulation of neural response tracked behavior.

In combination, evidence from single cell recording supports the localization of hedonic valuation in bilateral vmPFC/OFC. The instances of polymodal or multi-locus valuation cited above are germane to the present study first because they exemplify the independence of hedonic indexing or valuation from the processing of sensory characteristics. *A fortiori*, the sensory characteristics of one mode do not exist in another. We have seen that subpopulations of neurons in the OFC encode polymodal and multi-locus reward and punishment representations, including the reward value of the same stimulus presented in a different modality (e.g., Thorpe, Rolls and Maddison, 1983), the value of physically incommensurate classes of stimuli (e.g., Morrison and Salzman, 2009) and stimuli delivered to different locations on the body (e.g., Morrison and Salzman, 2009; Critchley and Rolls, 1996; Thorpe, Rolls and Maddison, 1983). This final observation is especially relevant to the present discussion because thermal *alliesthesia* requires thermosensory signals from the core and from the periphery¹⁷ (i.e., is multi-locus).

For primary rewards and punishers, whose hedonic value is indexed to regulatory processes, convergence of signals from multiple locations and modalities can be essential to the weighing of one sensory input in relation to another, which may contribute to the

¹⁷ The hedonic valuation processes engaged by our experimental manipulations necessarily involve multiple locations of thermosensation (i.e., core and skin). Concurrent somatosensory (i.e., feeling of the suit), visual, and auditory stimuli, do occur but at higher frequencies and without changes in value. We collect concurrent hedonic appraisals and sensory reports, rated on a visual analog scale. Thus, at minimum, the concurrent perceptual processes engaged include peripheral thermosensation and interoception.

determination of value. This is the case because determinants of immediate biological value can originate from other locations in the body and/or other sensory modalities (i.e., chemical, somato-visceral, thermosensory). Stating this is not to exclude the possibility that the modulation of hedonic signals can occur by means other than comparative weighting of multi-locus or polymodal inputs, but rather to highlight a principle feature of orbitomedial prefrontal function and anatomy that can help us organize the evidence.

In concluding this section, we reprise the foundational question stated above regarding how we might characterize the hedonic quality of affective experience in terms of states and processes of the central nervous system. Signal convergence is a general property of neural networks. Moreover, neural representations of the body and objects in the world depend on polymodal and multi-locus signals. With these axioms in mind, it is intriguing to consider precisely how representations of hedonic value exemplify these general principles. The spatial and temporal resolution of single cell recording studies permits the precise localization of neurons that selectively fire to different types of reward and punishment stimuli and neurons whose firing is modulated by changes in the hedonic value of stimuli. Thus, we have direct evidence that representing the hedonic value of stimuli is a polyvalent and polymodal function. Neuronal firing experimentally associated with hedonic valuation encodes signals from primary and secondary rewards and punishers, and the firing of these subpopulations is distinguishable from neuronal firing encoding sensory attributes. We will see in the following subsections that the convergence of inputs from all sensory modalities is a characteristic of the posterior orbito-medial prefrontal cortex (OMPFC). Recognition of this will aid us in understanding why diverse experimental paradigms produce correlates there.

A functional model of orbitomedial prefrontal cortex (OMPFC): segregated modal inputs converge for reward value representation

Price and colleagues have done comprehensive work on the orbitomedial prefrontal cortex (OMPFC) superstructure (Carmichael & Price, 1995, 1996; Price, 1999; Ongur & Price, 2000, 2003) and have described it as “a substrate to integrate viscerosensory information with affective signals” (Price, 1999, p.383). Their multiple staining method architectonic studies (in macaque, Carmichael and Price, 1994; in humans, Ongur, Ferry & Price, 2003) are complemented by retrograde and anterograde axonal tracer studies (Carmichael and Price, 1995, 1996) and synthesized in excellent reviews (Price, 1999; Ongur & Price, 2000). Taken together, this body of research amply demonstrates that the OMPFC itself is a highly interconnected and intra-connected network of subdivisions. Two classes of functional subdivision merit our attention. The posterior (i.e., caudal) subdivisions of OMPFC receive signals from all sensory modes: Visceral, somatosensory, olfactory, gustatory, auditory and visual signals have inputs there (see Figure 35., below; for the original maps, also see Price, 1999, p.385; Ongur & Price, 2000, p.212; for human architectonics, see Ongur, Ferry & Price, 2003). Furthermore, the medial anterior subdivisions (particularly area 11l, but also 11m, visible below) are convergence or “integration” sites for the hedonic valuation of these modal signals.

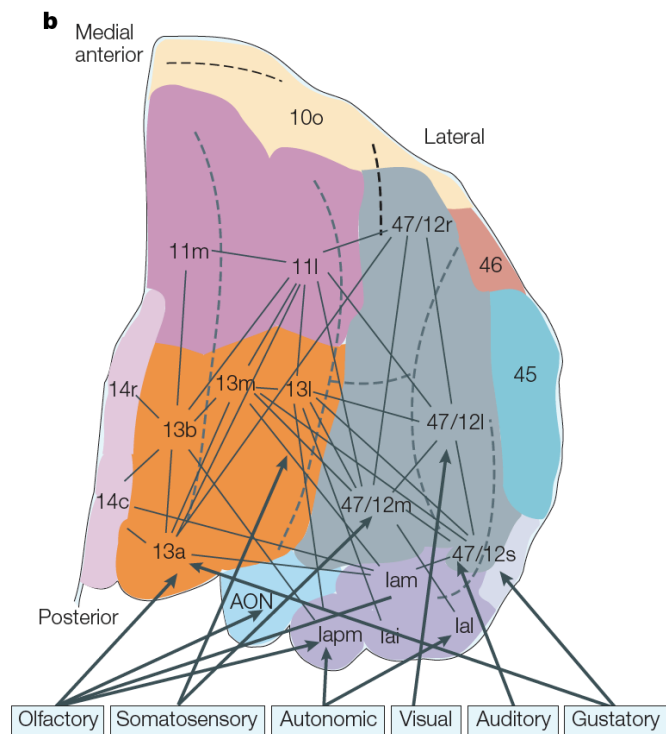


Figure 36. Orbitomedial prefrontal cortex (OMPFC) network (from Kringsbach, 2005, p.700, used by permission).

Most relevant to the present study are these two classes of function subdivision, which are consistent with our data in consequential respects. First, the posterior, ventral OMPFC areas of peak correlated BOLD signal observed in the present study are consistent with the segregated mapping of somatosensory inputs (see areas 47/12m and 13l above as compared to Figure 37., below). Peak voxels in our spatially conjoined z-maps for the normative *alliesthesia* model appear bilaterally within areas 13l and 47/12m, which have been characterized by Price and colleagues as somatosensory (compare Figure 36. above).

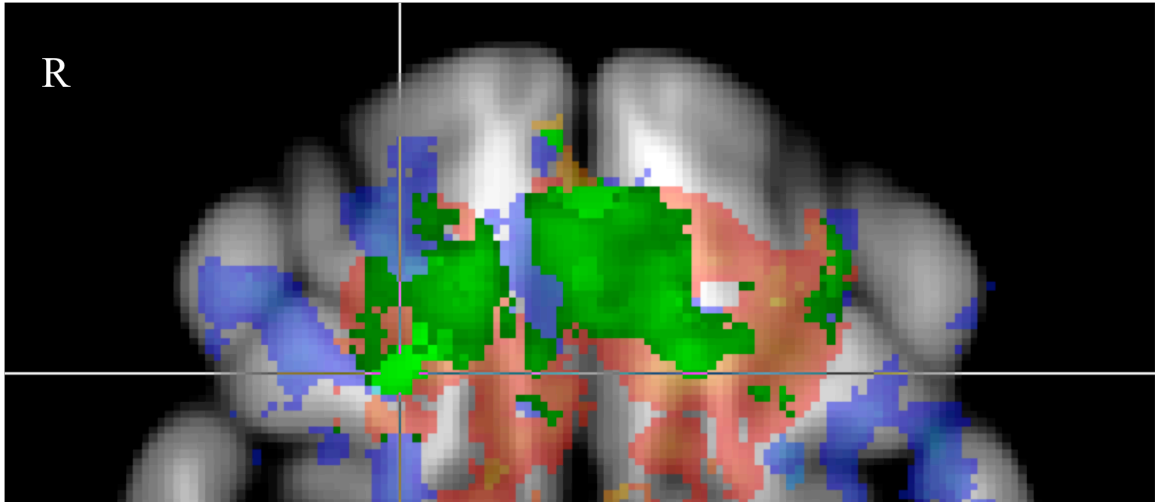


Figure 37. Normative Alliesthesia Conjunction Peak.

(areas 13l and 47/12m, right side, including anterior medial areas 14r and 11m, radiological convention: left side of image is right side of brain)

| Z | x | y | z |
|------|----|----|-----|
| 3.97 | 23 | 27 | -17 |

2.3  4.24

Second, as vividly depicted in the statistical map above, conjunctions in our data also span more anterior and medial subregions of the OMPFC network. The functional role of the more medial and anterior subregions of the vmPFC is determined by the input sources, which are exclusively the posterior, secondary sensory representations just mentioned. The functional role of anterior medial OMPFC has been delineated in two recent, complementary models.

Intriguingly, Craig (2002) has proposed a model of interoception (i.e., the sense of the physical condition of the body) that designates the right OFC as the final site for the representation of hedonic valence in mammals. His model is the culmination of many studies, but the results from one human imaging study in particular are relevant to our

discussion. In a PET study of the subjective evaluation of non-noxious peripheral thermal stimuli, Craig and colleagues showed that regional cerebral blood flow in the right OFC was strongly correlated with subjective ratings of a graded cool stimulus (Craig, Chen, et al., 2000).

Craig (2002) links his model of insula-to-OFC encoding of body states to the James-Lange theory of emotion (James, 1884) and the somatic marker hypothesis (Damasio, 1994), in which perception and evaluation of the state of the body are the basis for emotional responses. “Like all ‘feelings’ from the body,” Craig states, “thermal sensibility is inherently endowed with a characteristic affect that motivates behavior, and it reflexively generates autonomic responses that signal its primary role in thermoregulation and its integration with homeostasis” (p. 187). This interpretation suits our data as well, an idea to which we will return in the conclusion.

Kringelbach (2005) has developed a useful schematic model of OMPFC functional segregation, which integrates the connectivity maps of Ongur and Price (2000), single-cell recording data, and his review and meta-analysis of the neuroimaging evidence (Kringelbach and Rolls, 2004). According to this functional model, signals encoding the sensory features of a stimulus relay the identity and attributes from primary sensory areas (e.g., S1). The respective modality-specific signals then have secondary sensory inputs in the more posterior OMPFC. Signals from those posterior subregions converge in anterior/medial subregions of the OMPFC, where hedonic value is represented. The latter, more anterior areas have been functionally distinguished as regions where subpopulations of neurons encode modulated reward representations (as in single cell recording studies covered above, see Thorpe, Rolls and Maddison, 1983;

Critchley & Rolls, 1996; Morrison & Saltzman, 2009); and the specific connectivity and directionality have been characterized by axonal tracer and cytoarchitectonic studies (Carmichael & Price, 1995, 1996; Ongur & Price, 2000; Ongur, Ferry & Price, 2003).

Spatially conjoined areas in our *z*-maps of the hedonic ratings and the normative model of *alliesthesia* extend into these more anterior and medial subdivisions, such as 13m and 11l (see Figure 36., above). Particularly consequential to our interpretation of the present data is the regional specificity for somatosensory inputs. Our data fit this functional segregation. Furthermore, following up the argument regarding convergence above, the more anterior/medial subregions (i.e., 13m, 11m and 11l), where we also report conjunctions, do not receive secondary sensory input (Ongur & Price, 2000) but rather receive converging projections from the modality specific posterior OMPFC inputs.

In support of the claim that we have identified specific neural correlates of the hedonic valuation of somatosensory stimuli, it is of considerable importance that both modality specific correlates in posterior OMPFC and anterior/medial reward representations exist. We have observed conjoint peaks (i.e., areas 47/12m and 13l, in Figure 37. above) in both relevant subregions and these results are neuroanatomically specific to them. We do not, for example, observe conjunctions in gustatory, olfactory or auditory input areas. As a consequence, our observations have face validity and support Kringelbach's model.

Indeed, these observations are also consistent with the higher order processes described in Kringelbach's model and elsewhere (e.g., O'Doherty, 2004), which we might justifiably ascribe to our participants. To use Kringelbach's and Craig's terms,

these processes include monitoring the body state and hedonic experience. To the extent that we report conjoint peaks only in areas of specific modal input and in subregions designated as focal representation areas for subjective hedonic experience, our experiment has been successful. To more fully corroborate this, we will now consider the functional neuroimaging evidence for the localization of modulated hedonic responses, reward value representations and subjective hedonic experience, as distinguished from sensory processing.

FMRI studies of hedonic valuation

The concordance is strong among human neuroimaging studies designed to identify neural responses to stimuli of both hedonic signs and to distinguish those responses from other neural processes. A host of analogous experiments have yielded findings concordant with those under discussion from the present study (for reviews on OFC and reward representation, see Rolls, 2000, 2008; O'Doherty, 2004, 2007; Kringelbach, 2005; Rolls & Grabenhorst, 2008; for a meta-analysis on OFC in neuroimaging, see Kringelbach & Rolls, 2004; for meta-analysis of emotion induction and experience in neuroimaging see Steele & Lawrie, 2004; Phan et al., 2002; Murphy et al., 2003; Wager et al., 2003).

Importantly, a key positron emission tomography (PET) study (Royet et al., 2000) resolves questions as to how such a variety of stimulus presentations, subjects and imaging methods may have yielded comparable results in regard to the OMPFC. Among the methods used in neuroimaging studies to distinguish sensory from hedonic information processing, one is to present valenced stimuli (i.e., hedonically positive or

negative) in different sensory modalities and then identify common substrates by conjunction analysis. Using this method, Royet, Zald and colleagues (2000) report spatially conjoined increases in regional cerebral blood flow in left posterior OFC, subgenual cingulate and temporal pole during the presentation and hedonic rating of valenced stimuli in three sensory modalities. It is consequential that their common areas of increased blood flow overlap those reported in the present study, notably in the bilateral orbitofrontal gyri (26, 30, -12 and -30, 18, -12). Such observations of common functional localization of hedonic processes in humans, distinct from the sensory processing of the inducing stimuli, can serve as a reference point for this section of our discussion: With Royet and colleagues' results in mind, the aggregate of fMRI studies is more compelling evidence of the functional localization of hedonic valuation processes and their neuroanatomical dissociability from the variety of sensory or cognitive processes that may induce them, attend them or result from them.

A varied and growing list of stimuli evidently engage the vmPFC/OMPFC in the mode of hedonic valuation. These include olfactory and gustatory rewards and punishers (Anderson et al., 2003; Small et al., 2003; O'Doherty, Rolls et al., 2000, 2001; Zald & Pardo, 1997; de Araujo et al., 2005; Gottfried et al., 2002), auditory rewards and punishers (Blood, Zatorre, Bermudez & Evans, 1999); recalled emotions (Damasio et al., 2000, *inter alia*); food (Kringelbach et al., 2003, Small et al., 2001, *inter alia*); images of food (Bruce et al., 2010); images of attractive faces (Aharon et al., 2001; O'Doherty et al., 2003; Kawabata & Zeki, 2004); affective words (Lewis, Critchley, Rotshein & Dolan, 2007); pleasant and unpleasant touch (Rolls et al., 2003); peripheral temperature (Craig, Chen, Bandy & Reiman, 2000; Rolls & Grabenhorst, 2009); receipt and anticipation of

money (Elliot et al., 2003; Knutson et al., 2003; Hampton & O’Doherty, 2003; O’Doherty et al., 2001); emotional scenes and faces (Grimm et al., 2003; Anders et al., 2004; Dolcos et al., 2004; Posner et al., 2009; Nielen et al., 2009; *inter alia*); aversive pictures (Garrett & Maddock, 2006); evaluations of generosity and adherence to social mores (Cooper et al., 2010); predicted and anticipated rewards (Kahnt et al., 2010); imagined rewards (Bray, Shimojo & O’Doherty, 2010) and even architecture (Kirk et al., 2009), to list only some examples.

There is a common OMPFC super-structure indicated in the results of these studies, however, as described above in the end of the prior subsection, the underlying neuroanatomy is not homogeneous. Therefore, evidence from probabilistic, cytoarchitectural and connectivity studies (Carmichael & Price, 1995, 1996; Price, 1999; Ongur & Price, 2000, Ongur, Ferry & Price, 2003; Chiavaras and Petrides, 2002) has informed the inferences made from functional correlations (reviewed in Kringelbach and Rolls, 2004). Returning to Kringelbach’s model, there are complementary lines of evidence from functional neuroimaging that indicate further segregations between the OMPFC circuits encoding different classes of stimuli.

Of central importance to the present discussion are two patterns of functional segregation. We partially addressed the first in the foregoing, namely that between the representation of stimuli in the specialized, posterior “input” subregions of OMPFC versus the generalized reward value representations in adjacent anterior subregions. In the former, posterior areas, representations of stimuli in different modes do not overlap; in the latter, anterior areas, there are overlapping representations. Like many others, we have observed peak *z*-values in the anterior, medial areas. Such observations, when

consistent with the axonal tracer studies, form the basis for postulating a further signal convergence for the representation of hedonic value (see Figure 36. above, especially forward projections from single mode inputs, e.g., from 13l to 11l).

Situating our results in Ongur, Price and Ferry’s architectonic map (2003, reproduced in color and with higher resolution in Kringelbach, 2005) is a useful way of visualizing this functional and architectonic segregation. Furthermore, it helps us create a mental image to organize the fMRI results discussed in the following. Below is a representation of Ongur, Price and Ferry’s architectonic subdivisions followed by the hedonic conjunction and normative alliesthesia conjunction peaks in comparable axial views.

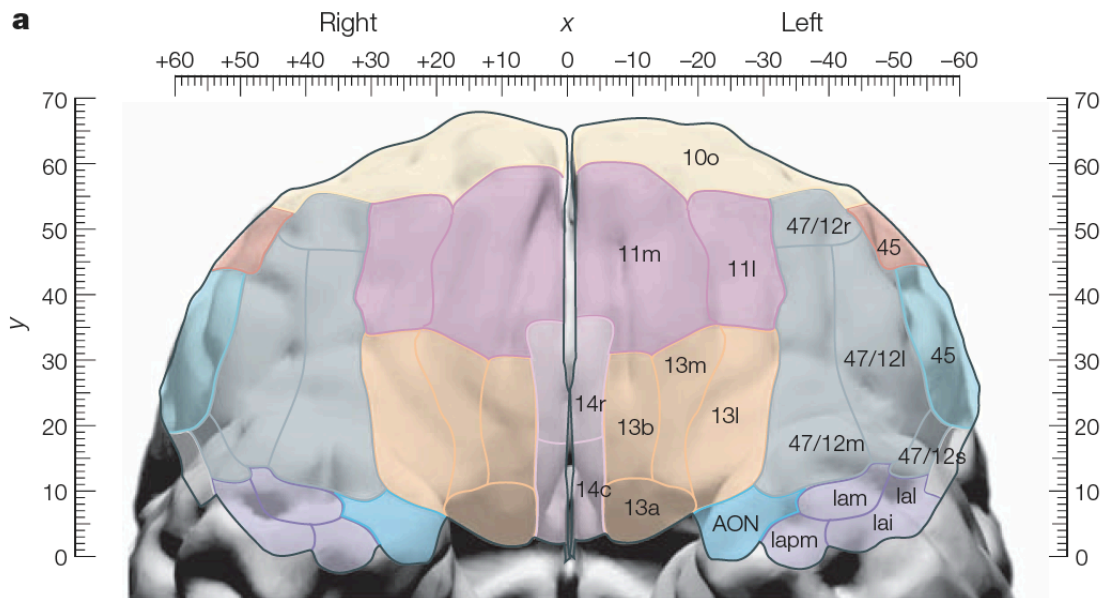


Figure 38. Ongur, Price and Ferry’s architectonic subdivisions. (orbital surface of prefrontal cortex, viewed from below, from Kringelbach, 2005, p.693, used by permission)

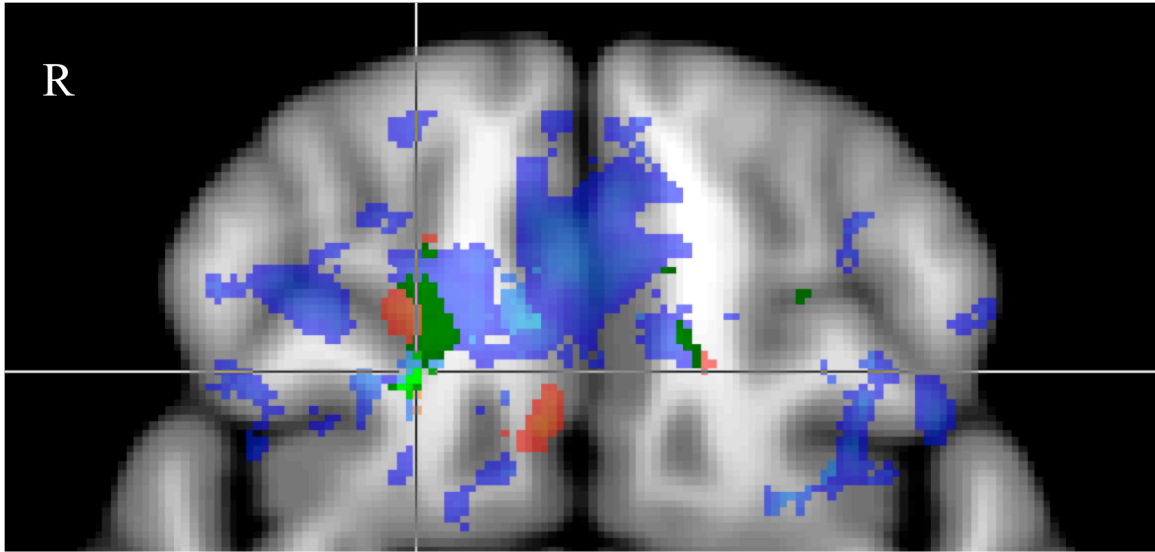


Figure 39. Hedonic Conjunction Peak (areas 13m, 13l and 11l, right side).

| Mean Z | x | y | z |
|--------|----|----|-----|
| 4.11 | 21 | 26 | -14 |

2.3  4.11

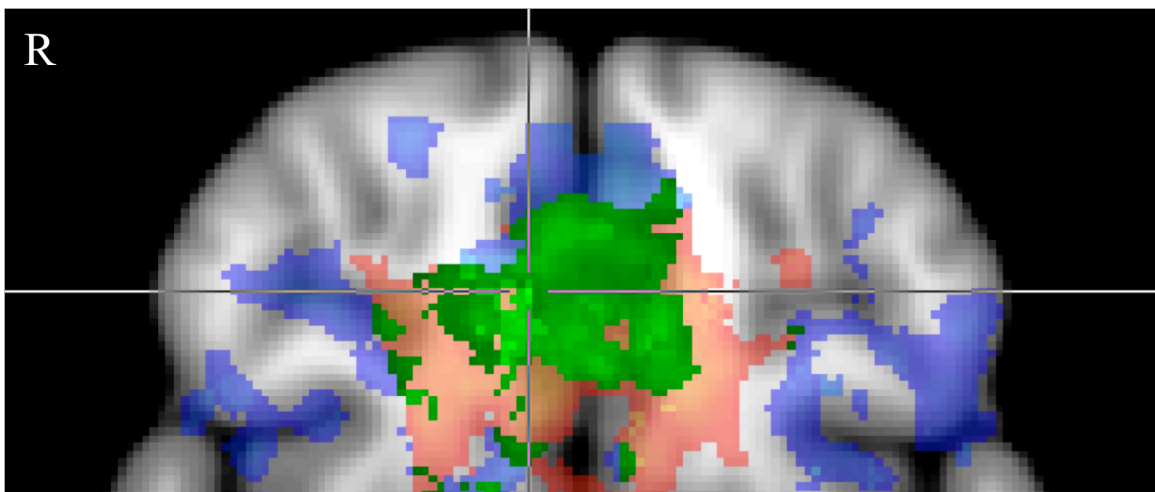
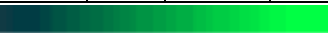


Figure 40. Normative Alliesthesia Conjunction Peak (areas 11m and 13m, 13b, right side, extending bilaterally).

| Mean Z | x | y | z |
|--------|---|----|-----|
| 4.24 | 7 | 37 | -12 |

2.3  4.24

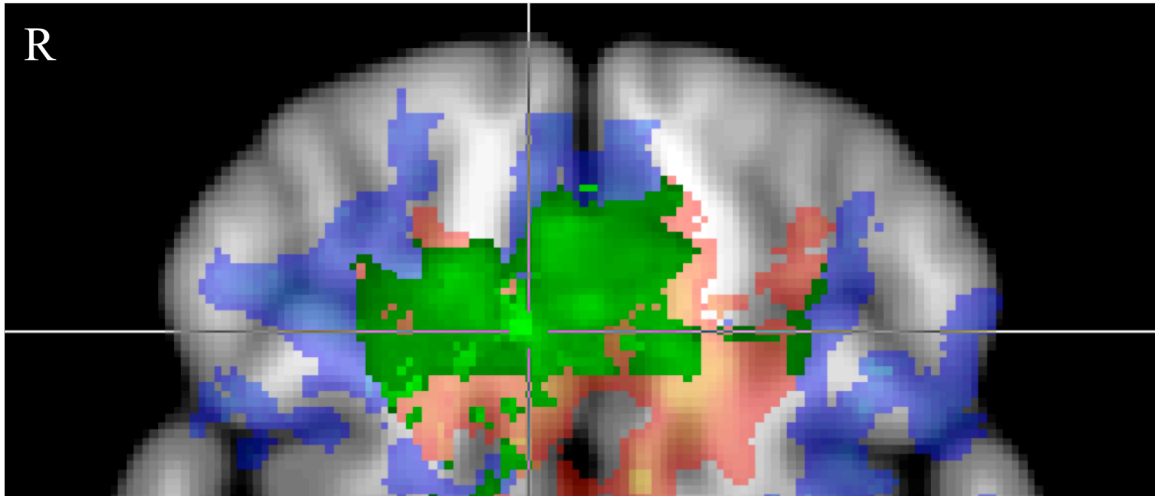


Figure 41. Normative Alliesthesia Conjunction Peak (areas 13b, 13m, 11m and 11l, right side, extending bilaterally).

| Mean Z | x | y | z |
|--------|---|----|-----|
| 4.24 | 7 | 32 | -14 |

2.3  4.23

The pattern emerging from comparisons of fMRI data, including that presented here, is that more anterior medial subdivisions of the OMFC represent the subjective hedonic value of primary reward stimuli¹⁸ (see meta-analysis in Kringelbach and Rolls, 2004; Kringelbach, 2004, 2005, for reviews). What is fascinating is that a seemingly contradictory pattern in the evidence can be viewed as complementary. In their meta-analysis and review, Kringelbach and Rolls (2004) formulate the explanatory hypothesis that the more complex the stimulus, the more anterior its value representation in the OFC. Relatively “uncompounded” primary rewards, like odors, have direct input pathways to the caudo-lateral OFC (e.g., Gottfried et al., 2002); Rolls and colleagues have observed,

¹⁸ However, we may question whether or not the best higher order descriptors for stimulus representation mapping have been produced.

consequently, that these stimuli have reward representations in more posterior-lateral areas of OFC.

As in the Royet and colleagues PET study (2000), among others, a common representation of pleasant and unpleasant stimuli has been observed in the caudolateral OFC. But this is the case when the reward value of the stimuli is not modulated. For example, when the hedonic value of olfactory and gustatory stimuli was modulated by satiety (Kringelbach et al., 2003), that hedonic value representation occurred in more anterior areas. It may be that the multiplex signal that determines conditional hedonic value is more complex than the unmodulated signal of an odor, to use one example (Kringelbach and Rolls, 2004; Kringelbach et al., 2003; Kringelbach, 2005).

Similarly, reward representations of combined sensory modes or combinations of attributes of stimuli have been observed in the most anterior OMFC subdivisions, extending even to the frontal pole. In our results as in those of other studies, the correlates of subjective ratings of pleasantness are observed in ventromedial, anterior areas. Therefore it merits consideration that modulated, conditional hedonic value is a more “complex” representation. Reward value representation and hedonic experience involve processing beyond the identification of a static stimulus and its attributes. In this respect, hedonic valuation is a complex instance of information processing, not least because of the integration of signals from the multiple sources potentially determining biological utility or the integration of contextual information determining reward and punishment association (e.g., Bray, Shimojo & O’Doherty, 2010, Morrison and Saltzman, 2009).

fMRI studies of primary rewards and punishers

Next, we will consider fMRI experiments that have involved scanning the response to primary rewards and punishers, principally those studies including modulated hedonic responses to, and subjective hedonic ratings of, such stimuli. For the purpose of focusing our discussion, we have adopted criteria derived from the behavioral level of analysis. The first criterion is the distinction of primary from secondary rewards (Rolls, 1999, Rolls et al., 2003; Kringelbach & Rolls, 2004) in experimental manipulations. Among studies of the former, the shared objective is to elucidate the neural correlates of the homeostatic value of a naturally occurring reward or punisher.

A secondary criterion is derived from the psychological level of analysis. Dimensional models of affect (Russell, 1980, 2003; Posner, Russell and Peterson, 2005) emphasize the orthogonality of affective valence processing and the processing of intensity or arousal. There is now evidence from neuroimaging that these separate dimensions have separable neural substrates (Posner et al., 2005, 2009; Colibazzi, Posner et al., 2010, Grimm et al., 2006). Lastly, we follow Kringelbach's (2005) model of the functional organization of the human OFC and ground this model in the excellent cytoarchitectonic studies and probabilistic atlases at our disposal (Carmichael & Price, 1995, 1996; Price, 1999; Ongur & Price, 2000, Ongur, Ferry & Price, 2003; Chiavaras and Petrides, 2000, 2001). Thus, inductively derived principles of functional subdivision can serve as a heuristic and neuroanatomical organization can serve as a definitive reference point.

In a translational experiment that bridges the primate single cell studies covered above and human neuroimaging, O'Doherty, Rolls and colleagues (2000) report OFC

BOLD signal decreases in response to the smell of a food eaten to satiety, but not to another food odor. In a second study (O'Doherty, Rolls et al., 2001), the same investigators delivered pleasant and aversive taste stimuli (i.e., glucose or salt) and report conjunction of localized BOLD response to the pleasant and aversive tastes in rostral, ventralmost OFC¹⁹, an area where BOLD signal was modulated by satiety.

The authors recognized that they had not isolated hedonic valuation with the latter experimental design, though they were able to conclude that both pleasant and unpleasant taste stimuli have separate and overlapping representations in the OFC (O'Doherty et al., 2001, p.1319, bottom right). They suggested two experimental approaches to demonstrating unambiguously the encoding of hedonic value in the OFC. These are: an fMRI replication of the selective satiety studies in which hedonic response to (whole food) gustatory stimuli was modulated by hunger in non-human primates (Rolls et al., 1983, 1986, 1989; Critchley & Rolls, 1996) and fMRI studies in other sensory modalities to test BOLD signal changes in OFC as a generalized index of the pleasant and aversive.

The Rolls group went on to execute both types of experiments, using selective satiety with whole food stimuli in one and somatosensory stimulation in another. Kringelbach, O'Doherty, Rolls and Andrews (2003) conducted an fMRI study that both extends the O'Doherty (2000) study of selective satiety and is a close analog of the present study in many respects. Specifically, the analogy includes the acquisition of two scans under different internal states. In their first scan they delivered two liquid food stimuli in alternating blocks, with rest periods during which they acquired subjective

¹⁹ Compare the results of O'Doherty et al., 2001, Figure 3., top row, p.1319, with the conjunction in OFC that we report above in Fig. 40 and 41., and to Chiavaras et al., 2001, Fig. 19, p. 490.

ratings of pleasantness and intensity on a visual analog scale. Participants then came out of the scanner and consumed one or the other liquid food to the point of satiety—literally to the point at which they simply could not take any more. Then the same trial sequence was repeated.

As with our study, the analysis comprised a general linear modeling of subjective pleasantness ratings and then a conjunction between the statistical maps from the respective stimulus conditions in two scans. As with our study, the conjunction maps show the areas of neural activity common to the modulated hedonic response to two different stimuli experienced during different motivational states (i.e., deviations from homeostasis: deprivation and satiety). Their finding was that bilateral OFC BOLD signal was conjoint, modulated by selective satiety and thus indexed the reward value of liquid foods. Furthermore, this activity was significantly correlated with subject ratings of pleasantness. Regardless of the sensory properties of the liquid foods, across subjects OFC BOLD signal tracked the decrease in the subjective pleasantness of the food eaten to satiety, while also tracking the unchanged subjective pleasantness of the food not eaten to satiety.

As with the single cell recording studies of non-human primates earlier run by the Rolls group (Rolls et al., 1983, 1986; Critchley and Rolls, 1996), this experiment (Kringelbach et al., 2003) has the merit of multi-modal stimulus presentation. Participants could taste, smell and feel the liquid food stimuli, yet the area of modulation by changing the motivational state (hunger in this case) was restricted to the bilateral OFC. This study illustrates an effective means of distinguishing the sensory from the hedonic; the concurrent sensory representations being diverse, conjunction analysis isolates the

common hedonic processes. The correlation with hedonic ratings serves to confirm that. Indeed, one significant advance from the primate studies is that neural activity could be statistically related to hedonic experience recorded in the form of subjective ratings.²⁰

In another fMRI study designed to distinguish the hedonic valuation of primary rewards and punishers from sensory perception, the Rolls group administered three types of touch to the hand (Rolls, O’Doherty, Kringelbach, et al., 2003): pleasant, neutral and moderately painful. The pleasant and neutral stimuli had been piloted in an earlier study (Francis, Rolls, et al., 1999), which indicated that the OFC was more responsive to pleasant than neutral touch. In the later study, the most statistically significant finding was a pronounced dissociation between bilateral OFC areas robustly activated by what they term the “affective aspects” of both the pleasant and unpleasant stimuli, and somatosensory areas activated only by a neutral control stimulus.

Another finding of note was segregation according to hedonic sign, whereby different areas of OFC (i.e., slightly more dorsal and medial) responded to the pleasant feeling of velvet as compared to areas that responded to the individually tuned, moderate pain of a pointed stylus (i.e., more ventral). The authors argue that this segregation further supports the conclusion that no single sensory property, such as the amount of force (mechanoreceptors) or the pain (nociceptors), engaged these two subregions of OFC. The localization of their results is striking close to our data (compare their Figure 2., p. 313, to the hedonic conjunction maps above in Figure 39., p. 109; 25 and 26, p. 68).

²⁰ The authors state their primary aim as “to obtain correlations between brain activity and the subjective emotion-related effects produced” by the stimuli (Kringelbach et al., 2003, p. 1064, right; see also p.1066, right)

Moreover, their observations also include activity of the subgenual cingulate in response to the pleasant stimulus.

Others have also sought to isolate the hedonic dimension of experience and thus identify its neural representation using fMRI. In a complementary pair of experiments, the first by Anderson and colleagues (2003), the second by Small and colleagues (2003), the investigators examined responses to olfactory and gustatory stimuli, respectively. Both experiments involved four stimulus conditions, comprising a 2 X 2 factorial design with two levels of stimulus intensity and two levels of affective valence²¹. Critically, this design facilitates comparisons between intensities or valences, while the other dimension is held constant: contrasts in BOLD signal could be modeled independently for valence or for intensity. Both groups report an anatomical dissociation between the neural representation of stimulus intensity, encoded by amygdala responses, and affective valence, encoded by subregions of the orbitofrontal cortex.

Specifically, Anderson and colleagues (2003) found, in concordance with prior studies of the hedonic valuation of olfactory stimuli (e.g., Critchley & Rolls, 1996; Rolls et al., 1989; O'Doherty et al., 2000), that BOLD response in right medial orbitofrontal gyrus was robust in response to the pleasant stimuli and equal at both intensity levels. This same region was also responsive to unpleasant stimuli, but to a lesser degree. Changes in left lateral OFC BOLD signal followed the presentation of unpleasant stimuli. In concordance with our observations, right OFC and subgenual cingulate activity

²¹ Anderson et al. and Small et al. follow Russell (1980, 2003); Posner, Russell and Peterson (2005); Posner et al., (2005, 2009); Colibazzi, Posner et al., (2010) *inter alia*, using the term “affective valence” to refer to one dimension in the circumplex or dimensional model of emotion. Affective valence is the equivalent of hedonic sign; it is “the hedonic tone of the subjectively experienced emotions, which may range from highly negative (i.e., unpleasant) emotions...to extremely positive (i.e., pleasant) ones” (Colibazzi, Posner et al., 2010, p.377).

correlated with subjective ratings of pleasantness, but not intensity, whereas bilateral OFC activity correlated with ratings of unpleasantness, but not intensity²².

Small and colleagues (2003) consummated these findings, applying the 2 X 2 design to gustatory stimuli and whole brain analyses, obtaining markedly similar results. They provide confirmatory evidence of the independence of hedonic value and stimulus intensity by virtue of their neural segregation. Acquiring scans during independent manipulation of hedonic sign and concentration, equated according to individual, pre-scan ratings, was critical to the validity of their comparisons. They report that right caudolateral OFC and subgenual cingulate (“subcallosal” in their terminology) BOLD correlates remained when the neutral condition was subtracted from the two levels of stimulus valence. Additional contrasts also indicated preferential response of the right caudolateral OFC to positive stimuli regardless of intensity (i.e., weak and intense pleasant minus weak and intense unpleasant). Left OFC showed preferential response to unpleasant stimuli, in subtractions of the neutral conditions from the unpleasant, but not in subtraction of the unpleasant from the pleasant conditions. Thus a similar constellation of associated structures in OFC and subgenual cingulate encodes hedonic sign, irrespective of intensity.

Finally, a recent fMRI study by Rolls, Grabenhorst and Parris (2009) demonstrates the neural representation of pleasant and unpleasant thermal stimuli applied to the hand. They delivered four non-noxious thermal stimuli, which were adjusted

²² Interestingly, the regions of interest (ROIs) in bilateral OFC and subgenual cingulate also were responsive to the clean air delivered through the olfactometer, which was the least intense stimulus. However, as dimensional models of affect dictate and these experiments confirm, intensity and valence are dissociable. Though “neutral” in respect to its intensity, in the Anderson experiment clean air could have a hedonic sign. It could be a relief or the termination of a reward, depending on context.

during a pre-scanning session to produce the desired pleasantness ratings. Their subjects rated a warm, pleasant stimulus; a cold, unpleasant, stimulus; and two graded mixtures, after each stimulus epoch. This latter detail is consequential, because the subjective ratings were not given during stimulus presentation, but instead a 4-second plateau period, during which the stimulus has reached its target temperature value, was indicated as the experience to be rated. In addition, the ratings of stimuli “tuned” for the desired hedonic results were to positive or negative ranges, respectively.

Rolls, Grabenhorst and Parris regressed subjective ratings of pleasantness or intensity against the BOLD signal and applied contrasts. The results of their region of interest analysis show that BOLD signal in medial OFC, subgenual cingulate, and ventral striatum correlated with pleasantness ratings, but not with intensity ratings. Moreover, their results are comparable with what we report in the present study and a direct comparison with our data is illuminating.

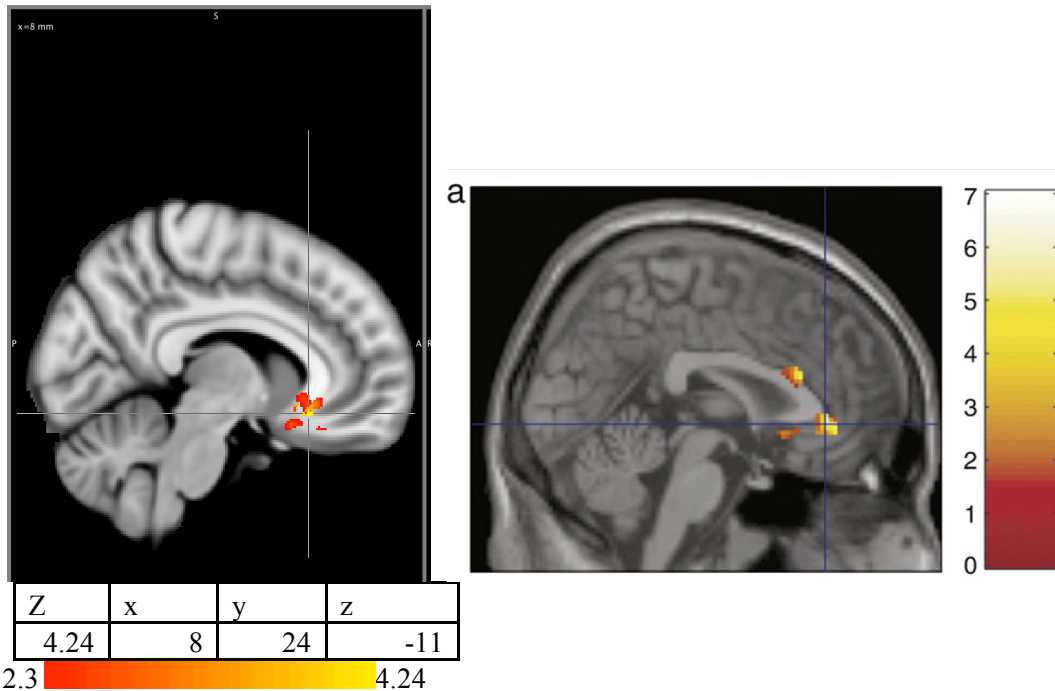


Figure 42. Left: Local maximum, hedonic ratings group analysis, hyperthermia scans Right: from Rolls, Grabenhorst & Parris, 2009, p. 1508, peak correlate of pleasantness ratings of warm, pleasant stimuli in subgenual OFC (peak at 4, 38, -2), used by permission.

The peak value in our hedonic ratings analysis of the hyperthermia scans is in a similar subgenual cingulate location to that reported by Rolls, Grabenhorst and Parris (2009)(see Figure 42., above). Yet there is a notable difference. In our data, while BOLD signal correlates in this area are conjoined between group maps from the two scanning conditions, interestingly the hypothermia peak correlates are elsewhere, in more lateral areas of the mid-OFC. As a consequence, the subgenual cingulate area in the figures above does not appear as a peak conjunction for the hedonic ratings analysis, even though this was the highest z-value we observed ($z=4.24$) in the hyperthermia condition group analysis.

This disparate result is very likely a function of key differences in experimental design. Rolls, Grabenhorst & Parris did not alter core temperature and therefore used the

cold stimulus only as a hedonically negative one. Their participants rated the cold stimulus on a scale from -2 to 0. Positive hedonic ratings of cold were thus not a possibility. In contrast, reversals of hedonic value are the key feature of our study: our participants experienced cold stimuli as hedonically positive when their core temperatures were elevated and warm stimuli as negative when their core temperatures were decreased. It is essential and suggestive to note that in the comparison of statistical maps above, the peak subgenual cingulate correlate from our data is derived from scans during which the hot stimulus was hedonically negative (i.e., unpleasant); while the Rolls data are functional correlates of hedonic ratings of a warm stimulus that was hedonically positive (i.e., ratings given on a scale from 0 to +2).

|

Limitations of the present study

We have reported that hedonic ratings tracked the sequence of and transitions between trials. However, the hedonic ratings acquired during hyperthermia scans vary in range, magnitude and frequency, as illustrated in Figure 15. (on page 53) of the Results section, and reproduced below.

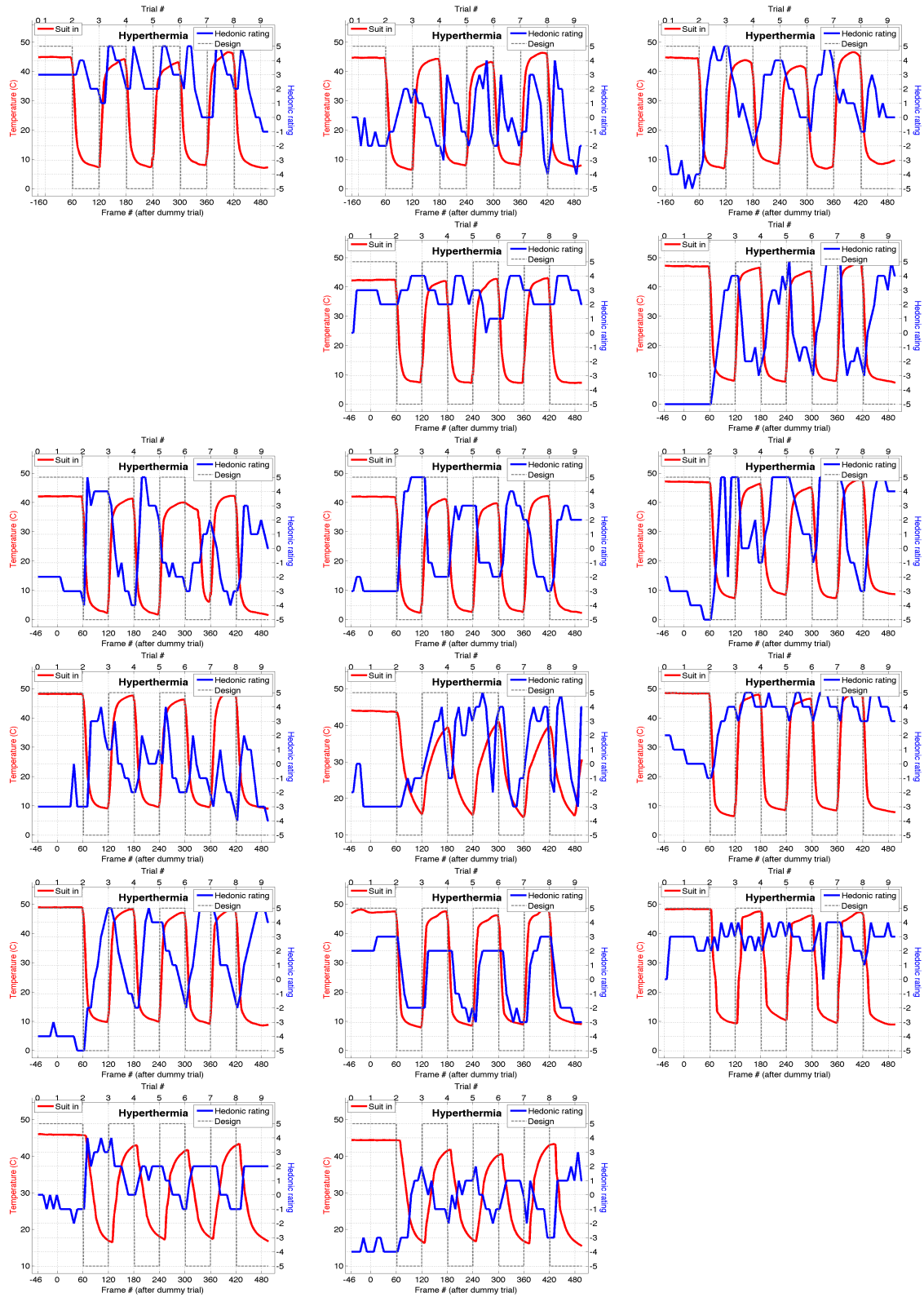


Figure 43. Hedonic ratings mosaic, hyperthermia scans (repeat of Figure 15.)

The variability in individual hedonic ratings given during the hyperthermia could have been a product of limitations in the present study. *Prima facie*, these behavioral data contradict our hypothesis. Some participants' hedonic ratings deviate from thermal *alliesthesia* when the temperature records indicate that they were, in fact, hyperthermic. To the extent that the cold stimuli were not experienced as pleasant during hyperthermia, it appears that our efforts at inducing hedonic experiences were not consistently successful. Moreover, the aberrant ratings affect statistical outcomes, because at the individual level of analysis, hedonic ratings are one of the vectors we used in our general linear model of the BOLD signal. In fact, the observed variability of hedonic ratings during the hyperthermia scans led us to construct the normative *alliesthesia* vectors from individual sensory ratings to model the predictions of our hypothesis. These normative vectors turned out to be a better fit to the data. The peak z values are higher²³ and there are a greater number of volume elements with correlated time courses.

One potential explanation is that because we did not monitor our participants' core temperatures across the nycthemeral cycle of thermoregulation (i.e., sleep/wake cycle). As a result, we simply do not know where the baseline temperatures we acquired were in that cycle. We took baseline temperatures at approximately 9:30 AM for all participants and always induced hyperthermia first. It is possible that within the respective nycthemeral cycles, some participants' core temperatures were still rising from values regulated during sleep. This would have consequences for both target temperatures. For hyperthermia, the deviation of +1°C may have actually been only 0.6°C or 0.7°C. While for hypothermia, the deviation may have exceeded -1°C. This

²³ Obviously, the reduced variability among the normative *alliesthesia* vectors contributed to the increased z-scores by minimizing the denominator value.

could account for the mismatch of hedonic ratings for some participants during hyperthermia and the consistency of ratings during hypothermia. A remedy for this limitation would be to sample baseline temperatures orally across the sleep-wake cycle in the days prior to scanning or to use ambulatory temperature monitoring devices.

A second potential explanation is that the range of peripheral or ambient temperatures that can be modulated hedonically by core temperature deviations does not extend indefinitely into the painful range. Cabanac's theory of thermal alliesthesia does not predict that all ranges of non-noxious thermal stimuli will be perceived as pleasant when core temperature is deviated (1971, 1979). Thermosensors in the skin will signal a temperature value that exceeds a hedonic threshold, despite the potential to remedy a core temperature deviation. The signal from peripheral thermosensors may have indicated that proximal tissue damage (or worse) would precede a return to normothermia, when an extremity was thermally stimulated. In that sense the cold stimulus could have been too intense, while a stimulus that indicated a more gradual return of core temperature to its normal range would have been more pleasant. More parsimoniously stated, it may simply have been that the cold stimulus was too cold for some: Even a team of reward researchers cannot please all of the people all of the time.

A third potential explanation entails the contribution of individual differences. The theory of alliesthesia may not completely account for the possibility of cognitive modulation of hedonic experience. If we take the hedonic ratings at face value, we might interpret the difference in the fit of the normative *alliesthesia* vectors and the hedonic ratings vectors to the BOLD signal changes in light of Craig's extensive work on interoception. Critically, the afferent pathway of interoception is neurally segregated

from the representations of sensory perception (see Craig, 2002, p.655, middle column). This dissociation maps onto that between the hedonic ratings, which reflect the individual's sense of the condition of their body, and sensory ratings, which are the basis of the normative alliesthesia vectors.

If individual differences in interoceptive awareness modulate hedonic ratings, they would do so without necessarily altering sensitivity to peripheral sensation. This might account for both the variability of the hedonic ratings and the accuracy of the sensory. Craig and colleagues (Craig, 2002; 2000), among others (Wiens, 2005; Pollatos et al., 2007a & b; Critchley et al., 2004), have shown that there are indeed significant individual differences in interoceptive awareness. These may be quantified using interoceptive awareness tasks, such as variants of heartbeat detection (Wiens et al., 2000, 2001; Critchley et al., 2004). If alliesthesia depends on internal signals (Cabanac, 1971, p. 1105), then alliesthesia requires interoception. The sense of core temperature deviation and the awareness of resulting thermoeffector responses should contribute to the modulation of the hedonic value of peripheral thermal stimulation. Our subsequent studies of thermal *alliesthesia* should include assessments of interoceptive awareness as a potential modulator of hedonic response.

It is plausible, considered at the psychological or phenomenological level of analysis, that the conscious hedonic experience of individual participants was simply more variable than predicted, given the theory of thermal *alliesthesia*. But even a glance at the hedonic ratings given under hypothermia (see Figure 16., above, p. 54) is sufficient to see conformity to the theory. If the pattern in behavioral data were simply a matter of variability due to individual differences (e.g., in interoceptive awareness, attention or

learned preferences), what explanation do we have for the observation that these individual differences did not manifest under both core temperature deviations? Why was the variability not more equally distributed in the two conditions?

It does not stand to reason, given that hyperthermia is much closer to the limit of survivable core temperatures than hypothermia (see Romanovsky, 2007, for review²⁴), that it would be a less potent modulator of hedonic responses. If anything, the thermoregulatory asymmetry might lead us to predict the opposite: hyperthermia should be a more potent modulator. Indeed, the biological utility of a warm stimulus during hypothermia might be less, in proportion to the distance between deviated core temperature and a dangerously low core temperature (i.e., over ten degrees for hypothermia).

It is also plausible that our participants were accustomed to elevated core temperatures because of their exercise routines and that the one-degree deviation we induced was easily within their range of comfort. This would account for the positive hedonic ratings that some participants gave even to the first “hot” trials under hyperthermia. Though designed to be aversive, the hedonic quality of a warm stimulus under +1°C hyperthermia may not be encoded as a threat of exacerbation. The “utility” may still have a positive value to someone who spends hours a day at +2.5°C. Indeed, when associated with peak performance, physical mastery and all the rewards that come with them, relative hyperthermia might become tolerable or even pleasant. For such a person, a warm stimulus at +1°C promises to shift core temperature further in a

²⁴ “First, our thermal physiology is “asymmetrical:” (body temperature) is positioned very closely, within just a few degrees Celsius, to the upper survival limit...but relatively far, a few tens of degrees, from the lower limit. Therefore, core overheating is much more dangerous than overcooling.” (Romanovsky, 2007, p. 37, right)

hedonically positive direction. In comparison, it is difficult to bring to mind a routine behavioral objective that results in becoming more and more cold, or seeking out a cold core temperature combined with increasingly cold skin temperature. This may represent one hedonic asymmetry.

Another hedonic asymmetry may be tied to the value of warmth for mammals. It is certain that the hedonic value of parental care, affection, feeding, affiliation within a pack, sexual relations, and much else is associated with warmth in a manner unmatched by cool or cold stimuli. We might well ask if it is possible that asymmetries in mammalian thermal preferences exemplify what Sander, Grandjean and Scherer (2005) characterized as genetically fixed schemata and overlearned associations, or Damasio characterized as the basic set of “preferences, criteria, biases or values” (1994, p.117), that serve to classify stimuli into categories of “good” and “bad”. Rolls, Grabenhorst and Parris (2009, p. 1504) remark that: “approach to warmth and avoidance of cold may be reinforcers or goals for action built into us during evolution to direct our behavior to stimuli that are important for survival.” In relation to such genetic and evolutionary factors, thermal alliesthesia may be limited in its modulatory power.

Interpreting the limitation

Beyond accounts of the individual differences in thermal preference that may have mediated the variability in ratings under hyperthermia, there is a weaker and a stronger version of the inference that we might draw from the fit of the normative *alliesthesia* vectors to the BOLD signal. The “weaker” version is that regulatory,

autonomic processes track the hedonic pattern of our design. These processes do have hedonic import and may result in hedonic experience if the magnitude or duration of the state-stimulus combination merits it. Yet during the given trial of our scan, these may not have triggered, or manifested as, conscious hedonic experience.

This position accords with Damasio's thinking on the functional role of hedonic responses (1994, 1999). His Jamesian emphasis on sensed body states, the "continuously updated image of the structure and state of our body" (1994, p.xiv) as the origin of felt emotion, is well suited to the present study. Considering "feelings (as) the sensors for the match or lack thereof between nature and circumstance" (1994, p.xv) coincides with the view of hedonic experience signaling the match or mismatch between a stimulus and a homeostatic imperative. But a more interesting question remains: Under what exact conditions are regulatory processes manifested as consciously experienced emotion, with a characteristic hedonic quality?

The stronger version of the inference that we might draw from the fit of the normative *alliesthesia* vectors to the BOLD signal is that they model the pattern of both conscious and unconscious affective processes. The latter, in fact, comprise the better part of hedonic valuation, in the manner that unconscious processes comprise the majority of the neurophysiological responses we term "affect". As such, unconscious affective processes include the engagement of neural modules with extremely fast, automatic processing, as well as autonomic responses and conditioned habits. Their manifestations are only intermittently conscious, as gated by attention; their existence is inferred from effects on behavior.

The “strong” view of unconscious affective processes is compatible with multi-stage appraisal models of emotion in that unconscious processing may account for an initial stage of encoding. Considering the single cell recording evidence from Kawasaki and colleagues (2001, 2005) described above, there is evidence that the OFC contributes to this early encoding and that selective neuronal responding occurs on a timescale that rules out conscious awareness. As formulated in Scherer’s componential appraisal model (Sander, Grandjean & Scherer, 2005; Grandjean, Sander, & Scherer, 2008), hedonic valuation is part of a continuous and recursive series of processes of which conscious affective states are one, minority component (see model in Grandjean, Sander, & Scherer, 2008, p. 487, Figure 3).

Finally, dimensional models (Russell, 1980, Posner, Russell and Peterson, 2005), like componential appraisal models of emotion (Sander, Grandjean & Scherer, 2005; Grandjean, Sander, & Scherer, 2008) include the feature of ambiguity in conscious affective experience. Like the communication of any ongoing affective process, concurrent hedonic rating is inherently challenging. In relation to the many concurrent processes, the many points of attentional focus, the area of valid self-report of emotional experience is relatively small. This has been comprehensively demonstrated by Ohman and colleagues (Ohman et al., 2007; Morris, Ohman & Dolan, 1999; Carlsson et al., 2004; Mineka & Ohman, 2002; Katkin, Wiens & Ohman, 2001; *inter alia*) and theoretically integrated by Scherer and colleagues (Sander, Grandjean & Scherer, 2005; Grandjean, Sander, & Scherer, 2008).

Future Directions

The variable hedonic ratings given during hyperthermia may have important implications for hedonic experience, yet if they were the result of limitations in our control of hedonic states, the remedies may be prosaic engineering and experimental design changes. First, we are in the process of addressing an engineering problem that contributed to this possible limitation in the study. Having observed that the heating units are not powerful enough to consistently deliver water heated to the set point of 52°C and reaching the suit at approximately 46°C, we have purchased an ancillary heater that will boost our heating capacity. The anticipated effect is not trivial: If the hot stimulus is attenuated, then the hedonic response to it and to the cold stimulus is attenuated. One reason that the hedonic ratings during hyperthermia were so variable may be that the hot water was not as hot as had been intended. Second, we plan to counterbalance the order of core temperature deviations and obtain the most accurate baseline temperatures possible by monitoring the changes in core temperature over the nycthemeral cycle.

Third, we plan to add an experimental session prior to scanning in which we “tune” the thermal stimuli to individual preferences (see Rolls, Grabenhorst & Parris, 2009). Participants would undergo a limited sequence of peripheral thermal stimulation (i.e., different from the subsequent scan) while hyperthermic and hypothermic. Very much like the experiment that Cabanac, Massonet and Belaiche (1972) executed, participants would adjust the stimuli to a temperature that is most pleasant during hedonically positive trials. We would then use the individually tuned mean temperature value as the hedonically positive stimuli during their subsequent scan (e.g., Rolls, Grabenhorst & Parris, 2009; Anderson et al., 2003; Small et al., 2003). If the engineering

difficulties could be surmounted, we might actually “yoke” the participants to their prior selections, by delivering exactly the sequence we recorded in the behavioral session (i.e., include any changes that were selected and present them over the same time scale).

The inextricable limitation of functional neuroimaging experiments is the existence of concurrent neural processes. Whole brain functional data acquisition, as applied in this study, cannot isolate any single process, no matter how adroit the experiment design. Though we have taken pains to design and execute an experiment in which hedonic valuation processes are distinguished from sensation by their pattern of modulation, we cannot discount the possibility that concurrent expectation, anticipation or dread contribute to the pattern of BOLD signal changes we have modeled statistically. Nor can we discount other affective, cognitive or physiological processes that might be concurrent and whose BOLD signal changes take the sinusoidal form of our explanatory variables of interest (i.e., the hedonic ratings or normative alliesthesia vectors).

Properly designed, intermediate term experiments might help clarify these questions. In them we would use the same general design of core temperature deviations, two scans and sequences of peripheral thermal stimulation. We would eliminate the potential limitations mentioned above by boosting our heating capacity, determining baseline temperatures in relation to the record of nycthemeral cyclic values, and including the pre-scan behavioral session to tune the hedonically positive stimuli. In one possible variant, we could take the approach of isolating hedonic experience from the appraisal of it. Our model would be a study by Grimm and colleagues (2006), who isolated valence encoding from the cognitive processes of judgment and attention. Their design matrix was a homolog of the 2 X 2 used in Anderson and colleagues (2003) and

Small and colleagues (2003), encompassing the following conditions: concurrent judgment versus passive experience/feeling, and cued versus uncued trials.

In another variant we would test the potential modulation of hedonic response during *alliesthesia* by interoceptive awareness and cues directing attention to the internal state. We would include a pre-scanning test of interoceptive awareness (Critchley, 2004; Critchley et al., 2004) and the Levels of Emotional Awareness Scale (LEAS, Lane et al., 1990). Pairs of ratings epochs from the current experimental design (i.e., blocks of 18s) would alternate between the appearance of rating scales and a static direction to close the eyes and concentrate on feeling the current state of the body. The resulting data could be modeled with an interpolated ratings vector, as we have done with the present experiment, and with a block-design vector that differentiated between “directed feeling” and “appraising” epochs.

Subsequent planned experiments in our laboratory have already been designed to isolate the array of expectancies that attend hedonic responses (e.g., desire, wanting, anticipation, dread). These experimental designs, elaborated elsewhere, will complement the present study and account for anticipatory processes, with particular reference to the prominent view that hedonic experience and the anticipation of it, “liking” and “wanting,” are distinguishable (Berridge & Kringelbach, 2007).

Conclusion

We have attempted to bridge the objective and the subjective in several ways through this experiment. We manipulated the objective physiological determinants of thermal alliesthesia to induce a pattern of subjective hedonic experiences. We confirmed our manipulation by acquiring objective measures of the constituent physiological changes and the sequences of thermal stimulation. We recorded subjective ratings of the stimuli. We acquired objective measures of brain activity in synchrony with hedonic experiences as communicated in the subjective ratings. Our results comprise evidence for the neural representation of hedonic value in the orbitomedial prefrontal cortex (OMPFC) network, inclusive of the subgenual cingulate and rostral temporal cortex. The unique contributions that we present include our modulation of the hedonic value of peripheral thermal stimuli without alteration of their physical attributes. We identify correlates of hedonic experience, which is paradigmatic of subjectivity, that are distinct from correlates of sensory information processing, which maps the objective world.

References

- Adolphs, R., Kawasaki, H., Oya, H., & Howard, M. (2006). Intracranial electrophysiology of the human orbitofrontal cortex. In Zald, D.H., & Rauch, S.L. (Eds.). (355-376). Oxford: Oxford University Press.
- Aharon, I., Etcoff, N., Ariely, D., Chabris, C., O'Connor, E., & Breiter, H. (2001). Beautiful faces have variable reward value: fMRI and behavioral evidence. *Neuron*, *32*, 537-551.
- Anders, S., Lotze, M., Erb, M., Grodd, W., & Birbaumer, N. (2004). Brain activity underlying emotional valence and arousal: A response-related fMRI study. *Human Brain Mapping*, *23*, 200-209.
- Anderson, A., Christoff, K., Stappen, I., Panitz, D., Ghahremani, D., Glover, G., et al. (2003). Dissociated neural representations of intensity and valence in human olfaction. *Nature Neuroscience*, *6*, 196-202.
- Attia, M. (1984). Thermal pleasantness and temperature regulation in man. *Neuroscience & Biobehavioral Reviews*, *8*, 335-342.
- Attia, M., & Engel, P. (1981). Thermal alliesthesial response in man is independent of skin location stimulated. *Physiology & behavior*, *27*, 439-444.
- Attia, M., & Engel, P. (1982). Thermal pleasantness sensation: an indicator of thermal stress. *European Journal of Applied Physiology and Occupational Physiology*, *50*, 55-70.
- Beckmann, C., Jenkinson, M., & Smith, S. (2002). General multilevel linear modeling for group analysis in FMRI. *NeuroImage*, *20*, 1052-1063.
- Beckmann, C., & Smith, S. (2004). Probabilistic independent component analysis for functional magnetic resonance imaging. *Medical Imaging, IEEE Transactions on Medical Imaging*, *23*(2), 137-152.
- Berridge, K., & Kringelbach, M. (2007). Affective neuroscience of pleasure: reward in humans and animals. *Psychopharmacology*, *199*, 457-480.
- Block, N. (1990). Inverted earth. *Philosophical perspectives*, *4*, 53-79.
- Boulant, J., & Dean, J. (1986). Temperature receptors in the central nervous system. *Annual review of physiology*, *48*, 639-654.
- Bray, S., Shimojo, S., & O'Doherty, J. (2010). Human medial orbitofrontal cortex is recruited during experience of imagined and real rewards. *Journal of Neurophysiology*, *103*, 2506.

- Cabanac, M. (1969). Plaisir ou déplaisir de la sensation thermique et homeothermie. *Physiology & behavior*, 4, 359-364.
- Cabanac, M. (1971). Physiological role of pleasure. *Science*, 173, 1103.
- Cabanac, M. (1979). Sensory pleasure. *Quarterly Review of Biology*, 54, 1-29.
- Cabanac, M., & Massonnet, B. (1977). Thermoregulatory responses as a function of core temperature in humans. *The Journal of Physiology*, 265, 587.
- Cabanac, M., Massonnet, B., & Belaiche, R. (1972). Preferred skin temperature as a function of internal and mean skin temperature. *Journal of Applied Physiology*, 33, 699.
- Carlsson, K., Peterson, K.M., Lundqvist, D., Karlsson, A., Ingvar, M., Ohman, A. (2004). Fear and the amygdala: Manipulation of awareness generates differential cerebral responses to phobic and fear-relevant (but nonfeared) stimuli. *Emotion*, 4, 340-353.
- Chiavaras, M. M., LeGoualher, G., Evans, A., & Petrides, M. (2001). Three-dimensional probabilistic atlas of the human orbitofrontal sulci in standardized stereotaxic space. *NeuroImage*, 13, 479-496.
- Chiavaras, M. M., & Petrides, M. (2000). Orbitofrontal sulci of the human and macaque monkey brain. *The Journal of comparative neurology*, 422, 35-54.
- Churchland, P. (1985). Reduction, qualia, and the direct introspection of brain states. *The Journal of Philosophy*, 82, 8-28.
- Colibazzi, T., Posner, J., Wang, Z., Gorman, D., Gerber, A., Yu, S., et al. (2010). Neural systems subserving valence and arousal during the experience of induced emotions. *Emotion*, 10, 377-389.
- Craig, A. (2002). How do you feel? Interoception: the sense of the physiological condition of the body. *Nature Reviews Neuroscience*, 3, 655-666.
- Craig, A. (2003). Interoception: the sense of the physiological condition of the body. *Current opinion in neurobiology*.
- Craig, A. (2004). Human feelings: why are some more aware than others? *Trends in cognitive sciences*, 8, 239-241.
- Craig, A., Chen, K., Bandy, D., & Reiman, E. (2000). Thermosensory activation of insular cortex. *Nature Neuroscience*, 3, 184-190.
- Critchley, H. D., & Rolls, E. T. (1996). Hunger and satiety modify the responses of olfactory and visual neurons in the primate orbitofrontal cortex. *Journal of Neurophysiology*, 75, 1673-1686.

- Critchley, H. (2004). The human cortex responds to an interoceptive challenge. *Proceedings of the National Academy of Sciences of the United States of America*, 101, 6333.
- Critchley, H., Wiens, S., Rotshtein, P., Ohman, A., & Dolan, R. (2004). Neural systems supporting interoceptive awareness. *Nature Neuroscience*, 7, 189-195.
- Damasio, A., Grabowski, T., Bechara, A., Damasio, H., Ponto, L., Parvizi, J., et al. (2000). Subcortical and cortical brain activity during the feeling of self-generated emotions. *Nature Neuroscience*, 3, 1049-1056.
- Damasio, A. R. (1994). *Descartes' Error*. New York: Putnam.
- Damasio, A. R. (1999). *The Feeling of What Happens*. New York: Harcourt.
- Dolan, R. J., Lane, R., Chua, P., Fletcher, P. (2000). Dissociable temporal lobe activations during emotional episodic memory retrieval. *Neuroimage*, 11, 203-209.
- Dolan, R. J. (2002). Emotion, cognition, and behavior. *Science*, 298, 1191-1194.
- Dolan, R. J. (2007). Keynote address: revaluing the orbital prefrontal cortex. *Annals of the New York Academy of Sciences*, 1121, 1-9.
- Dolcos, F., LaBar, K., & Cabeza, R. (2004). Dissociable effects of arousal and valence on prefrontal activity indexing emotional evaluation and subsequent memory: an event-related fMRI study. *NeuroImage*, 23, 64-74.
- Drevets, W., Raichle, M.E. (1992). Neuroanatomical circuits in depression: implications for treatment mechanisms. *Pharmacological Bulletin* 28 (3), 261--274.
- Drevets, W. (2000). Neuroimaging studies of mood disorders. *Biological Psychiatry* 48, 813-829.
- Drevets, W., Price, J., Simpson, J., Todd, R., Reich, T., Vannier, M., et al. (1997). Subgenual prefrontal cortex abnormalities in mood disorders. *Nature*, 386, 824-827.
- Drevets, W., Savitz, J., & Trimble, M. (2008). The subgenual anterior cingulate cortex in mood disorders. *CNS spectrums*, 13, 663.
- Drevets, W., Price, J., Furey, M.L. (2008). Brain structural and functional abnormalities in mood disorders: implications for neurocircuitry models of depression. *Brain Structure and Function*, 213, 93-118.
- Drevets, W. C. (1998). Functional neuroimaging studies of depression: the anatomy of melancholia. *Annual review of medicine*, 49, 341-361.

- Drevets, W. C., Ongur, D., & Price, J. L. (1998). Neuroimaging abnormalities in the subgenual prefrontal cortex: implications for the pathophysiology of familial mood disorders. *Mol Psychiatry*, 3(3), 220-226, 190-221.
- Drevets, W. C., Ongur, D., & Price, J. L. (1998). Reduced glucose metabolism in the subgenual prefrontal cortex in unipolar depression. *Mol Psychiatry*, 3(3), 190-191.
- Francis, S., Rolls, E., Bowtell, R., McGlone, F., O'Doherty, J., Browning, A., et al. (1999). The representation of pleasant touch in the brain and its relationship with taste and olfactory areas. *Neuroreport*, 10, 453.
- Gottfried, J., Deichmann, R., Winston, J., & Dolan, R. (2002). Functional heterogeneity in human olfactory cortex: an event-related functional magnetic resonance imaging study. *Journal of Neuroscience*, 22, 10819.
- Grabenhorst, F., & Rolls, E. T. (2009). Different representations of relative and absolute subjective value in the human brain. *NeuroImage*, 48(1), 258-268.
- Grandjean, D., Sander, D., & Scherer, K. (2008). Conscious emotional experience emerges as a function of multilevel, appraisal-driven response synchronization. *Consciousness and cognition*, 17, 484-495.
- Grimm, S., Schmidt, C., Bermpohl, F., Heinzl, A., Dahlem, Y., Wyss, M., et al. (2006). Segregated neural representation of distinct emotion dimensions in the prefrontal cortex--an fMRI study. *NeuroImage*, 30, 325-340.
- Heinzl, A., Bermpohl, F., Niese, R., Pfennig, A., Pascual-Leone, A., Schlaug, G., et al. (2005). How do we modulate our emotions? Parametric fMRI reveals cortical midline structures as regions specifically involved in the processing of emotional valences. *Cognitive Brain Research*, 25, 348-358.
- Hemenover, S.H. (2003). Individual differences in rate of affect change: studies in affective chronometry. *Journal of Personality and Social Psychology*, 85(1), 121-131.
- James, W. (1884). What is an Emotion? *Mind*, 9, 188-205.
- James, W. (1894). The physical basis of emotion. *Psychological review*, 1, 516-529.
- Jenkinson, M. & Beckmann, C. (2001). ICA in FMRI: A Basic Introduction. FMRIB Technical Report TR01MJ2. Retrieved from:
(<http://www.fmrib.ox.ac.uk/analysis/research/melodic/melodic/?searchterm=technical%2>

Oreport)

- Kahnt, T., Heinzle, J., Park, S., & Haynes, J. (2010). The neural code of reward anticipation in human orbitofrontal cortex. *Proceedings of the National Academy of Sciences*, *107*, 6010.
- Kalisch, R., Wiech, K., Critchley, H., & Dolan, R. (2006). Levels of appraisal: a medial prefrontal role in high-level appraisal of emotional material. *NeuroImage*, *30*, 1458-1466.
- Katkin, E., Wiens, S., & Ohman, A. (2001). Nonconscious fear conditioning, visceral perception, and the development of gut feelings. *Psychological Science*, *12*, 366.
- Kawabata, H. & Zeki, S. (2008). The neural correlates of desire. *PLoS ONE* *3*(8):e3027. doi:10.1371/journal.pone.0003027.
- Kawasaki, H., Adolphs, R., Kaufman, O., Damasio, H., Damasio, A., Granner, M., et al. (2001). Single-neuron responses to emotional visual stimuli recorded in human ventral prefrontal cortex. *Nature Neuroscience*, *4*, 15-16.
- Kawasaki, H., Adolphs, R., Oya, H., Kovach, C., Damasio, H., Kaufman, O., et al. (2005). Analysis of single-unit responses to emotional scenes in human ventromedial prefrontal cortex. *Journal of cognitive neuroscience*, *17*, 1509-1518.
- Kirk, U., Skov, M., Christensen, M. S., & Nygaard, N. (2009). Brain correlates of aesthetic expertise: A parametric fMRI study. *Brain and cognition*, *69*(2), 306-315.
- Knutson, B., Fong, G., Bennett, S., Adams, C., & Hommer, D. (2003). A region of mesial prefrontal cortex tracks monetarily rewarding outcomes: characterization with rapid event-related fMRI. *NeuroImage*, *18*, 263-272.
- Kringelbach, M. L. (2004). Food for thought: hedonic experience beyond homeostasis in the human brain. *Neuroscience*, *126*, 807-819.
- Kringelbach, M. L. (2005). The human orbitofrontal cortex: linking reward to hedonic experience. *Nature Reviews Neuroscience*, *6*, 691-702.
- Kringelbach, M. L., O'Doherty, J., Rolls, E. T., & Andrews, C. (2003). Activation of the human orbitofrontal cortex to a liquid food stimulus is correlated with its subjective pleasantness. *Cerebral cortex*, *13*, 1064-1071.
- Kringelbach, M. L., & Rolls, E. T. (2004). The functional neuroanatomy of the human orbitofrontal cortex: evidence from neuroimaging and neuropsychology. *Progress in neurobiology*, *72*, 341-372.
- Lang, P.J. & Ohman, A. (1988). The international affective picture system (photographic slides). Gainesville, FL: Center for Research in Psychophysiology.

- Lewis, P., Critchley, H., Rotshtein, P., & Dolan, R. (2007). Neural correlates of processing valence and arousal in affective words. *Cerebral Cortex*, *17*, 742.
- Liotti, M., Mayberg, H., Brannan, S., McGinnis, S., Jerabek, P., & Fox, P. (2000). Differential limbic-cortical correlates of sadness and anxiety in healthy subjects: implications for affective disorders. *Biological psychiatry*, *48*, 30-42.
- Loar, B. (1990). Phenomenal states. *Philosophical Perspectives*, *4*, 81-108.
- Marks, L., & Gonzalez, R. (1974). Skin temperature modifies the pleasantness of thermal stimuli. *Nature*, *247*, 473-475.
- Mayberg, H., Liotti, M., Brannan, S., McGinnis, S., Mahurin, R., Jerabek, P., et al. (1999). Reciprocal limbic-cortical function and negative mood: converging PET findings in depression and normal sadness. *American Journal of Psychiatry*, *156*, 675.
- McAllen, R., Farrell, M., Johnson, J., Trevaks, D., Cole, L., McKinley, M., et al. (2006). Human medullary responses to cooling and rewarming the skin: a functional MRI study. *Proceedings of the National Academy of Sciences of the United States of America*, *103*, 809.
- Mineka, S. & Ohman, A. (2002). Phobias and preparedness: The selective, automatic, and encapsulated nature of fear. *Biological Psychiatry*, *52*, 927–937.
- Morris, J.S., Ohman, A., & Dolan, R.J. (1999). A subcortical pathway to the right amygdala mediating “unseen” fear. *Proceedings of the National Academy of Sciences*, *96*, 1680–1685.
- Morrison, S. E., & Salzman, C. D. (2009). The convergence of information about rewarding and aversive stimuli in single neurons. *The Journal of neuroscience: the official journal of the Society for Neuroscience*, *29*, 11471-11483.
- Mower, G. (1976). Perceived intensity of peripheral thermal stimuli is independent of internal body temperature. *Journal of Comparative and Physiological Psychology*, *90*, 1152-1155.
- Murphy, F., Nimmo-Smith, I., & Lawrence, A. (2003). Functional neuroanatomy of emotions: a meta-analysis. *Cognitive, Affective, & Behavioral Neuroscience*, *3*, 207.
- Nielen, M., Heslenfeld, D., Heinen, K., Strien, J. V., Witter, M., Jonker, C., et al. (2009). Distinct brain systems underlie the processing of valence and arousal of affective pictures. *Brain and cognition*, 1-10.
- Northoff, G., & Bermpohl, F. (2004). Cortical midline structures and the self. *Trends in Cognitive Science*, *8*, 102-107.
- Northoff, G., Heinzl, A., de Greck, M., Bermpohl, F., Dobrowolny, H., & Panksepp, J. (2006).

Self-referential processing in our brain- A meta-analysis of imaging studies on the self. *NeuroImage*, 31, 440-457.

- Northoff, G., & Panksepp, J. (2008). The trans-species concept of self and the subcortical-cortical midline system. *Trends in cognitive sciences*, 12, 259-264.
- O'Doherty, J.P., Rolls, E., Francis, S., Bowtell, R., & McGlone, F. (2000). Sensory-specific satiety-related olfactory activation of the human orbitofrontal cortex. *NeuroReport*, 11, 893-897.
- O'Doherty, J.P., Rolls, E., Francis, S., Bowtell, R., & McGlone, F. (2001). Representation of pleasant and aversive taste in the human brain. *Journal of Neurophysiology*, 85, 1315.
- O'Doherty, J.P., Winston, J., Critchley, H., Perrett, D., Burt, D., & Dolan, R. (2003). Beauty in a smile: the role of medial orbitofrontal cortex in facial attractiveness. *Neuropsychologia*, 41, 147-155.
- O'Doherty, J. P. (2004). Reward representations and reward-related learning in the human brain: insights from neuroimaging. *Current opinion in neurobiology*, 14, 769-776.
- O'Doherty, J. P. (2004). Lights, camembert, action! The role of the human orbitofrontal cortex in encoding stimuli, rewards and choices. *Annals of the New York Academy of Sciences*, 1121: 254-272.
- Ohman, A., Carlsson, K., Lundqvist, D., & Ingvar, M. (2007). On the unconscious subcortical origin of human fear. *Physiology & behavior*, 92, 180-185.
- Ongur, D., Ferry, A. T., & Price, J. L. (2003). Architectonic subdivision of the human orbital and medial prefrontal cortex. *The Journal of comparative neurology*, 460, 425-449.
- Ongur, D., & Price, J. L. (2000). The organization of networks within the orbital and medial prefrontal cortex of rats, monkeys and humans. *Cerebral cortex*, 10, 206-219.
- Ongur, D., Ferry, A. T., & Price, J. L. (2003). Architectonic subdivision of the human orbital and medial prefrontal cortex. *J Comp Neurol*, 460(3), 425-449.
- Pessiglione, M., Petrovic, P., Daunizeau, J., Palminteri, S., Dolan, R., & Frith, C. (2008). Subliminal instrumental conditioning demonstrated in the human brain. *Neuron*, 59, 561-567.
- Petrides, M., & Pandya, D. (2001). Comparative cytoarchitectonic analysis of the human and the macaque ventrolateral prefrontal cortex and corticocortical connection patterns in the monkey. *European Journal of Neuroscience*, 16, 291-310.
- Phan, K., Wager, T., Taylor, S., & Liberzon, I. (2002). Functional neuroanatomy of emotion: a meta-analysis of emotion activation studies in PET and fMRI. *NeuroImage*, 16, 331-348.

- Phan, K., Taylor, S., Welsh, R.C., Ho, S.-H., Britton, J.C., & Liberzon, I. (2004). Neural correlates of individual ratings of emotional salience: A trial-related fMRI study. *NeuroImage, 21*, 768-780.
- Poldrack, R., Fletcher, P., Henson, R., Worsley, K., Brett, M., & Nichols, T. (2008). Guidelines for reporting an fMRI study. *NeuroImage, 40*, 409-414.
- Pollatos, O., Gramann, K., & Schandry, R. (2007a). Neural systems connecting interoceptive awareness and feelings. *Human Brain Mapping, 28*, 9-18.
- Pollatos, O., Traut-Mattausch, E., Schroeder, H., & Schandry, R. (2007b). Interoceptive awareness mediates the relationship between anxiety and the intensity of unpleasant feelings. *Journal of anxiety disorders, 21*, 931-943.
- Pollatos, O., Schandry, R., Auer, D., & Kaufmann, C. (2007c). Brain structures mediating cardiovascular arousal and interoceptive awareness. *Brain research, 1141*, 178-187.
- Posner, J., Russell, J. A., Gerber, A., Gorman, D., Colibazzi, T., Yu, S., et al. (2009). The Neurophysiological Bases of Emotion: An fMRI Study of the Affective Circumplex Using Emotion-Denoting Words. *Human Brain Mapping, 30*, 883-895.
- Posner, J., Russell, J. A., & Peterson, B. S. (2005). The circumplex model of affect: an integrative approach to affective neuroscience, cognitive development, and psychopathology. *Development and psychopathology, 17*, 715-734.
- Price, J. L. (1999). Prefrontal cortical networks related to visceral function and mood. *Annals of the New York Academy of Sciences, 877*, 383-396.
- Price, J. L. & Drevets, W.C. (2010). Neurocircuitry of mood disorders. *Neuropsychopharmacology Reviews 35*, 192-216.
- Rolls, E., Murzi, E., Yaxley, S., Thorpe, S., & Simpson, S. (1986). Sensory-specific satiety: food-specific reduction in responsiveness of ventral forebrain neurons after feeding in the monkey. *Brain Research, 368*, 79-86.
- Rolls, E., Sienkiewicz, Z.J., & Yaxley, S. (1989). Hunger modulates the responses to gustatory stimuli of single neurons in the caudolateral orbitofrontal cortex of the macaque monkey. *European Journal of Neuroscience, 1*, 53-60.
- Rolls, E. T., Yaxley, S., & Sienkiewicz, Z. J. (1990). Gustatory responses of single neurons in the caudolateral orbitofrontal cortex of the macaque monkey. *Journal of Neurophysiology, 64*, 1055-1066.

- Rolls, E. (1999). The functions of the orbitofrontal cortex. *Neurocase*, 5, 301-312.
- Rolls, E. (2000). The orbitofrontal cortex and reward. *Cerebral Cortex*, 10, 284.
- Rolls, E., O'Doherty, J., Kringelbach, M., Francis, S., Bowtell, R., & McGlone, F. (2003). Representations of pleasant and painful touch in the human orbitofrontal and cingulate cortices. *Cerebral Cortex*, 13, 308.
- Rolls, E. T. (2004). The functions of the orbitofrontal cortex. *Brain and cognition*, 55, 11-29.
- Rolls, E. T., & Grabenhorst, F. (2008). The orbitofrontal cortex and beyond: from affect to decision-making. *Progress in neurobiology*, 86, 216-244.
- Rolls, E., Grabenhorst, F., & Parris, B. (2009). Warm pleasant feelings in the brain. *NeuroImage*, 41, 1504-1513.
- Romanovsky, A. (2007). Thermoregulation: some concepts have changed. Functional architecture of the thermoregulatory system. *American Journal of Physiology-Regulatory, Integrative and Comparative Physiology*, 292, R37.
- Royet, J., Zald, D., Versace, R., Costes, N., Lavenne, F., Koenig, O., et al. (2000). Emotional responses to pleasant and unpleasant olfactory, visual, and auditory stimuli: a positron emission tomography study. *Journal of Neuroscience*, 20, 7752.
- Russell, J. A. (1980). A circumplex model of affect. *Journal of personality and social psychology*.
- Russell, J. (2003). Core affect and the psychological construction of emotion. *Psychological review*, 110, 145-172.
- Sander, D., Grandjean, D., & Scherer, K. (2005). A systems approach to appraisal mechanisms in emotion. *Neural Networks*, 18, 317-352.
- Small, D., Gregory, M., Mak, Y., Gitelman, D., Mesulam, M., & Parrish, T. (2003). Dissociation of neural representation of intensity and affective valuation in human gustation. *Neuron*, 39, 701-711.
- Smith, S. (2001). Overview of fMRI analysis. In Jezzard, P., Matthews, P.M., & Smith, S. M. (Eds.). *Functional MRI*. (215-228). Oxford: Oxford University Press.
- Smith, S. (2002). Fast robust automated brain extraction. *Human Brain Mapping*, 17(3): 143-155.
- Smith, S., Jenkinson, M., Woolrich, M., Beckmann, C., Behrens, T., Johansen-Berg, H., et al. (2004). Advances in functional and structural MR image analysis and implementation as

- FSL. *NeuroImage*, 23, S208-S219.
- Steele, J., & Lawrie, S. (2004). Segregation of cognitive and emotional function in the prefrontal cortex: a stereotactic meta-analysis. *NeuroImage*, 21, 868-875.
- Thorpe, S., Rolls, E., & Maddison, S. (1983). The orbitofrontal cortex: neuronal activity in the behaving monkey. *Experimental Brain Research*, 49, 93-115.
- Verduyn, P., Delvaux, E., Van Coillie, H., Tuerlinckx, F., & Van Mechelen, I. (2009). Predicting the duration of emotional experience: Two experience sampling studies. *Emotion*, 9, 83.
- Waugh, C. E., Hamilton, J. P., & Gotlib, I. H. (2010). The neural temporal dynamics of the intensity of emotional experience. *NeuroImage*, 49(2), 1699-1707.
- Wiens, S. (2005). Interoception in emotional experience. *Current opinion in neurology*, 18, 442.
- Wise, R., Ide, K., Poulin, M., & Tracey, I. (2004). Resting fluctuations in arterial carbon dioxide induce significant low frequency variations in BOLD signal. *NeuroImage*, 21, 1652-1664.
- Woolrich, M., Jbabdi, S., Patenaude, B., Chappell, M., Makni, S., Behrens, T., et al. (2009). Bayesian analysis of neuroimaging data in FSL. *NeuroImage*, 45, S173-S186.
- Worsley, K. (2001). Statistical analysis of activation images. In Jezzard, P., Matthews, P.M., & Smith, S. M. (Eds.). *Functional MRI*. (251-270). Oxford: Oxford University Press.
- Worsley, K. (2003). Detecting activation in fMRI data. *Statistical Methods in Medical Research*, 12, 401.
- Yaxley, S., Rolls, E., Sienkiewicz, Z.J., & Scott, T.R. (1985). Satiety does not affect gustatory activity in the nucleus of the solitary tract of the alert monkey. *Brain Research*, 347, 1, 85-93.
- Zajonc, R.B. (1980). Feeling and thinking: Preferences need no inferences. *American Psychologist*, Vol. 35, 2, 151-175.
- Zajonc, R.B. (1984). On the primacy of affect. *American Psychologist*, Vol. 39, 2, 117-123.

Appendix A

Magnetic Resonance Imaging Screening Form



Subject last name: _____ First name: _____

Date of birth: _____
dd / mm / yy

Sex: F / M

| Previous surgery? | NO | YES | If yes indicate the type |
|-------------------|--------------------------|--------------------------|--------------------------|
| Head | <input type="checkbox"/> | <input type="checkbox"/> | |
| Heart | <input type="checkbox"/> | <input type="checkbox"/> | |
| Eyes | <input type="checkbox"/> | <input type="checkbox"/> | |
| Abdomen | <input type="checkbox"/> | <input type="checkbox"/> | |
| Extremities | <input type="checkbox"/> | <input type="checkbox"/> | |
| Spine | <input type="checkbox"/> | <input type="checkbox"/> | |

Others: _____

| Do you have a: | NO | YES | |
|--|--------------------------|--------------------------|---|
| Cardiac Pacemaker / Defibrillator | <input type="checkbox"/> | <input type="checkbox"/> | |
| Cochlear implant or implanted hearing aid | <input type="checkbox"/> | <input type="checkbox"/> | |
| Implanted insulin pump | <input type="checkbox"/> | <input type="checkbox"/> | <i>If yes, must be removed for scan</i> |
| Coloured contact lenses | <input type="checkbox"/> | <input type="checkbox"/> | <i>If yes, must be removed for scan</i> |
| Transdermal delivery system (e.g. patch) | <input type="checkbox"/> | <input type="checkbox"/> | <i>If yes, must be removed for scan</i> |
| Body piercing | <input type="checkbox"/> | <input type="checkbox"/> | <i>If yes, must be removed for scan</i> |
| IUD | <input type="checkbox"/> | <input type="checkbox"/> | |
| Foreign metallic objects (e.g. bullets or metal splinters) | <input type="checkbox"/> | <input type="checkbox"/> | |
| Permanent make-up / tattoos | <input type="checkbox"/> | <input type="checkbox"/> | |
| Ocular implants or devices | <input type="checkbox"/> | <input type="checkbox"/> | |
| Cardiac valve prosthesis | <input type="checkbox"/> | <input type="checkbox"/> | ▶ <u>Specify type</u> |
| Neurostimulator | <input type="checkbox"/> | <input type="checkbox"/> | ▶ _____ |
| Artificial limb or joint | <input type="checkbox"/> | <input type="checkbox"/> | ▶ _____ |
| Implanted orthopedic device | <input type="checkbox"/> | <input type="checkbox"/> | ▶ _____ |
| Penile implant | <input type="checkbox"/> | <input type="checkbox"/> | ▶ _____ |
| Aneurysm Clip | <input type="checkbox"/> | <input type="checkbox"/> | ▶ _____ |
| Filter, catheter or stent in a blood vessel | <input type="checkbox"/> | <input type="checkbox"/> | ▶ _____ |
| Shunt (programmable) | <input type="checkbox"/> | <input type="checkbox"/> | ▶ _____ |

Are you pregnant? NO YES

Have you ever been injured by a metallic piece? (e.g. in your eyes) NO YES

Have you ever undergone Magnetic Resonance Imaging? NO YES
If yes when: _____

Do you suffer from claustrophobia? NO YES

Subject signature

Date (dd-mm-yy)

Physician / Researcher signature

Date (dd-mm-yy)

Appendix B
Informed Consent Form

CONSENT FORM
MONTREAL NEUROLOGICAL INSTITUTE AND HOSPITAL
McConnell Brain Imaging Centre

1. TITLE OF PROJECT

Neural Correlates of Thermal Comfort and Discomfort: Functional Magnetic Resonance Imaging (Principal Investigator: Peter Shizgal, Ph.D.)

2. REASON FOR THE STUDY

Sensations of comfort and discomfort help us maintain physiological balance and thereby survive. When we are chilled, sources of warmth are pleasant, and the cold is unpleasant. When we are overheated, entering a cool setting is pleasant, and continuous exposure to the hot sun may be unpleasant. By seeking out warmth and avoiding the cold when chilled, or seeking out cool shelter when hot, we help bring our body temperature back to normal. The purpose of the study is to identify areas of the brain involved in such thermal comfort and discomfort and the motivation to act that often follows from them.

3. PROCEDURES

Your participation will include two sessions. The first will consist of a screening visit including a test of cardiovascular fitness carried out by a cardiologist, and the second will consist of Magnetic Resonance Imaging (MRI) scans carried out while your body temperature is slightly higher than normal and slightly lower than normal.

3.1 Screening visit and Fitness test. You will be asked to provide a urine sample for drug screening; pregnancy screening will also be carried out on the samples from female subjects. The purpose of the drug screening is to protect you from increased risks posed by any drugs of abuse, prescription drugs, or even over the counter drugs in your system. Such drugs and their residual effects may increase the chance of reacting adversely to the fitness test and changes in body temperature involved in the experimental procedure. As a precaution, pregnant women will be excluded from participating. You may choose not to participate in the urine screening, but this will exclude you from further involvement in the study.

Following the collection of the urine sample, you will be asked to participate in medical and psychological interviews, and to complete a set of questionnaires concerning your mood and mental health. The interview and questionnaires will include inquiries of a personal nature regarding, for example, your use of medications, past history of mental illness or use of alcohol and illegal drugs. Females will also be asked to estimate the dates of their last and next menstruation. You may decide not to participate in these components of the study, but this will exclude you from further involvement in the study.

Regular performance of aerobic exercise and at least average physical fitness are required for your participation in this study. For this reason, your cardiovascular health will be assessed by monitoring your heart while you exercise at different rates on a treadmill. This cardiac stress test will be performed following successful completion of the urine screening, psychological interview and questionnaires. As part of the test, twelve (12) sensors will be arranged on your chest to measure your heart's electrical activity while you perform exercise. You will be directed to walk on the treadmill as readings of your cardiovascular function are recorded for assessment by a cardiologist.

The principal investigator and study physicians reserve the right to exclude any potential participant from the study for any reason based on their medical or psychological judgment.

3.2 Raising body temperature.

If you are eligible for participation, the urine screening (including drug and pregnancy) will be repeated on the morning of the study visit. Following successful completion of the urine screening and a brief mood questionnaire, you will proceed with the thermal control experiment. You will wear a tube-suit, which consists of long underwear (shirt and pants) into which plastic tubing has been sewn. Insulating clothing will be worn over the tube-suit. While hot water circulates through the suit, you will perform mild exercise on a stationary bicycle. Beginning at this time, your temperature will be monitored with oral thermometers mounted in a snorkel mouthpiece and with temperature sensors taped to your skin. The snorkel mouthpiece must remain in your closed mouth throughout the study procedure. You will be provided with pen and paper in order to communicate with the research team.

Once your body temperature has reached the target level, approximately one degree above your recorded temperature taken that day, you will participate in a Magnetic Resonance Imaging scan (MRI).

3.3 Lowering body temperature. Following the first MRI scan, the insulating clothing will be removed, and you will sit in a cool room in front of a fan while cold water circulates through the tube-suit. Your temperature will be monitored and allowed to drop to approximately one degree below your recorded temperature taken that day. Once your body temperature has reached the target level you will then participate in a second functional Magnetic Resonance Imaging scan (fMRI).

3.4 Magnetic Resonance Imaging

The MRI scanner uses a powerful magnetic field and radio frequencies to derive images of the structure and blood flow in your brain. The scans do not involve radiation of any kind, and you should not feel any effects of the scanning.

You will be asked to lie on a bed that will be moved into a cylindrical opening where brain scans will be taken during a period of 30 to 40 minutes. Your head will rest inside an apparatus, resembling a baseball catcher's mask, which serves as a receiving antenna for the scanner. You will be asked to remain as still as possible during the scans, and pads will be placed around your head to assist you in remaining immobile. The MRI scanner will be quite noisy during the scan. To reduce the noise, you will be given earplugs. During the scanning, the temperature of the tube-suit will be varied, and you will be asked to rate your level of comfort and the temperature of the water in the tubesuit. A display will be visible to you through a mirror set on an angle above eye level. You may be asked to rate your desire to change the temperature in the tube-suit, or to press a button that either causes or prevents a change in suit temperature. You will be able to communicate with the MRI technician at all times through a microphone, and you are free to end the scanning procedure at any time if you experience discomfort.

After the scanning procedures, you will complete another mood questionnaire, and remain in the MR suite to be assessed by the study physician before leaving. A shower at the facility and transportation home will be provided for your comfort and convenience.

4. CONTRAINDICATIONS

The following is a list of physical issues that would exclude you from participation in a Magnetic Resonance Imaging study. Please read the list carefully and inform the researchers if you have any of the following:

- *Pacemaker*
- *Aneurysm Clip*
- *Heart/Vascular Clip*
- *Prosthetic Valve*
- *Metal Prosthesis*
- *Pregnancy*
- *Claustrophobia*
- *Metal fragments in body*
- *Piercings or other metal that cannot be removed from your body*
 - *Pins, screws, plates or any other metal implants*
 - *Extensive tattooing*
 - *Transdermal Patches (Must be removed prior to scanning. You are advised to bring an additional patch to reapply post scanning.)*
 - *Pregnancy*

5. ADVANTAGES OF THE PROPOSED STUDY

The MRI scans are tests, not treatments. It is hoped that the information obtained will increase our understanding of the function of the human brain and the mechanisms that maintain physiological balance.

6. DISADVANTAGES OF THE PROPOSED STUDY

6.1 Fitness test. The stress on the heart during the fitness test is similar to what is experienced during a vigorous aerobic workout. In young, healthy, aerobically trained individuals such as you, the risk of any cardiac incident is very small. A cardiologist will conduct this test in a medical facility.

6.2 Raising body temperature. The small increase in body temperature (~1 °C) that you will experience while performing mild exercise does not pose a significant risk in young, healthy, aerobically trained individuals such as yourself. Regular aerobic activity at a level that qualifies you for this study entails exercise of similar or greater intensity and at similar or higher body temperatures. However, if your body temperature is kept elevated for a very long time while wearing the tube-suit, there is a risk of fainting. This risk will be controlled by limiting the time your temperature will be raised and by having you lie down during scanning with your legs elevated.

6.3 Lowering body temperature. The small decrease in body temperature (~1 °C) that you will experience while wearing the tube-suit does not pose a significant risk. This change in body temperature is smaller than the normal variation over the 24-hour cycle.

6.4 Scalding. The water flowing through the tube suit will be as hot as 50 °C. Nonetheless, the risk of scalding is very low. The suit has been found not to leak at a pressure greater than three times the value that will be used in this study.

6.5 Magnetic Resonance Imaging. During these sessions, you will be exposed to a strong magnetic field. However, no long-term negative side-effects have been observed from this type of study. As mentioned above, the magnetic resonance scanner is very noisy and you will be given earplugs to reduce this effect. Metallic objects can be attracted with great force by the magnetic field. You will be asked to remove all such objects from your person and clothing prior to the session.

7. CONFIDENTIAL NATURE OF THIS STUDY

Your participation is strictly confidential. The investigators will take all reasonable measures to protect the confidentiality of your records. Your identity will not be revealed in any presentation or publication that results from this project. Our complete research records, which contain personal information about you (name, date of birth, address and telephone number), may have to be forwarded to the MNI/MNH Research Ethics Board, upon request. You should also be aware that the Research Ethics Board or Quality Assurance Officers duly authorized by it might access study data.

8. DISCONTINUATION OF THE STUDY BY THE INVESTIGATOR

At any time during the testing, the investigators have the right to terminate the study for any reasons.

9. WITHDRAWAL FROM THE STUDY

Your participation in this research study is voluntary and you may withdraw at any time, including during the procedures. If the investigators obtain useful data prior to your withdrawal, they will keep it in their records and use it for research purposes and data analysis unless you provide written refusal to do so. Any secondary use of these data would be restricted to a research protocol in the same or related area of study and subject to the approval of the MNI/MNH Research Ethics Board.

10. INCIDENTAL FINDINGS

Research scans and fitness-test results are not subject to clinical review. However, any incidental findings will be communicated to you and, upon your request, to your physician.

11. EFFECTS OF PARTICIPATION IN THIS STUDY

Magnetic Resonance Imaging does not interfere with any treatment or other diagnostic tests.

12. SUBJECT'S AGREEMENT TO BE CONTACTED BY THE RESEARCH ETHICS BOARD

Participants in this research study may be contacted by a member of the Research Ethics Board, at the discretion of the board.

13. COMPENSATION

Following completion of the screening visit or any portion thereof, you will receive a fee of \$100 as compensation for your time and inconvenience; if you are eligible, following completion of experimental procedure and the MRI scans or any portion thereof, you will receive an additional fee to \$200. Thus the total fee for completion of the entire study will be \$300. The time required for the study is approximately six (6) hours: 2 hours for the interview and fitness test, and 4 hours for the MRI scans at the Montreal Neurological Institute and Hospital (McConnell Brain Imaging Centre). The screening visit (including the fitness test) and MRI scans will be carried out on separate days.

14. CONTACT INFORMATION FOR SUBJECT

If you have any further questions concerning the study, please call Prof. Peter Shizgal: (514) 848-2424 ext 2191. If you have any questions regarding your rights as a research subject and you wish to discuss them with someone not conducting the study, you may contact the Montreal Neurological Hospital (MNH) Patient Ombudsman at (514) 934-1934, extension 48306. If you have any other kind of comments or concerns, or need assistance regarding your participation as a research subject in this project, please contact the MNH Patient's Committee, room 354, telephone: (514) 398-5358.

I HAVE CAREFULLY STUDIED THE ABOVE AND UNDERSTAND THIS AGREEMENT.
I FREELY CONSENT AND VOLUNTARILY AGREE TO PARTICIPATE IN THIS STUDY.

NAME (please print) _____

SIGNATURE _____

NAME OF WITNESS (please print) _____

SIGNATURE OF WITNESS _____

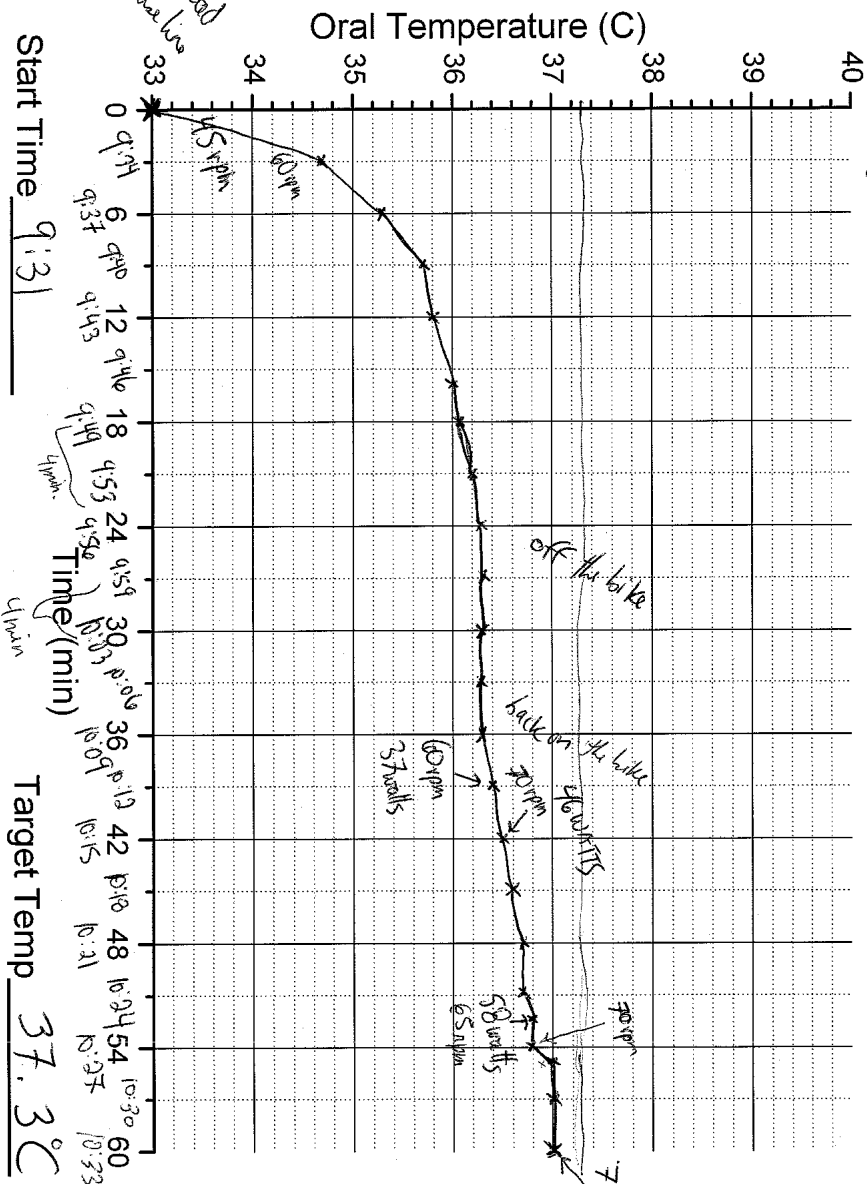
Appendix C

Exemplary Hyper- and Hypothermia Induction Sheets

Set bottom box out put to 6

Phase hypokinesia Subject IF090325 Date 25/3/19

Shizgal Thermal Experiment



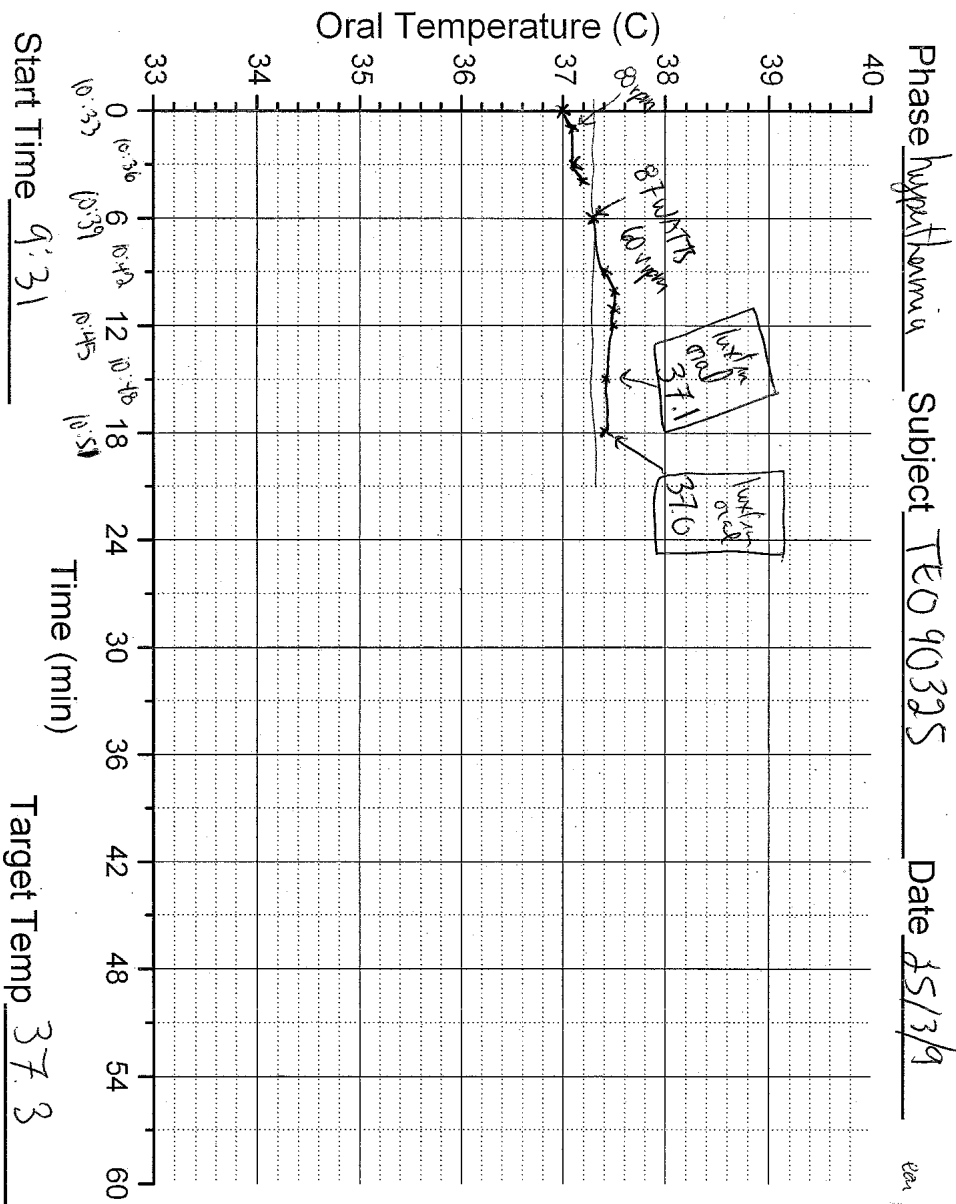
203
Lushin
reading
please

Start Time 9:31 Target Temp 37.3°C

head size: 59 cm

baseline 36.3°C

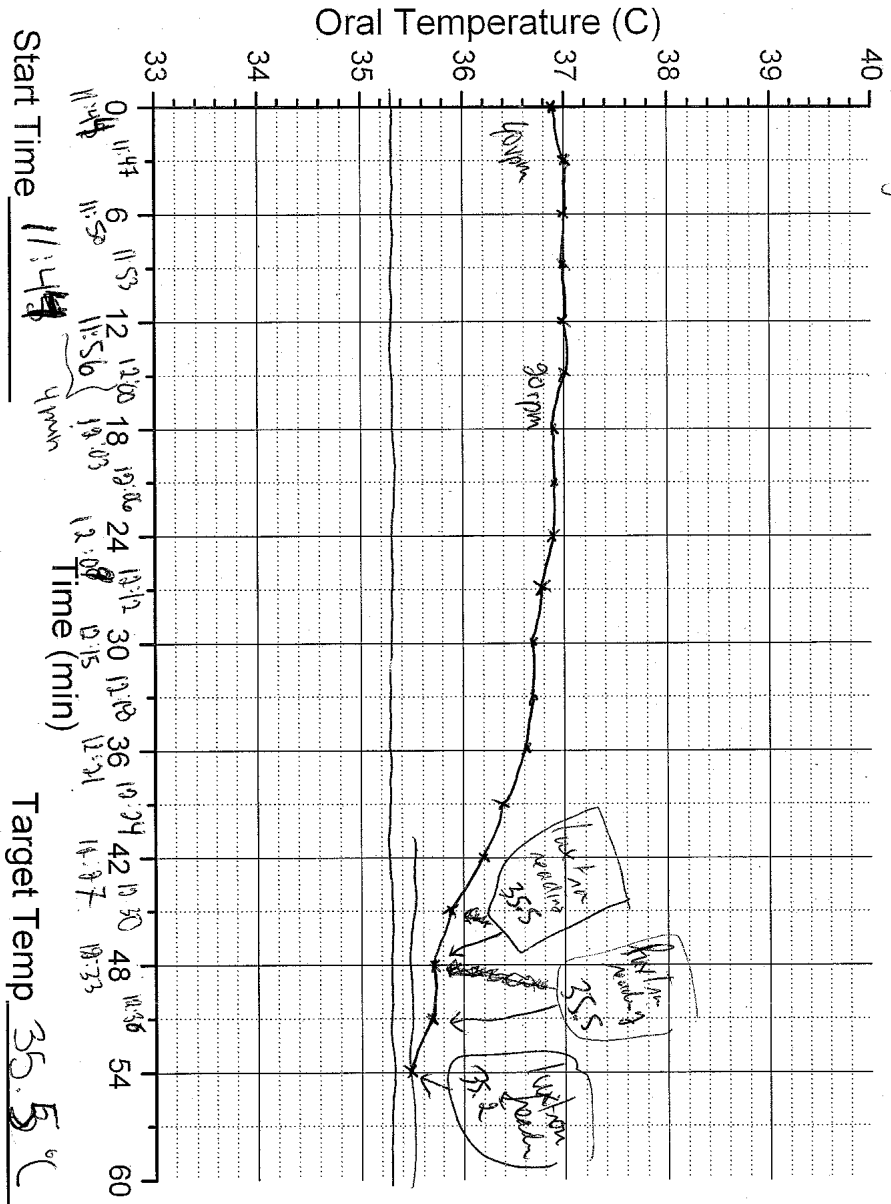
Shizgal Thermal Experiment



page 2/2

Shizgal Thermal Experiment

Phase hyperthermia Subject TEG 90325 Date 95/3/9



Appendix D
Rating Directions

During the scans, you will be asked to rate your experience. Alternating rating scales will appear on the screen at frequent intervals for this purpose. You will be asked to rate your sensations of temperature and *thermal* comfort level.

Please concentrate on your thermal sensations, especially on your skin. Rate the temperature of the water in the tube suit as you feel it at this very moment.

A scale from 0 to 10 will appear at frequent intervals for this purpose. Use the right button to move the cursor to the right, and the left button to move the cursor left.

Zero (0) indicates the coldest that the water in the suit can get. Ten indicates (10) the hottest that the water in the suit can get.

Please concentrate on your thermal comfort. Rate how good or bad the temperature in the suit feels at this very moment.

A scale from -5 (indicating “Bad”) to 5 (indicating “Good”) will appear at frequent intervals for this purpose. Use the right button to move the cursor to the right, and the left button to move the cursor left.

Your ratings should reflect the range of feeling that the present circumstances generate, not the worst (most uncomfortable) or best (most comfortable) you have ever felt.

Rate your relative *thermal* comfort, not whether you are feeling well or feeling ill.

Do the best you can to pay attention to the rating scales as they change and make your ratings promptly.

Appendix E
Individual FEAT Script

```

# FEAT version number
set fmri(version) 5.98
# Are we in MELODIC?
set fmri(inmelodic) 0
# Analysis level
# 1 : First-level analysis
# 2 : Higher-level analysis
set fmri(level) 1
# Which stages to run
# 0 : No first-level analysis (registration and/or group stats only)
# 7 : Full first-level analysis
# 1 : Pre-Stats
# 3 : Pre-Stats + Stats
# 2 :      Stats
# 6 :      Stats + Post-stats
# 4 :      Post-stats
set fmri(analysis) 7
# Use relative filenames
set fmri(relative_yn) 0
# Balloon help
set fmri(help_yn) 1
# Run Featwatcher
set fmri(featwatcher_yn) 1
# Cleanup first-level standard-space images
set fmri(sscleanup_yn) 0
# Output directory
set fmri(outputdir) /Users/Shared/cbig/te/lib/grp/all/feat/nat/hed/021/vmt/ft1/glm/hyper/te090525
# TR(s)
set fmri(tr) 2.25
# Total volumes
set fmri(npts) 504
# Delete volumes
set fmri(ndelete) 0
# Perfusion tag/control order
set fmri(tagfirst) 1
# Number of first-level analyses
set fmri(multiple) 1
# Higher-level input type
# 1 : Inputs are lower-level FEAT directories
# 2 : Inputs are cope images from FEAT directories
set fmri(inputtype) 1
# Carry out pre-stats processing?
set fmri(filtering_yn) 1
# Brain/background threshold, %
set fmri(brain_thresh) 10
# Critical z for design efficiency calculation
set fmri(critical_z) 5.3
# Noise level
set fmri(noise) 0.66

```

```

# Noise AR(1)
set fmri(noisear) 0.34
# Post-stats-only directory copying
# 0 : Overwrite original post-stats results
# 1 : Copy original FEAT directory for new Contrasts, Thresholding, Rendering
set fmri(newdir_yn) 0
# Motion correction
# 0 : None
# 1 : MCFLIRT
set fmri(mc) 0
# Spin-history (currently obsolete)
set fmri(sh_yn) 0
# B0 fieldmap unwarping?
set fmri(regunwarp_yn) 0
# EPI dwell time (ms)
set fmri(dwell) 0.47
# EPI TE (ms)
set fmri(te) 30
# % Signal loss threshold
set fmri(signallossthresh) 10
# Unwarp direction
set fmri(unwarp_dir) y-
# Slice timing correction
# 0 : None
# 1 : Regular up (0, 1, 2, 3, ...)
# 2 : Regular down
# 3 : Use slice order file
# 4 : Use slice timings file
# 5 : Interleaved (0, 2, 4 ... 1, 3, 5 ... )
set fmri(st) 0
# Slice timings file
set fmri(st_file) ""
# BET brain extraction
set fmri(bet_yn) 0
# Spatial smoothing FWHM (mm)
set fmri(smooth) 0
# Intensity normalization
set fmri(norm_yn) 0
# Perfusion subtraction
set fmri(perfsub_yn) 0
# Highpass temporal filtering
set fmri(temphp_yn) 0
# Lowpass temporal filtering
set fmri(templp_yn) 0
# MELODIC ICA data exploration
set fmri(melodic_yn) 0
# Carry out main stats?
set fmri(stats_yn) 1
# Carry out prewhitening?
set fmri(prewhiten_yn) 1
# Add motion parameters to model

```

```

# 0 : No
# 1 : Yes
set fmri(motionevs) 0
# Robust outlier detection in FLAME?
set fmri(robust_yn) 0
# Higher-level modelling
# 3 : Fixed effects
# 0 : Mixed Effects: Simple OLS
# 2 : Mixed Effects: FLAME 1
# 1 : Mixed Effects: FLAME 1+2
set fmri(mixed_yn) 2
# Number of EVs
set fmri(evs_orig) 1
set fmri(evs_real) 1
set fmri(evs_vox) 0
# Number of contrasts
set fmri(ncon_orig) 1
set fmri(ncon_real) 1
# Number of F-tests
set fmri(nftests_orig) 0
set fmri(nftests_real) 0
# Add constant column to design matrix? (obsolete)
set fmri(constcol) 0
# Carry out post-stats steps?
set fmri(poststats_yn) 1
# Pre-threshold masking?
set fmri(threshmask) ""
# Thresholding
# 0 : None
# 1 : Uncorrected
# 2 : Voxel
# 3 : Cluster
set fmri(thresh) 3
# P threshold
set fmri(prob_thresh) 0.05
# Z threshold
set fmri(z_thresh) 2.3
# Z min/max for colour rendering
# 0 : Use actual Z min/max
# 1 : Use preset Z min/max
set fmri(zdisplay) 0
# Z min in colour rendering
set fmri(zmin) 2
# Z max in colour rendering
set fmri(zmax) 8
# Colour rendering type
# 0 : Solid blobs
# 1 : Transparent blobs
set fmri(rendertype) 1
# Background image for higher-level stats overlays
# 1 : Mean highres

```

```

# 2 : First highres
# 3 : Mean functional
# 4 : First functional
# 5 : Standard space template
set fmri(bgimage) 1
# Create time series plots
set fmri(tsplot_yn) 0
# Registration?
set fmri(reg_yn) 1
# Registration to initial structural
set fmri(reginitial_highres_yn) 0
# Search space for registration to initial structural
# 0 : No search
# 90 : Normal search
# 180 : Full search
set fmri(reginitial_highres_search) 90
# Degrees of Freedom for registration to initial structural
set fmri(reginitial_highres_dof) 3
# Registration to main structural
set fmri(reghighres_yn) 1
# Search space for registration to main structural
# 0 : No search
# 90 : Normal search
# 180 : Full search
set fmri(reghighres_search) 90
# Degrees of Freedom for registration to main structural
set fmri(reghighres_dof) 6
# Registration to standard image?
set fmri(regstandard_yn) 1
# Standard image
set fmri(regstandard) "/usr/local/fsl/data/standard/MNI152_T1_1mm_brain"
# Search space for registration to standard space
# 0 : No search
# 90 : Normal search
# 180 : Full search
set fmri(regstandard_search) 90
# Degrees of Freedom for registration to standard space
set fmri(regstandard_dof) 12
# Do nonlinear registration from structural to standard space?
set fmri(regstandard_nonlinear_yn) 0
# Control nonlinear warp field resolution
set fmri(regstandard_nonlinear_warpres) 10
# High pass filter cutoff
set fmri(paradigm_hp) 405
# Number of lower-level copes feeding into higher-level analysis
set fmri(ncopeinputs) 0
# 4D AVW data or FEAT directory (1)
set feat_files(1)
"/Users/Shared/cbig/te/lib/grp/all/cmn/nii/hyper/te090525_hyper_fnc_bpf_mcf_X38.nii"
# Add confound EVs text file
set fmri(confoundevs) 1

```

```

# Confound EVs text file for analysis 1
set confoundev_files(1)
"/Users/Shared/cbig/te/lib/grp/all/feat/nat/hed/021/vmt/ft1/glm/hyper/te090525/te090525_ev_cv.t
xt"
# Subject's structural image for analysis 1
set highres_files(1)
"/Users/Shared/cbig/te/lib/grp/all/cmn/nii/hyper/TE090525_Hyper_ana_swp_bet.nii"
# EV 1 title
set fmri(evtitle1) "Ev1"
# Basic waveform shape (EV 1)
# 0 : Square
# 1 : Sinusoid
# 2 : Custom (1 entry per volume)
# 3 : Custom (3 column format)
# 4 : Interaction
# 10 : Empty (all zeros)
set fmri(shape1) 2
# Convolution (EV 1)
# 0 : None
# 1 : Gaussian
# 2 : Gamma
# 3 : Double-Gamma HRF
# 4 : Gamma basis functions
# 5 : Sine basis functions
# 6 : FIR basis functions
set fmri(convolve1) 2
# Convolve phase (EV 1)
set fmri(convolve_phase1) 0
# Apply temporal filtering (EV 1)
set fmri(tempfilt_yn1) 1
# Add temporal derivative (EV 1)
set fmri(deriv_yn1) 0
# Custom EV file (EV 1)
set fmri(custom1)
"/Users/Shared/cbig/te/lib/grp/all/feat/nat/hed/021/vmt/ft1/glm/hyper/te090525/te090525_ev_pv.t
xt"
# Gamma sigma (EV 1)
set fmri(gammasigma1) 3
# Gamma delay (EV 1)
set fmri(gammadelay1) 6
# Orthogonalise EV 1 wrt EV 0
set fmri(ortho1.0) 0
# Orthogonalise EV 1 wrt EV 1
set fmri(ortho1.1) 0
# Contrast & F-tests mode
# real : control real EVs
# orig : control original EVs
set fmri(con_mode_old) real
set fmri(con_mode) real
# Display images for contrast_real 1
set fmri(conpic_real.1) 1

```

```

# Title for contrast_real 1
set fmri(conname_real.1) ""
# Real contrast_real vector 1 element 1
set fmri(con_real1.1) 1
# Display images for contrast_orig 1
set fmri(conpic_orig.1) 1
# Title for contrast_orig 1
set fmri(conname_orig.1) ""
# Real contrast_orig vector 1 element 1
set fmri(con_orig1.1) 1
# Contrast masking - use >0 instead of thresholding?
set fmri(conmask_zerothresh_yn) 0
# Do contrast masking at all?
set fmri(conmask1_1) 0
#####
# Now options that don't appear in the GUI
# Alternative example_func image (not derived from input 4D dataset)
set fmri(alternative_example_func) ""
# Alternative (to BETting) mask image
set fmri(alternative_mask) ""
# Initial structural space registration initialisation transform
set fmri(init_initial_highres) ""
# Structural space registration initialisation transform
set fmri(init_highres) ""
# Standard space registration initialisation transform
set fmri(init_standard) ""
# For full FEAT analysis: overwrite existing .feat output dir?
set fmri(overwrite_yn) 0

```

Appendix F
Group FEAT Script

```

# FEAT version number
set fmri(version) 5.98

# Are we in MELODIC?
set fmri(inmelodic) 0

# Analysis level
# 1 : First-level analysis
# 2 : Higher-level analysis
set fmri(level) 2

# Which stages to run
# 0 : No first-level analysis (registration and/or group stats only)
# 7 : Full first-level analysis
# 1 : Pre-Stats
# 3 : Pre-Stats + Stats
# 2 :      Stats
# 6 :      Stats + Post-stats
# 4 :      Post-stats
set fmri(analysis) 6

# Use relative filenames
set fmri(relative_yn) 0

# Balloon help
set fmri(help_yn) 1

# Run Featwatcher
set fmri(featchecker_yn) 1

# Cleanup first-level standard-space images
set fmri(sscleanup_yn) 0

# Output directory
set fmri(outputdir)
"/Users/Shared/cbig/te/lib/grp/thn16/feat/nat/nrm/021/vmt/ft2/flm1+2/glm/hyper"

# TR(s)
set fmri(tr) 2.25

# Total volumes
set fmri(npts) 16

# Delete volumes
set fmri(ndelete) 0

# Perfusion tag/control order
set fmri(tagfirst) 1

# Number of first-level analyses

```

```
set fmri(multiple) 16

# Higher-level input type
# 1 : Inputs are lower-level FEAT directories
# 2 : Inputs are cope images from FEAT directories
set fmri(inputtype) 1

# Carry out pre-stats processing?
set fmri(filtering_yn) 0

# Brain/background threshold, %
set fmri(brain_thresh) 10

# Critical z for design efficiency calculation
set fmri(critical_z) 5.3

# Noise level
set fmri(noise) 0.66

# Noise AR(1)
set fmri(noisear) 0.34

# Post-stats-only directory copying
# 0 : Overwrite original post-stats results
# 1 : Copy original FEAT directory for new Contrasts, Thresholding, Rendering
set fmri(newdir_yn) 0

# Motion correction
# 0 : None
# 1 : MCFLIRT
set fmri(mc) 1

# Spin-history (currently obsolete)
set fmri(sh_yn) 0

# B0 fieldmap unwarping?
set fmri(regunwarp_yn) 0

# EPI dwell time (ms)
set fmri(dwell) 0.7

# EPI TE (ms)
set fmri(te) 35

# % Signal loss threshold
set fmri(signallossthresh) 10

# Unwarp direction
set fmri(unwarp_dir) y-

# Slice timing correction
```

```
# 0 : None
# 1 : Regular up (0, 1, 2, 3, ...)
# 2 : Regular down
# 3 : Use slice order file
# 4 : Use slice timings file
# 5 : Interleaved (0, 2, 4 ... 1, 3, 5 ... )
set fmri(st) 0

# Slice timings file
set fmri(st_file) ""

# BET brain extraction
set fmri(bet_yn) 1

# Spatial smoothing FWHM (mm)
set fmri(smooth) 5

# Intensity normalization
set fmri(norm_yn) 0

# Perfusion subtraction
set fmri(perfsub_yn) 0

# Highpass temporal filtering
set fmri(temphp_yn) 1

# Lowpass temporal filtering
set fmri(templp_yn) 0

# MELODIC ICA data exploration
set fmri(melodic_yn) 0

# Carry out main stats?
set fmri(stats_yn) 1

# Carry out prewhitening?
set fmri(prewhiten_yn) 1

# Add motion parameters to model
# 0 : No
# 1 : Yes
set fmri(motionevs) 0

# Robust outlier detection in FLAME?
set fmri(robust_yn) 1

# Higher-level modelling
# 3 : Fixed effects
# 0 : Mixed Effects: Simple OLS
# 2 : Mixed Effects: FLAME 1
# 1 : Mixed Effects: FLAME 1+2
```

```

set fmri(mixed_yn) 2

# Number of EVs
set fmri(eps_orig) 1
set fmri(eps_real) 1
set fmri(eps_vox) 0

# Number of contrasts
set fmri(ncon_orig) 1
set fmri(ncon_real) 1

# Number of F-tests
set fmri(nftests_orig) 0
set fmri(nftests_real) 0

# Add constant column to design matrix? (obsolete)
set fmri(constcol) 0

# Carry out post-stats steps?
set fmri(poststats_yn) 1

# Pre-threshold masking?
set fmri(threshmask) ""

# Thresholding
# 0 : None
# 1 : Uncorrected
# 2 : Voxel
# 3 : Cluster
set fmri(thresh) 3

# P threshold
set fmri(prob_thresh) 0.05

# Z threshold
set fmri(z_thresh) 2.3

# Z min/max for colour rendering
# 0 : Use actual Z min/max
# 1 : Use preset Z min/max
set fmri(zdisplay) 0

# Z min in colour rendering
set fmri(zmin) 2.3

# Z max in colour rendering
set fmri(zmax) 8

# Colour rendering type
# 0 : Solid blobs
# 1 : Transparent blobs

```

```

set fmri(rendertype) 1

# Background image for higher-level stats overlays
# 1 : Mean highres
# 2 : First highres
# 3 : Mean functional
# 4 : First functional
# 5 : Standard space template
set fmri(bgimage) 5

# Create time series plots
set fmri(tsplot_yn) 1

# Registration?
set fmri(reg_yn) 0

# Registration to initial structural
set fmri(reginitial_highres_yn) 0

# Search space for registration to initial structural
# 0 : No search
# 90 : Normal search
# 180 : Full search
set fmri(reginitial_highres_search) 90

# Degrees of Freedom for registration to initial structural
set fmri(reginitial_highres_dof) 3

# Registration to main structural
set fmri(reghighres_yn) 1

# Search space for registration to main structural
# 0 : No search
# 90 : Normal search
# 180 : Full search
set fmri(reghighres_search) 90

# Degrees of Freedom for registration to main structural
set fmri(reghighres_dof) 6

# Registration to standard image?
set fmri(regstandard_yn) 1

# Standard image
set fmri(regstandard) "/usr/local/fsl/data/standard/MNI152_T1_1mm_brain"

# Search space for registration to standard space
# 0 : No search
# 90 : Normal search
# 180 : Full search
set fmri(regstandard_search) 90

```

```

# Degrees of Freedom for registration to standard space
set fmri(regstandard_dof) 12

# Do nonlinear registration from structural to standard space?
set fmri(regstandard_nonlinear_yn) 1

# Control nonlinear warp field resolution
set fmri(regstandard_nonlinear_warpres) 10

# High pass filter cutoff
set fmri(paradigm_hp) 100

# Number of lower-level copes feeding into higher-level analysis
set fmri(ncopeinputs) 1

# Use lower-level cope 1 for higher-level analysis
set fmri(copeinput.1) 1

# 4D AVW data or FEAT directory (1)
set feat_files(1)
"/Users/Shared/cbig/te/lib/grp/all/feat/nat/nrm/021/vmt/ft1/glm/hyper/te070806.feats"

# 4D AVW data or FEAT directory (2)
set feat_files(2)
"/Users/Shared/cbig/te/lib/grp/all/feat/nat/nrm/021/vmt/ft1/glm/hyper/te070807.feats"

# 4D AVW data or FEAT directory (3)
set feat_files(3)
"/Users/Shared/cbig/te/lib/grp/all/feat/nat/nrm/021/vmt/ft1/glm/hyper/te070808.feats"

# 4D AVW data or FEAT directory (4)
set feat_files(4)
"/Users/Shared/cbig/te/lib/grp/all/feat/nat/nrm/021/vmt/ft1/glm/hyper/te080125.feats"

# 4D AVW data or FEAT directory (5)
set feat_files(5)
"/Users/Shared/cbig/te/lib/grp/all/feat/nat/nrm/021/vmt/ft1/glm/hyper/te080328.feats"

# 4D AVW data or FEAT directory (6)
set feat_files(6)
"/Users/Shared/cbig/te/lib/grp/all/feat/nat/nrm/021/vmt/ft1/glm/hyper/te080723.feats"

# 4D AVW data or FEAT directory (7)
set feat_files(7)
"/Users/Shared/cbig/te/lib/grp/all/feat/nat/nrm/021/vmt/ft1/glm/hyper/te080806.feats"

# 4D AVW data or FEAT directory (8)
set feat_files(8)
"/Users/Shared/cbig/te/lib/grp/all/feat/nat/nrm/021/vmt/ft1/glm/hyper/te080912.feats"

```

```

# 4D AVW data or FEAT directory (9)
set feat_files(9)
"/Users/Shared/cbig/te/lib/grp/all/feat/nat/nrm/021/vmt/ft1/glm/hyper/te080919.feats"

# 4D AVW data or FEAT directory (10)
set feat_files(10)
"/Users/Shared/cbig/te/lib/grp/all/feat/nat/nrm/021/vmt/ft1/glm/hyper/te090325.feats"

# 4D AVW data or FEAT directory (11)
set feat_files(11)
"/Users/Shared/cbig/te/lib/grp/all/feat/nat/nrm/021/vmt/ft1/glm/hyper/te090429.feats"

# 4D AVW data or FEAT directory (12)
set feat_files(12)
"/Users/Shared/cbig/te/lib/grp/all/feat/nat/nrm/021/vmt/ft1/glm/hyper/te090525.feats"

# 4D AVW data or FEAT directory (13)
set feat_files(13)
"/Users/Shared/cbig/te/lib/grp/all/feat/nat/nrm/021/vmt/ft1/glm/hyper/te090814.feats"

# 4D AVW data or FEAT directory (14)
set feat_files(14)
"/Users/Shared/cbig/te/lib/grp/all/feat/nat/nrm/021/vmt/ft1/glm/hyper/te091217.feats"

# 4D AVW data or FEAT directory (15)
set feat_files(15)
"/Users/Shared/cbig/te/lib/grp/all/feat/nat/nrm/021/vmt/ft1/glm/hyper/te100301.feats"

# 4D AVW data or FEAT directory (16)
set feat_files(16)
"/Users/Shared/cbig/te/lib/grp/all/feat/nat/nrm/021/vmt/ft1/glm/hyper/te100426.feats"

# Add confound EVs text file
set fmri(confoundevs) 0

# EV 1 title
set fmri(evtitle1) ""

# Basic waveform shape (EV 1)
# 0 : Square
# 1 : Sinusoid
# 2 : Custom (1 entry per volume)
# 3 : Custom (3 column format)
# 4 : Interaction
# 10 : Empty (all zeros)
set fmri(shape1) 2

# Convolution (EV 1)
# 0 : None
# 1 : Gaussian
# 2 : Gamma

```

```
# 3 : Double-Gamma HRF
# 4 : Gamma basis functions
# 5 : Sine basis functions
# 6 : FIR basis functions
set fmri(convolve1) 0

# Convolve phase (EV 1)
set fmri(convolve_phase1) 0

# Apply temporal filtering (EV 1)
set fmri(tempfilt_yn1) 0

# Add temporal derivative (EV 1)
set fmri(deriv_yn1) 0

# Custom EV file (EV 1)
set fmri(custom1) "dummy"

# Orthogonalise EV 1 wrt EV 0
set fmri(ortho1.0) 0

# Orthogonalise EV 1 wrt EV 1
set fmri(ortho1.1) 0

# Higher-level EV value for EV 1 and input 1
set fmri(evg1.1) 1

# Higher-level EV value for EV 1 and input 2
set fmri(evg2.1) 1

# Higher-level EV value for EV 1 and input 3
set fmri(evg3.1) 1

# Higher-level EV value for EV 1 and input 4
set fmri(evg4.1) 1

# Higher-level EV value for EV 1 and input 5
set fmri(evg5.1) 1

# Higher-level EV value for EV 1 and input 6
set fmri(evg6.1) 1

# Higher-level EV value for EV 1 and input 7
set fmri(evg7.1) 1

# Higher-level EV value for EV 1 and input 8
set fmri(evg8.1) 1

# Higher-level EV value for EV 1 and input 9
set fmri(evg9.1) 1
```

```
# Higher-level EV value for EV 1 and input 10
set fmri(evg10.1) 1

# Higher-level EV value for EV 1 and input 11
set fmri(evg11.1) 1

# Higher-level EV value for EV 1 and input 12
set fmri(evg12.1) 1

# Higher-level EV value for EV 1 and input 13
set fmri(evg13.1) 1

# Higher-level EV value for EV 1 and input 14
set fmri(evg14.1) 1

# Higher-level EV value for EV 1 and input 15
set fmri(evg15.1) 1

# Higher-level EV value for EV 1 and input 16
set fmri(evg16.1) 1

# Group membership for input 1
set fmri(groupmem.1) 1

# Group membership for input 2
set fmri(groupmem.2) 1

# Group membership for input 3
set fmri(groupmem.3) 1

# Group membership for input 4
set fmri(groupmem.4) 1

# Group membership for input 5
set fmri(groupmem.5) 1

# Group membership for input 6
set fmri(groupmem.6) 1

# Group membership for input 7
set fmri(groupmem.7) 1

# Group membership for input 8
set fmri(groupmem.8) 1

# Group membership for input 9
set fmri(groupmem.9) 1

# Group membership for input 10
set fmri(groupmem.10) 1
```

```

# Group membership for input 11
set fmri(groupmem.11) 1

# Group membership for input 12
set fmri(groupmem.12) 1

# Group membership for input 13
set fmri(groupmem.13) 1

# Group membership for input 14
set fmri(groupmem.14) 1

# Group membership for input 15
set fmri(groupmem.15) 1

# Group membership for input 16
set fmri(groupmem.16) 1

# Contrast & F-tests mode
# real : control real EVs
# orig : control original EVs
set fmri(con_mode_old) real
set fmri(con_mode) real

# Display images for contrast_real 1
set fmri(conpic_real.1) 1

# Title for contrast_real 1
set fmri(conname_real.1) "group mean"

# Real contrast_real vector 1 element 1
set fmri(con_real1.1) 1

# Contrast masking - use >0 instead of thresholding?
set fmri(conmask_zerothresh_yn) 0

# Do contrast masking at all?
set fmri(conmask1_1) 0

#####
# Now options that don't appear in the GUI

# Alternative example_func image (not derived from input 4D dataset)
set fmri(alternative_example_func) ""

# Alternative (to BETting) mask image
set fmri(alternative_mask) ""

# Initial structural space registration initialisation transform
set fmri(init_initial_highres) ""

```

```
# Structural space registration initialisation transform  
set fmri(init_highres) ""
```

```
# Standard space registration initialisation transform  
set fmri(init_standard) ""
```

```
# For full FEAT analysis: overwrite existing .feat output dir?  
set fmri(overwrite_yn) 0
```